Dynamic adaptation of human motions

Ludovic Hoyet

Thèse

THESE INSA Rennes
sous le sceau de l'Université européenne de Bretagne
pour obtenir le titre de
DOCTEUR DE L'INSA DE RENNES
Spécialité : Informatique

présentée par
Ludovic Hoyet
ECOLE DOCTORALE : *MATISSE*
LABORATOIRE : *IRISA*

Adaptation dynamique de mouvements humains

Dynamic Adaptation of Human Motions

Thèse soutenue le 18.11.2010
devant le jury composé de :

Bruno Arnaldi
Professeur des Universités, INSA de Rennes / *Président*
Ronan Boulic
Maître d'Enseignement et de Recherche, Virtual Reality Lab, Suisse / *Rapporteur*
Jean-Paul Laumond
Directeur de Recherche, LAAS-CNRS, Toulouse / *Rapporteur*
Arjan Egges
Assistant Professor, Université d'Utrecht, Pays-Bas / *Examinateur*
Taku Komura
Assistant Professor, Université d'Edimbourg / Co-directeur de thèse
Franck Multon
Professeur des Universités, Université de Rennes 2 / Directeur de thèse

Adaptation dynamique de mouvements humains

Dynamic Adaptation of Human Motions

Ludovic Hoyet

En partenariat avec

Equipe Projet Bunraku
IRISA – INRIA Rennes

Centre INRIA Rennes
Bretagne Atlantique

Mouvement Sport Santé
Université de Rennes 2

School of Informatics
Université d'Edimbourg

Remerciements - Acknowledgement

Je tiens tout d'abord à remercier Bruno Arnaldi qui m'a fait l'honneur de présider mon jury de thèse. Je remercie ensuite Jean-Paul Laumond et Ronan Boulic d'avoir accepté d'être mes deux rapporteurs de thèse et pour leurs commentaires extrêment constructifs sur ce travail. Je remercie aussi Arjan Egges d'avoir accepté de participer à ce jury et pour les différentes recommandations qu'il m'a fait parvenir. J'espère que cette rencontre sera une bonne occasion pour d'entamer de futures collaborations.

I would also like to thank Taku Komura for being my co-supervisor since my Master of Sciences, and for hosting me during six months in Edinburgh during my PhD. Without these collaborations it would have been far more difficult to write and defend my PhD in English.

Je remercie aussi tout particulièrement Franck qui m'a encadré depuis le début de mon stage de Master Recherche et qui m'a donné ma chance de travailler dans ce domaine que j'affectionnais depuis plusieurs années. Je te remercie pour tous les nombreux échanges que nous avons pu avoir au cours de ces quatres années de collaboration, que ce soit du point de vue scientifique, humain, ainsi que pour les histoires abracadabrantes que tu as à raconter :D. Je te remercie surtout pour ta disponibilité, car tu as su trouver du temps à m'accorder même lorsque ton emploi du temps était déjà plus que chargé. C'est en tout cas avec le plus grand plaisir que je continuerai à collaborer avec toi.

Je tiens aussi à remercier tous les membres de l'IRISA/INRIA Rennes que j'ai pu cotoyer au cours de toutes ces années. Je tiens à remercier principalement tous les membres de SIAMES, Bunraku et futurs ex-Bunraku que j'ai cotoyé au jour le jour. Je remercie Julien, Marc, Fabrice et Anatole pour tous leurs conseils avisés en matière de rédaction d'articles, rédaction de dossiers et discussions diverses concernant le monde de l'enseignement et de la recherche. Je remercie aussi Richard, à qui je pense que l'on peu décerner le diplôme de Zukari squatteur honoraire, Georges pour ses conseils et pour ses blagues d'introduction de séminaire que je ne pourrai oublier, Valérie, Maud, Alain, Kadi, Thierry et tous les autres.

Je remercie aussi tous les autres membres de l'équipe qui ont davantage accompagné ces trois années de doctorat au jour le jour pendant nos pauses café pluri-journalières, mémorables soirées de séminaires au vert, soirées poker et toutes les diverses activités que nous avons pu organiser. La liste est heureusement trop longue pour être énumérée ici.

Je remercie aussi l'AGOS, et particulièrement Marie, pour toutes les activités que nous avons pu lancer. Qui aurait cru que nous aurions déclenché un tel entousiasme dans ce laboratoire pour monter une équipe de Hockey sur Glace en si peu de temps :D. Merci d'avoir cru en nous, car ce n'est clairement partout que nous aurions eu le soutien pour lancer ce genre d'activité. De fil en aiguille, je remercie tous les membres de l'équipe pour ces séances de glisse qui ne sont que du bonheur. Et je n'oublie pas non

plus Laurence et Pierrette qui par leur bonne humeur nous permettent de profiter d'un cadre de travail privilégié.

Je tiens bien entendu à remercier ma famille pour leur soutien: mes parents, pour qui j'espère la soutenance technique d'une heure et demie en anglais n'a pas été un trop long calvaire :p, et celui qui restera toujours mon petit frère malgré le fait que nous vieillissons tous les deux :D. Je remercie aussi tous mes amis: Bibi en premier car il est surement l'un de ceux qui comprend le mieux la difficulté de la thèse, Steph et Emilie pour m'avoir accueilli dans les moments où j'étais seul, Thomas (double casquette Bunraku) pour les trajets en covoit et les scéances photo à la piscine, Anthony, Julien, Victor, Coralie, Rémy, Cyril et bien entendu tous les autres dont la liste serait un peu longue à citer. A special thank to Hubert and Masashi whom I met in Edinburgh for all the good moments, and I am still waiting for my chocolate muffin string.

Mes derniers remerciements, et pas les moindres, s'adressent bien entendu à toi Hélène pour m'avoir supporté (et le mot est sûrement faible) surtout en cette fin de thèse :D. Et surtout merci de toujours m'accompagner lorsque je pars travailler à l'étranger car j'ai toujours le rôle facile...

Table of contents

Introduction

Nowadays, virtual humans are widely used in many applications, such as entertainment, training, digital mock-ups, film production... The key problem is to produce virtual humans that behave and move like real humans would have done in the same situation. It is an important issue especially for interactive applications where users have to interact with virtual humans. The naturalness of the interaction is clearly affected by the way the virtual human behaves and moves, leading to more or less involvement of the user in the experiment (named the feeling of Presence in VR).

In such applications, virtual humans have to interact with their environment. They have to displace on more or less complex grounds, carry objects with various masses, and interact with objects or other virtual humans. Hence, to perform all of these tasks, virtual humans have to deal with the following constraints:

- **Kinematic constraints**, which handle constraints based on positions, such as the position of an object to grasp in a virtual environment,
- **Kinetic constraints**, which handle the balance of virtual humans under a quasi-static assumption (without accelerations) by driving the center of mass of the character,
- **Dynamic constraints**, which handle the intrinsic dynamic laws, which is especially important when external perturbations are applied,
- **Other constraints** such as style, morphology or diseases which enhance the naturalness of a motion by taking care of various specific effects.

Simulation of virtual humans is a very active field of research that has offered a wide range of methods and algorithms to drive virtual humans in complex scenes while taking the above constraints into account. Broadly two main families of methods raised in the last two decades. The first one consists in reusing motion capture data in a clever manner. The main advantage of this type of method is that the resulting simulation is based on natural motions measured on real actors. The problem consists in organizing or adapting motion capture data in order to deal with all the possible situations that could occur during an application. Indeed, it's impossible to capture all the possible motions for all possible virtual humans. This problem is then partially compensated by algorithms (and thus computation time) to reuse motion capture data in any new situation.

The second approach consists in designing motions without the direct help of motion capture data. This approach offers a high level of control of the virtual human with accurate responses to external perturbations. It is very similar to what has been developed in robotics to control the motion of autonomous entities. However, the key point here is naturalness. How to ensure that an algorithm is able to generate

natural virtual humans? Among all the possible motions that a virtual human can perform, how to select those that a real human would have done in the same situation?

Whatever the approach used, the virtual human should behave and move in a natural manner in order to make users get involved in the application. However, naturalness is very difficult to define and to formalize. On the one hand, some cartoons may look natural while they do not obey the physical laws. On the other hand, virtual humans are not very natural when they do not obey the physical laws in ballistic motions. One key point here is the subjective feeling of the user who is watching to the virtual human. As a result, perception of natural motions is also a very important issue in order to ensure that users are involved in the application.

In this PhD, we propose to use this last statement as a guideline. On the one hand, we wish to examine which dynamic properties are relevant for ensuring natural motions for virtual humans that has to interact with their environment. On the other hand, we wish to improve our knowledge about the users' perception of natural motions subject to strong physical constraints. The key idea is to generate motions that would be perceived as natural while applying relevant simplifications in order to deal with dynamic constraints.

Hence, the first contribution consists in getting more information about the relevant dynamic parameters used by people to react to external perturbations. Among all the possible parameters that are affected by external perturbations, we propose to focus on balance, especially in dynamic situations. Indeed, balance strongly affects the way people interact with their environment. As humans stand on their two feet (leading to a very small area of interaction with their environment), their balance status is weak leading to continuously controlling balance. As a consequence, applying external forces to humans generally leads to adapting their balance status. Many researchers have proposed methods to analyze and control balance in static or quasi-static situations but the problem is less clear for dynamic situations. Our first contribution aims at comparing various methods to model dynamic balance by carrying-out specific experiments. The goal is to determine if there exists a criterion that is able to detect loss of balance in biological motions subject to dynamic constraints. This knowledge would be usefully reused to simulate more natural motions.

As stated above, the key problem is to generate motions that are perceived as natural rather than accurate physically-valid motions. Therefore, the second contribution aims at better understanding the relevant information perceived by users when watching biological motions subject to various physical constraints. We thus carried-out experiments in order to quantify the accuracy of human perception for lifting motions with various weights. This knowledge can be reused to design a perception-based simulation method for generating natural-looking virtual humans that interact with their physical environment.

Hence, the last contribution consists in reusing the above knowledge to develop a new method for simulating natural-looking reactions to physical external perturbations. As stated above, there exists a large quantity of physically-valid reactions to given external perturbations. The key idea is to use one example of reaction (a motion clip) and to adapt it to the new constraints (new skeleton and new kinematic and physical constraints). Knowledge about dynamic balance is reused to adapt the poses at interaction time while taking recent advances in biomechanics and neurosciences into account. Hence, contrary to classical approaches that are based on costly optimizations, we directly apply motor strategies of humans in order to select a natural reaction to the physical constraints. The perceptual experiment exposed above is also used to simplify the solving process. Instead of solving complex nonlinear differential equations, the problem is divided into two simpler sub-problems: adapting each pose assuming zero accelerations

and then retiming the resulting motion. We assume here that the error linked to this simplification may not be perceived by the users.

Hence, this PhD is organized as follows. Chapter I introduces global knowledge about computer animation and presents a state of the art about virtual human animation. Chapter II studies different criteria that have been proposed in the literature to measure the balanced/unbalanced state of a character, as it is a key point in dynamic adjustments to changes in external perturbations. Another key point is the ability of users to perceive this type of adjustments to dynamic constraints. Thus, chapter III presents a biomechanical and a perceptual study to evaluate if human beings are able to distinguish differences in biological captured motions subject to various external perturbations. Based on these two first contributions, Chapter IV presents a new real-time interactive approach to adapt a unique motion to various physical perturbations while considering the perceptual skills and the natural behavior of people described in biomechanics and neurosciences. A last Chapter summarizes the main contributions of this PhD, concludes and provides some perspectives.

Chapter I

Background

Animation of virtual humans requires to define a model of the human. Based on the complexity of a real human body, it is necessary to define the level of precision required to animate a virtual character: human being is made of different layers, from bones and joints to skin, through muscles and tendons. Therefore, it is important to define the relevant information needed to animate a virtual character. This is addressed by Section I.1.

Section I.2 shortly presents different representations commonly used to describe human motion. It also presents existing methods for the production and modification of motions.

However, whatever the method used to produce or modify motions, human motion is highly driven by dynamic laws. Section I.4.1 presents dynamic laws that are used in the contributions presented in this PhD.

Then, Section I.5 concludes this short state of the art and introduces our main motivations.

I.1 Human body representation

Human body is a complex assembly of bones, joints, muscles, tendons, soft tissues, skin as much as decision and transmission systems. As it is impossible to accurately model its whole complexity, it is important to define a simplified set of these elements in order to animate a virtual character. Thus, the complexity of the animated virtual character is decreased, as for the computational cost of the animating system, while preserving the naturalness of the animation.

For animation purpose, Chadwick et al. [Chadwick 89] separated the human body into three distinct layers: **skeleton**, **muscles** and **skin**. The skeleton defines the hierarchy of bones of the character, with a father-child relation between bones, with bones being linked using joints. Muscles are then connected to this structure to actuate the bones. They act in both bone motions and skin deformation. When activated, the muscle length decreases, making the attached bones move. At the same time, the skin also moves as the muscle section increases. The last layer, skin, gives the final appearance of the character for rendering.

This decomposition in layers is then used to animate a virtual character in two steps. The first step takes care of the virtual human's motion (effects of muscles on the skeleton). Then, the second step uses the output from the previous step (motion) to simulate and render muscle contractions and skin

deformations. In this report, we are mainly interested in the adaptation of human motions which consists in driving the joints along time (first step). We now address how the human body can be modeled for this step.

I.1.1 Hierarchical representation of the skeleton

As we are used to see human motions since our childhood, we are extremely critical about the naturalness of virtual human motions. Johansson [Johansson 73] showed that it is possible to recognize the properties of motions, such as differences between male and female walking styles, only by watching at bright patches (Point Light Display) positioned on an actor. To represent a character's motion, a simple solution is to define a skeleton based on joint positions. However, this representation based on the position of the different joints does not ensure a constant distance between joints. This can lead to the dislocation of the skeleton.

To solve this problem, a **hierarchical representation** is usually used in computer animation. The skeleton structure is stored in a tree, each joint being represented by a node of the tree and each bone by an arc between two nodes. In this kind of representation, the root usually represents the pelvis of the character. Then, the animation of the character is done by driving the rotational degrees of freedom of each joint, which ensure the constant length of each segment.

This **hierarchical representation** (Figure I.1) gives an intuitive solution to animate virtual humans. It is described in the H-Anim standard [H-Anim 01]. However, a few geometric simplifications are used, such as perfect joint center of rotation or various structure simplifications (subsets of the skeleton grouped in rigid parts to decrease the complexity). The Z-up coordinate system presented in Figure I.1 will be our reference in this report.

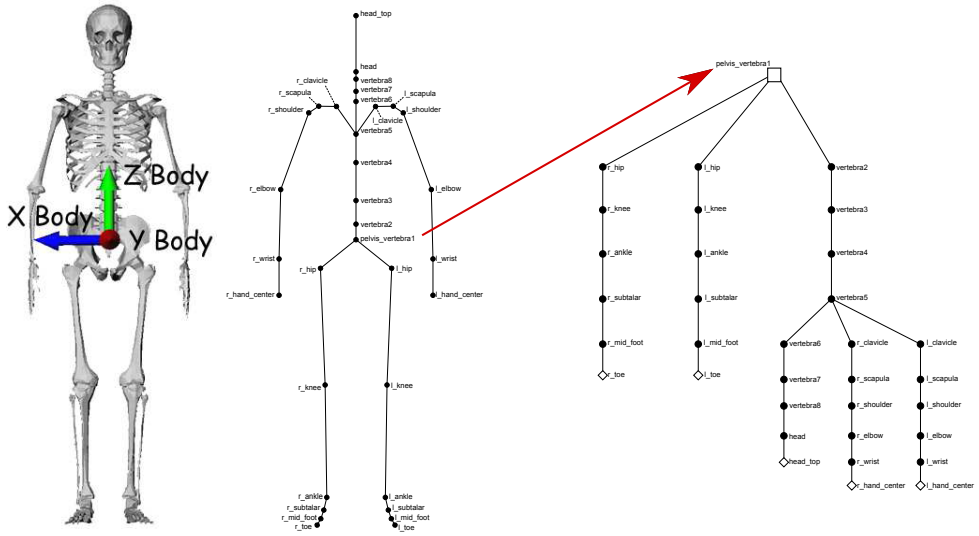

Figure I.1: Hierarchical representation of the skeleton. Left: representation of the bones. Center: simplified skeleton. Right: hierarchy of the simplified skeleton with the root as the pelvis joint.

Applying rotations on these joints modifies the pose of the character. A joint is usually composed of three degrees of freedom (DOF), corresponding to rotations applied to the main axes. In some cases, a

joint can be driven by only one degree of freedom. It can be the case of elbow, knee or finger joints. Another special joint, the root of the hierarchy, is given three additional degrees of freedom, representing the translations on the three axes of the world coordinate system.

A pose $q(t)$ is then defined at the time t as:

$$q(t) = \{p(t), \theta_0(t), \{\theta_i, i \in \{1; ..; n\}\}\} \tag{I.1}$$

where p and θ_0 are the position (3 DOF) and orientation (3 DOF) of the root, θ_i is the value of the i^{st} DOF of the skeleton and n is the total number of DOF of the skeleton.

With this representation, the position X of a given point, such as a joint or an end effector position, only depends on the angles applied to each DOF θ_i:

$$X = f(q) \tag{I.2}$$

This function f is called the geometric function. The result X is the accumulation of the geometric transformations from the world coordinate system to the local coordinate system of each segment:

$$X = \prod_{s \in E_s} M_{s_i \to s_{i+1}} \tag{I.3}$$

where $M_{s_i \to s_{i+1}}$ is the coordinate system of the local transformation from the segment s_i to the segment s_{i+1} and E_s is the sorted set of segments belonging to the kinematic chain from the root to the wanted segment.

I.1.2 Morphology independent representation

Representations based on joint angle transformations allow to manipulate a skeleton and to successfully animate a virtual character when the trajectories are adapted to the character's skeleton and morphology. However, when the same angles are applied to another skeleton, nothing ensures that the final animation will be natural, even for two skeletons with the same hierarchy. Figures I.2.a and I.2.b show that the hand contact cannot be guaranteed when the same joint angles are applied to two different skeletons. To solve this problem, it is necessary to apply motion adaptation techniques (Figure I.2.c), leading to an increase of computation time [Kulpa 05a].

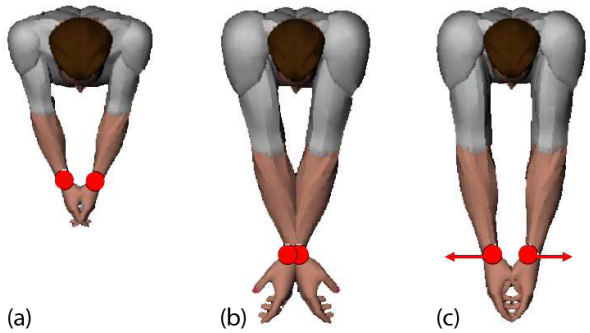

Figure I.2: Same angles applied to two characters with different morphologies (a) and (b). Figure (c) shows the pose which satisfies the initial contact between the hands.

To solve these problems, Ménardais [Ménardais 03] proposed a morphology independent skeleton representation. In this representation, the skeleton is composed of three different kinds of segments (Figure I.3.a):

- a limb (arm or leg) is represented by a unique segment with a variable length (in red),
- the spine is represented by a set of splines (in blue),
- the other segments, called **normalized links**, correspond to a simple segment with a fixed length (in black).

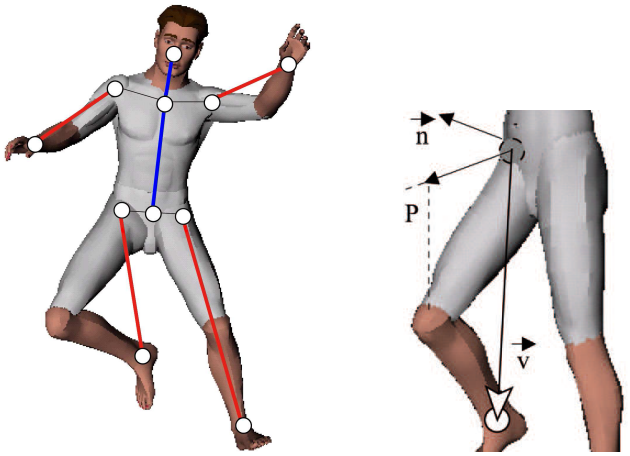

(a) (b)

Figure I.3: a) Morphology independent skeleton representation. b) Normalized representation of the leg. The half plane containing the knee is defined by the coordinate system $(\vec{v}, \vec{P}, \vec{n})$ [Ménardais 03].

The main advantage of this representation is that it includes both angular and cartesian data. Each kinematic chain is then computed from the cartesian positions of the joints of the original skeleton. A kinematic chain CC composed of the set of segments s_j is computed from its root joint position R and its extremity joint position E. The vector $(R, \vec{E})$ is then normalized by the sum of the length lg_j of the segments s_j:

$$CC_{normalized} = \frac{E - R}{\sum_j lg_j} \tag{I.4}$$

This normalization allows to instantly recover the position of the extremity E' of a kinematic chain with another morphology. Given the position R' of the root of this chain and the new lengths lg'_j of the segments s_j, the new position E' is given by:

$$E' = CC_{normalized} \times \sum_j lg'_j + R' \tag{I.5}$$

This representation ensures the consistency of the data when using the same skeleton, with $lg = lg'$.

As shown in Figure I.3.a, intermediate joints are not directly stored into this representation (elbows, knees and intermediate vertebrae). However, they can still be instantly computed when needed, for instance to render 3D poses. The limb intermediate joint I is computed from the following data:

- an additional coordinate system is linked to the limb, defined by the vector $(R,\vec{E})$ and the half plan containing R, E and I (Figure I.3.b),
- a variable length corresponding to the norm of the vector $(R,\vec{E})$, representing the current folding of the limb.

Vertebrae are immediately computed by discretizing the splines modeling the spine.

The position of the root of the character is normalized by the height of the character, corresponding to the rest length of the legs. The character can thus be automatically positioned at the good height relatively to the floor. However, this can be a limitation as it is difficult, for instance, to directly represent walking-on-the-hands motions. This representation is used in the MKM animation system developed in our team [Kulpa 05b, Multon 09]. This system has been used during this PhD.

I.2 Motion representation

I.2.1 Image based representation

The simplest way do define a motion is to consider it as a sequence of poses at fixed time intervals. From the beginning of the 19th century [Marey 94], this technique allowed to describe and analyze human motion. The problem comes from that a motion is described by poses separated by a fixed time step. However, in animation, the frame rate may vary upon the time. Then, there is usually a need to have access to poses between the fixed time intervals.

I.2.2 Key-framed based representation

As it is often necessary to have access to poses using a unpredictable time step, key-framed based animation has been introduced to allow the specification of only a set of representative poses. In-between poses are then computed automatically by interpolating the corresponding key frames. Key-frame based representation is usually used to compute joint trajectories (in cartesian or angular space).

However, results highly depend on the chosen type of interpolation (linear, cubic, spherical, etc). Furthermore, hand creation of key-framed motions implies to use a trial an error process to check if the defined key frames produce the wanted result with the given interpolation method: it is necessary to check the quality and the sampling of the key poses. This lack of flexibility is then carried over the skills of the animator. Assa et al [Assa 05] proposed to compute automatically key frames using positions, rotations and angular velocities of each joint.

I.2.3 Signal processing

Using signal processing, it is possible to extract the dominant characteristics of a trajectory. Angular trajectories θ_i for joint i are thus decomposed as *Fourier series* [Unuma 91] or *Wavelets* [Bruderlin 95] and defined as:

$$\theta_i(t) = \alpha_0 + \sum_{k\geq 1} \alpha_k \sin(kt + \phi_k) \tag{I.6}$$

where the angular trajectory θ_i is decomposed as the sum of k sinusoids of amplitude α_k, with a period of $\frac{2\pi}{k}$ and a phase difference ϕ_k. A low-pass filtering of this trajectory enables us to represent θ_i with a finite set of parameters (α_j, ϕ_j). Thus, the main problem consists in choosing an adequate number of parameters while preserving the major characteristics of the motion.

This representation gives a simple way to extract the main characteristics of a motion. Unuma et al. [Unuma 91, Unuma 93, Unuma 95] computed Fourier series to extract parameters representing human walks and generated new locomotions by interpolating in the frequency domain: they modified normal walks into tired walks or runs. Other authors have proposed to blend locomotion sequences in a control space using this Fourier representation [Pettré 06]. However, if the main characteristics of a motion (emotions, style, dynamic, etc) are included in the representation, it is not straightforward to work on the frequency space to modify motions or to separate the main characteristic parameters. Moreover, this method is mostly appropriate for periodic motions.

Provisional conclusion

Whatever the chosen representation, it is only a support to store human motions. If the frequency-based representation integrates various human characteristics, it is difficult to separate them to express one specific characteristic. For this reason, key-frame based representations are commonly used in computer animation to store human motions.

I.3 Kinematic animation

I.3.1 Motion capture

The most intuitive way to obtain natural motions is to capture them on real actors. With the advances made in the last years in motion capture techniques, more and more human motion data is nowadays available to animate virtual characters. The principle consists in capturing the trajectories of a real actor's motions, using emitters and receptors positioned either on the subject's body or in the captured room (Figure I.4).

(a) Optical Vicon System. (b) Magnetic ShapeWrap II System.

Figure I.4: Motion capture systems.

As these systems use markers positioned on the human body, they provide information linked to the exterior of the body. To animate virtual humans, it is necessary to transform this external data into

internal joint centers. However, the topology of the skeleton usually differs from the real actor. The spine, for instance, is simplified to a few segments while it is composed of 24 vertebrae in humans. Therefore, animating a simplified virtual human always introduces errors. Furthermore, each different technology leads to its own limitations/advantages and creates its own artifacts. It is then necessary to use algorithms to correct these errors (noise correction, simplification of the virtual skeleton, adaptation of the motion to a new skeleton or to a different environment, etc) [Molet 96, Molet 97, Boulic 98, Herda 00, Herda 01, Ménardais 01, Ménardais 03].

Even so, motion capture systems have the main advantage of capturing the naturalness of the actor's own motions and style, while usually keeping original velocity and acceleration profiles.

However, human motion is so complex and there are so many ways to perform a motion depending on the environment configuration that it is impossible to capture all the possible motions. For instance, it is impossible to capture locomotions at all possible speeds for all morphologies on all kinds of floors. One key issue in computer animation consists in reusing motion capture data in new situations without performing new capture sessions. To use captured motions under new environment conditions and constraints, such as changing the speed of a locomotion, it is then more interesting to modify captured motions to create a variety of specific animations. To this end, different families of techniques modifying captured motions have been introduced in the last few years.

I.3.2 Forward and Inverse kinematics

Forward kinematics consists in specifying the joint angle configuration $q(t)$ of the hierarchical structure over time to define a whole animation sequence. However, the exclusive use of forward kinematics makes it difficult to adapt the motion to new constraints, such as preventing foot penetration into the ground during support phases or specifying a new target position of the hand for a grasping task.

To solve these constraints, Inverse Kinematics is commonly used. It consists in adapting the kinematic chain according to constraints expressed in the cartesian frame. The goal is to find the angular configuration q (in angular coordinate system) satisfying the wanted constraint X (in cartesian coordinate system). The solution is then obtained by inversing the geometric function f:

$$f(q) = X \qquad \Rightarrow \qquad q = f^{-1}(X) \tag{I.7}$$

However, f is usually not bijective and not linear. As a consequence, in many cases it is impossible to directly compute f^{-1}. For instance, if the shoulder of a virtual character is fixed and a constraint is set on the position of the wrist, infinity of solutions exist, positioning the elbow on a circle [Korein 82] (Figure I.5.a). This problem comes from the over actuation of the system: the number of degrees of freedom is higher than the number of constraints. Furthermore, the solution space increases with the increase of the number of degrees of freedom (Figure I.5.b).

As f is usually not linear, a common Inverse Kinematics technique consists in locally linearizing f around the current configuration. The angular variations Δq are then linked to the end-effector position variations ΔX given:

$$J\Delta q = \Delta X \tag{I.8}$$

where the Jacobian matrix J maps the variations of the angular degrees of freedom θ_i with the variations of the end-effector constraints X. Hence J is a $M \times N$ matrix made from the partial derivatives of parameters X (M parameters) relatively to the degrees of freedom θ (N DOF), with:

$$J_{m,n} = \frac{\partial f_m}{\partial \theta_n} \tag{I.9}$$

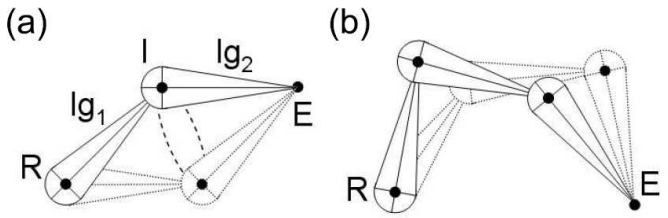

Figure I.5: a) Inverse Kinematics on a two body structure, with R and E being fixed. The joind I has a infinity of solution on the drawn circle. b) Same problem with a three body structure where the solution space is higher.

where f_m corresponds to the variation of the m^{st} parameter of the effector. Then the Inverse Kinematics problem is solved by inversing Equation I.8:

$$\Delta q = J^{-1}\Delta X \tag{I.10}$$

However, the Jacobian matrix J is generally not directly invertible, due to the different dimensions of X and q. Moore-Penrose pseudo-inverse [Penrose 55] is usually used to solve this problem:

$$\Delta q = J^{+}\Delta X \quad \text{with} \quad J^{+} = \begin{cases} (J^tJ)^{-1}J^t & \text{if } M > N \\ J^t(JJ^t)^{-1} & \text{if } M < N \end{cases} \tag{I.11}$$

If this formulation works for solving simultaneous constraints, they are however restricted to have the same degree of importance. In some cases, it is however necessary to strictly satisfy a constraint, then solve the remaining ones as much as possible. To handle multiple constraints with different levels of priority, Hanafusa et al. [Hanafusa 81] proposed to solve them in the inverse order of their priorities. When two constraints X_1 and X_2 are applied, with priorities p_1 and p_2 ($p_1 > p_2$), they enforce X_2 on the null space of X_1 using:

$$\Delta q = J_1^{+}(q)\Delta X_1 + [J_2(I - J_1^{+}J_1)]^{+}(\Delta X_2 - J_2(J_1^{+}\Delta X_1)) \tag{I.12}$$

As a result, the main constraint X_1 is satisfied, when possible, while X_2 is satisfied as much as possible without affecting the achievement of X_1. It has been extended to handle any number of tasks by Siciliano et al. [Siciliano 91]. Baerlocher et al. [Baerlocher 98, Baerlocher 04] proposed various solutions to decrease the complexity of the generalization.

When the hierarchical structure is really simple, a direct analytical solution can be computed. These analytical methods are usually mainly used with a two-segments kinematic chain, such as human limbs [Kondo 91, Lee 99, Wang 99, Tolani 00, Shin 01, Ménardais 03]. Ménardais [Ménardais 03] used this method to adapt a character on uneven grounds. By specifying the position of the footprints on the ground, they compute the optimal position of the root of the character, and adapt both legs using an analytical inverse kinematics method [Kulpa 05b].

Most of the kinematic approaches used for generating virtual human motions combine biomechanical knowledge with forward and inverse kinematics to compute motions [Boulic 92]. Using results obtained from the biomechanics field, it is possible to define joint trajectory characteristics for a specified motion

and to predict the evolution of these trajectories. Thus, kinematic techniques use high level parameters (such as step length, phase duration, velocities, etc) to generate virtual motions. It has also usually the advantage of low computation time, but it can increase with the number of simulated joints or the chosen inverse kinematics algorithm. Furthermore, the quality of the generated motions highly depends on the quality of the model, whose necessary knowledge is only available for the most studied motions. Therefore, it is necessary to search for the specific law ruling each new specific motion.

I.3.3 Displacement maps

Inverse kinematics enables us to adapt a kinematic chain to given constraints. However, discontinuities appear in the final sequence if constraints are activated in a discontinuous manner (Figure I.6.b). To prevent these discontinuities, different authors proposed to modify an original sequence s by adding a variation function Δ to joint trajectories [Witkin 95, Bruderlin 95]. Thus, the new sequence s' is obtained by:

$$s' = s + \Delta \tag{I.13}$$

This variation function Δ corresponds to the variation that should be added to the original sequence s to satisfy the given constraints. This function, called *Displacement map*, is computed by filtering the key frames of the sequence $(s' - s)$. Thus, the resulting sequence s' retains the subtle details of the original sequence s while satisfying the given constraints.

With this method, motions can be adapted to satisfy kinematic constraints only when they are activated [Gleicher 97, Gleicher 98, Gleicher 01]. Inverse kinematic methods are then used to satisfy these constraints. Figure I.6.a shows an original trajectory (blue) and different constraints that should be satisfied (red diamonds). Inverse Kinematics applied to the specified frames associated with constraints leads to discontinuities (Figure I.6.b). Thus, a displacement map is computed to correct these discontinuities. The difference Δ between adapted and original trajectories is filtered (Figure I.6.c) and added to the original trajectory (Figure I.6.d). This operation is repeated until satisfying the given constraints (Figure I.6.e). Even if the number of iterations can be important, the complexity of the method depends only on the number of constraints and on the chosen Inverse Kinematic algorithm.

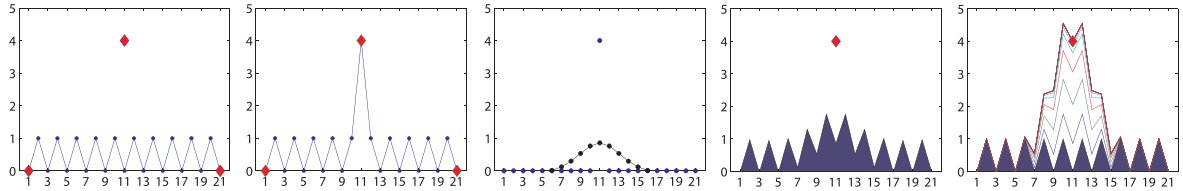

(a) (b) (c) (d) (e)

Figure I.6: Discontinuities in displacement maps [Gleicher 01]. a) Original trajectory (blue) with given constraints (red diamonds). b) Same trajectory with the constraints solved locally: a discontinuity appears. c) The displacement map Δ is filtered. d) Original trajectory with the filtered displacement map. e) Result after several iterations of the process.

I.3.4 Motion Blending

With the previous techniques, it is difficult to handle simultaneously complex tasks. If it is possible to generate walking or grasping motions, it is difficult to generate natural trajectories for walking while grasping an object for instance. To produce new complex sequences, authors proposed to consider them as the blending of simple tasks. This technique is called Motion blending.

However, it is necessary to verify that motions are compatibles to ensure the correctness of the resulting motion. For instance, it is not possible to blend a right foot hoping motion with a left foot hoping motion without ensuring that the change of contact leg is performed in the air and not during the contact phase. Motion blending techniques thus involve synchronizing motions to ensure a temporal coherence between them. This synchronization is mainly controlled by events. For instance, locomotion is mainly driven by events such as foot contact, foot landing, etc. Intuitively, after a foot contact on the floor, it seems reasonable to use a motion with a similar foot contact pattern [Ménardais 04b].

Dynamic Time Warping has been presented by Bruderlin [Bruderlin 95] to synchronize motions for animation purpose. It handles the non-uniform compression or dilatation of parts of a motion (Figure I.7.a) to minimize its distance to another one. However, the time association function giving the correspondence between the original time and the adapted time must be monotonous and continuous. This is necessary to prevent return in the past and discontinuities. As compressions and dilatations might create velocity discontinuities, it is necessary that the time adaptation function is C^2 continuous (Figure I.7.b)

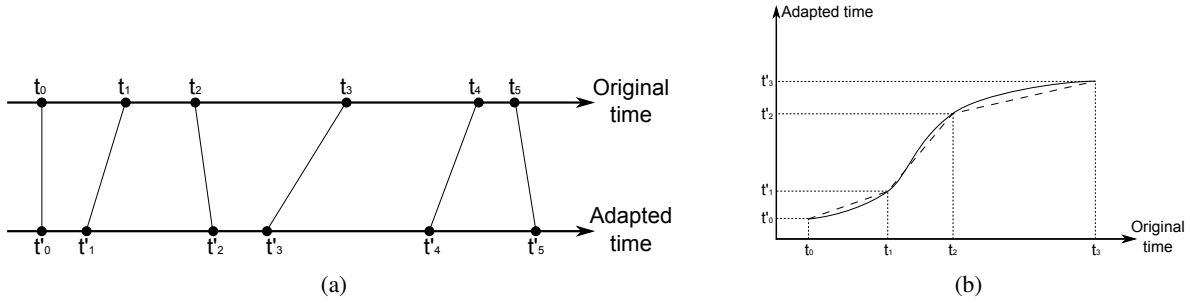

Figure I.7: Dynamic Time Warping [Guo 96]. a) The different time events are associated on both motions. b) The temporal monocity and continuity are necessary to prevent discontinuities [Ménardais 04a].

A first possibility to generate complex tasks using Motion blending consists in blending a set of sequences. Basically, the blending of the different trajectories is done using linear combination (weighted sum) [Guo 96, Wiley 97, Ashraf 00, Park 02, Park 04]. Using four different walking motion types (small step walk – *SSW*, long step walk – LSW, small step running – SSR, long step running – LSR), Guo [Guo 96] applied this method to generate different walking and running motions. A new locomotion is then defined as a linear interpolation of these four motions (Figure I.8).

However, these approaches need to know the future actions to be able to synchronize them. In interactive applications, it is almost impossible to have a long term knowledge of what is going to happen. Different approaches have thus been proposed to handle the blending of different motions in interactive applications. In these case, different priorities are associated on different motions or on subsets of the skeleton [Boulic 97, Ménardais 04a]. For instance, it is possible to combine the lower body part of a walking motion with a right arm grasping motion when close to the object to catch. The continuity of the resulting motion is then obtained by using continuous and derivable priority functions. However, in some cases the produced results can be less natural than approaches using the whole sequence.

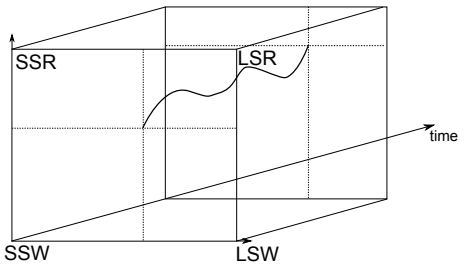

Figure I.8: A joint trajectory defined as a weighted sum of four reference trajectories [Guo 96].

If complex tasks can be defined as a mix of simple actions, in some cases it is necessary to considered them as a succession of simple tasks rather than a mixing to create complex sequences. However, the end of a simple sequence does not usually match the beginning of the following. In these cases, discontinuities appear at the transition between successive sequences. To prevent these discontinuities, Motion blending can be used to generate smooth transitions between successive motions. Dynamic Time Warping is used to automatically synchronize these successive motions using foot contact constraints [Ménardais 04b]. A mathematical operator checks the different supports compatibility and allow the transition to another motion when possible. For instance, a transition between a right foot sequence and a left foot sequence is not valid. When an incompatibility is detected, they dynamically change the local time scale of one of the two motions until its cancellation. However this method is limited to foot contact compatibilities. Other authors have proposed different compatibility criteria [Ashraf 00, Ashraf 01, Ashraf 03].

I.3.5 Motion graphs

If Motion blending enables us to generate new sequences by blending existing motions, resulting motions can be unnatural if not correctly blended [Safonova 05]. To generate natural motions while using only captured poses, the problem consists in defining a method to reuse and reorder all poses of captured motions. Motion graphs [Kovar 02] is one solution to reorder and navigate through huge amount of captured motions. It gives information about the possible transitions from one pose of a motion to another.

In this graph, a node represents one configuration of the skeleton in the database (one frame) and an arc represents an admissible transition from a pose to another. As a first step, a transition exists between two successive poses belonging to the same motion clip (Figure I.9.a). However, Kovar [Kovar 02] proposed that these transitions are not only related to a link in the original motion, but also with a notion of pose similarity: two poses with a similar configuration may be associated with a transition from one to another (Figure I.9.b). To compute these similarities, different distance metrics exist in the literature (distance between joint angles and joint angular velocity [Lee 02, Wang 03], torso velocity and acceleration in the local coordinate system [Arikan 02], etc).

This graph is automatically built offline by computing possible transitions between each motion or pose of the set of motions. Then, the synthesis of a new motion consists in finding a path in the graph between a starting and a goal pose. Lee et al. [Lee 06] improved the model by gathering successive nodes where only one path is possible. They obtained a simplified motion graph, which nodes represent key poses where it is possible to transit to different motions.

By navigating through the Motion Graph, characters can satisfy constraints such as following a path

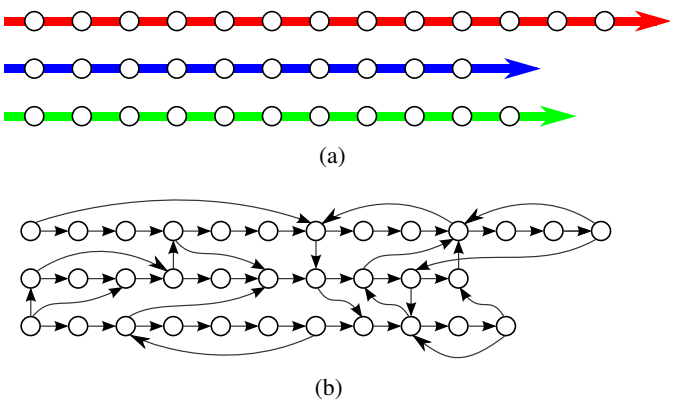

Figure I.9: a) Three different motions as a succession of poses. b) Transitions are created between similar poses.

or performing a succession of tasks. As Motion Graphs handle transitions between motions, the quality of the resulting animation highly depends on the number and diversity of motions in the database. To cover a wide range of possible actions, it is then necessary to have a huge amount of motions.

I.4 Dynamic animation

As human motion is subject to mechanical laws, previous approaches generally fail in satisfying the dynamical laws. Dynamic laws link forces applied to an object with corresponding accelerations, and torques with angular positions. **Forward dynamics** corresponds to the process of calculating the motion generated by given accelerations. On the contrary, **Inverse dynamics** is the process calculating the forces that would generate a given motion.

I.4.1 Dynamic Laws

To take dynamics into account in human motions, a key point is to satisfy the dynamic laws. To handle these laws, two formalisms are mainly used in the literature: Newton-Euler or Lagrange formalism.

Using Newton's laws, a solid moving under different forces verifies:

$$\begin{cases} \sum \mathbf{F}_{ext} &= m.\mathbf{a} \\ \sum \tau_{ext} &= \dot{\mathbf{H}} \end{cases} \tag{I.14}$$

where $\sum \mathbf{F}_{ext}$ is the sum of the external forces applied to the solid, m is the mass of the solid, $\mathbf{a}$ is its acceleration, $\sum \tau_{ext}$ is the sum of the external torques applied to the solid and $\dot{\mathbf{H}}$ is the derivative of the angular momentum of the solid. Details about the computation of the angular momentum are given in Appendix C.

Assuming that the system is in contact with the ground, Equation I.14 becomes:

$$\begin{cases} \mathbf{P} + \mathbf{GRF} + \sum_j \mathbf{F}_j &= m.\mathbf{a} \\ \mathbf{OG} \times \mathbf{P} + \mathbf{OCoP} \times \mathbf{GRF} + \sum_j \mathbf{OA_j} \times \mathbf{F}_j &= \dot{\mathbf{H}}_{/O} \end{cases} \tag{I.15}$$

where $\mathbf{P} = m\mathbf{g}$ is the weight acting on the system applied to the center of mass G and **GRF** is the ground reaction force applied to the position of the center of pressure (CoP). The system is also subject to j external forces $\mathbf{F}_j$ applied respectively to the point A_j. O is a reference point.

Another possibility is to use Lagrange formalism. It is based on the Lagrangian $\mathbf{L}$:

$$\mathbf{L} = \mathbf{E}_c - \mathbf{E}_p \tag{I.16}$$

where $\mathbf{E}_c$ and $\mathbf{E}_p$ respectively correspond to the kinetic and potential energies. Lagrange formalism is then based on the virtual work principle:

$$\frac{d}{dt}\left(\frac{\partial \mathbf{L}}{\partial \dot{\theta}_i}\right) - \frac{\partial \mathbf{L}}{\partial \theta_i} = \tau_{\mathbf{i}} \qquad i = 1, .., n \tag{I.17}$$

where θ_i is the i^{st} parameter of the system and $\tau_{\mathbf{i}}$ is the generalized force (torque) applied to the i^{st} parameter.

The equation of motion can be reformulated as:

$$\tau = \mathbf{M}(\theta)\ddot{\theta} + \mathbf{V}(\theta, \dot{\theta}) + \mathbf{G}(\theta) \tag{I.18}$$

where τ is the $n \times 1$ torque vector, $\mathbf{M}(\theta)$ is the $n \times n$ inertia acceleration-related symmetric matrix, $\mathbf{V}(\theta, \dot{\theta})$ is the $n \times 1$ nonlinear Coriolis and centrifugal force vector and $\mathbf{G}(\theta)$ is the $n \times 1$ gravity loading force vector.

In this report, we only to use the Newton-Euler representation to present our work.

I.4.2 Dynamic controllers

Motion synthesis using controllers is one of the most popular method to handle the dynamics of human motion. Controllers are defined to animate virtual humans using forward dynamics, which allows to automatically take into account the effects of the interactions of the virtual character with its physical virtual environment. According to the physical laws, it is possible to compute the motion equation of the mechanical system (using Euler or Lagrange formalism). The resulting mechanical model is able to compute the state of the system according to external forces and actuators. The problem consists in finding the forces to apply on the virtual human in order to produce a controllable and natural motion.

Hodgins et al. [Hodgins 95, Wooten 96, Wooten 00] designed controllers to synthesize dynamic-based running, vaulting, cycling and diving motions. The mechanical model is generally embedded in a feedforward control loop that enables the controller to compute the appropriate forces to drive the system to the desired state (Figure I.10).

A possible solution to specify these forces is to use a proportional-derivative controller (PD controller) that specify the force f to apply as:

$$f = K_p(q - q_d) - K_v(\dot{q} - \dot{q_d}) \tag{I.19}$$

where K_p and K_v are respectively proportional and derivative gains, $(q, \dot{q})$ and $(q_d, \dot{q_d})$ are respectively the current and the desired states of the system.

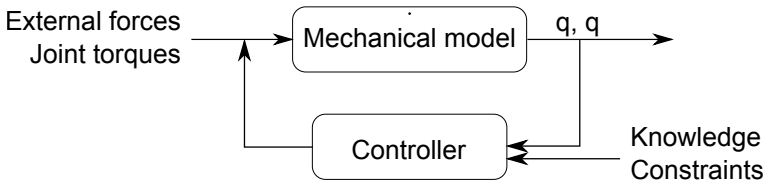

Figure I.10: Controller representation. Given external forces and joint torques, the controller drives q and $\dot{q}$ to obtain a dynamically correct motion while satisfying input constraints and knowledge.

To design a controller, it is necessary to study the motion that we want to simulate. This step allows the extraction of the principal characteristics of a motion, needed to define the controller. It usually corresponds to the different phases of the motion. For instance, a running motion can be separated in alternated flight and one foot contact phases, each phase being defined by its own characteristics (time length, trajectory of the center of mass, configuration to reach, etc). Then, the controller generates a motion while satisfying as much as possible the user defined constraints (velocity of the motion, trajectory to follow, etc). Different works embedded a finite state machine in the controller, each state being associated with a pose, and transition between adjacent states are performed thanks to PD controllers [van de Panne 94, Raibert 91, Hodgins 95].

One of the key problems addressed by controllers is to maintain balance even when the character is subject to external perturbations. Different works focus on generating walking motions while automatically maintaining balance [Laszlo 96, Yin 07] or recovery and reactions to falling [Faloutsos 01b]. Yin et al. [Yin 07] developed a simple control strategy, based on the COM location and velocity, to generate a large variety of gaits and styles in real-time, including walking in all directions (forwards, backwards, sideways, turning). Different works improved this control strategy using an inverted pendulum model to handle the balance of the character [Tsai 10, Mordatch 10, Coros 10]. The inverted pendulum model is used to compute the COM trajectory and the landing position of the feet. Coros et al. [Coros 10] proposed to add continuous balance adjustments using a Jacobian transpose control to mimic the effect of virtual forces, such as gravity or additional external forces. To handle locomotion in complex environments, Mordatch et. al [Mordatch 10] plan the locomotion over multiple phases of gait using a simplified Spring-Load Inverted Pendulum model. Wu and Popović [Wu 10] handle uneven terrain at run-time by planning end-effector trajectories. Then, they solve a quadratic program at each frame, which computes the torques driving the biped while taking the features of the surrounding terrain into account. However, depending on the environment or the task, many factors are unknown by the controller (such as external forces, control torques and user control inputs). Thus, Wang et al. [Wang 10] proposed to use a physics-based optimization process to increase the robustness of walking controllers to these uncertainties.

However, most of previous controller-based approaches do not use any example to generate motions, which leads to sequences that do not possess the naturalness of human motions. Thus, it is necessary to use knowledge in the controller design process to enhance the naturalness of the resulting motions. A interesting solution consists in tracking motion capture reference data [Zordan 02, Abe 07, da Silva 08a, da Silva 08b, Macchietto 09, Liu 10, Ye 10].

Zordan and Hodgins [Zordan 02] proposed to combine motion capture with a controller for response to dynamic perturbations. By controlling the simulation with motion capture data using a PD-controller, they capture the subtle humanlike details of the original subject while adding responsiveness to external perturbations. When a collision happens with the environment, a physical collision model computes the

involved external forces. These forces are fed into the controller while lowering the PD gains, allowing the passive dynamics to take over during impacts. When the perturbation disappears, they smoothly return to the captured data. As strong perturbations may lead to an unbalanced motion, they integrate a balance controller that drives the center of mass of the character to ensure its balance.

To increase the balance control of standing characters subject to external perturbations, Macchietto et al. [Macchietto 09] proposed to drive in real-time the center of mass and the center of pressure of the character by controlling the linear and angular momentum (Figure I.11). Their method tracks a reference motion while an optimization routine ensures wanted linear and angular momentums.

To allow re-planning of long-term goals, Ye and Liu [Ye 10] presented a controller tracking a reference motion while generating dynamically consistent full-body motions. They use an abstract model that captures the essential relation between contact forces and momenta. In an offline optimization, they solve an optimal feedback control policy for the abstract model. Then, an online optimization process synthesizes full-body motions with consistent dynamics to the abstract, model while tracking a reference motion.

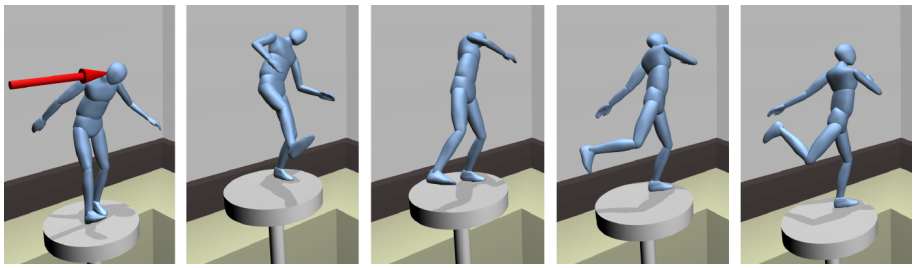

Figure I.11: Character balancing after a external perturbation [Macchietto 09].

Instead of tracking captured motions, another solution consists in using these captured motions in the design of the controllers. Shiratori et al. [Shiratori 09] used a biomechanical study which presents that two main strategies exist for trip recovery responses that may occur during walking. Then, they designed corresponding controllers using biomechanical literature and motion capture data. Thus, when a character trips in the virtual environment, the trip recovery controller is activated to produce a natural recovery response, as a real human would do. Coupling biomechanical knowledge and captured motions is good solution to avoid unnatural motions.

However, the design of a new controller is usually a tedious task, requiring to specifically define and design the controller for the specific motion. Sometimes, it is possible to generalize a family of motions into one controller [Wooten 00] or to combine different controllers together [Faloutsos 01a, Faloutsos 01b]. If dynamic-based controllers synthesize dynamically correct motions, the resulting motion are not always natural. Thus, a controller can generate dynamically correct motions still not generate the motion that a human would have performed in the same situation.

I.4.3 Spacetime constraints

The design of a new controller is usually a long task, needing to study the desired motion and extract its main characteristics. Furthermore, results are not always natural even if satisfying physical

laws. To increase the naturalness of generated motions, Witkin and Kass [Witkin 88] introduced *space-time constraints* to compute the trajectories of the motion for the whole sequence instead of computing poses sequentially in time. The discrete values of forces, velocities and positions over time are set in a very large vector of unknowns while a set of constraints between these unknowns is specified. These constraints include initial, final and intermediary targets, velocities or accelerations, force and torque limitations, models of contacts with the ground and physical constraints.

The whole process consists in computing the best sequence $q(t)$ minimizing an objective function h, while satisfying the user defined constraints X:

$$\min_q h(q, \dot{q}, \ddot{q}) \qquad \text{under} \qquad f(q) = X \tag{I.20}$$

However, the choice of the cost function is a key issue to obtain natural motions. It is often set to the sum of squared muscular forces over time, which makes the optimization process look for the sequence that spends as little energy as possible given the user-defined constraints. For instance, Liu and Cohen [Liu 94] proposed to minimize the squared sum of the joint torques τ_i, using the following function:

$$h(q, \dot{q}, \ddot{q}) = \int_{t=t_0}^{t_f} \Big(\sum_{i=1}^{n} \tau_i^2(q, \dot{q}, \ddot{q}, t) \Big) dt \tag{I.21}$$

while proposing a method based on the optimization of this function in order to synthesize virtual human diving. However, this objective function requires the computation of joint torques. This process, called Inverse Dynamics, is computation costly, even for simple motions.

Different works focus on decreasing the complexity of the optimization process [Liu 02, Fang 03, Safonova 04]. Liu and Popović [Liu 02] defined objective functions controlling linear and angular momentums while minimizing mass displacement and velocity to generate realistic highly dynamic motions (Figure I.12). However, this technique only worked with highly dynamic motions and is unable to handle the synthesis of walking or reaching motions for example. Fang and Pollard [Fang 03] represented joint trajectories with parametric curves and partially analytically solved the optimization equation by reformulating different dynamic constraints (Equation I.20). However, if this improvement avoids the computation of joint torques, it still requires high computation time.

As human joint motions are usually correlated, such as legs and arm tending to move in a similar pattern during locomotion, Safonova et al. [Safonova 04] used Principal Component Analysis (PCA) to reduce the dimensionality of the optimization process. By using PCA, they extracted the main dynamic characteristics of a set of motions. Then, they ran the optimization process in this extracted low-dimension and managed to produce high and low dynamic motions, close to samples from given data sets.

Unlike highly dynamic motions, low-energy motions such as locomotion are more difficult to generate by optimization, as it requires a much more detailed model of dynamics and style. Liu et al. [Liu 05] presented a dynamic model incorporating several factors of locomotion, derived from the biomechanical literature. This model includes muscles relative preferences, joint elastic mechanisms, joint stiffness, etc. When fed in an optimization process, this model addresses a wide range of styles of natural human movement. However, the hand-designed of these parameters is extremely difficult due to the complexity of biological motion. Thus, they propose a nonlinear inverse optimization process to automatically estimate these dynamic-based parameters from motion capture data. Once estimated, these parameters can be used to generate motions in the same style but performing different tasks.

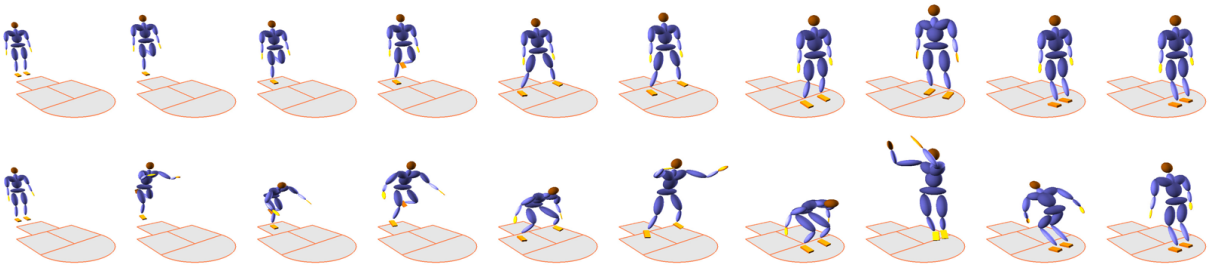

Figure I.12: Optimization result example from [Liu 02]. Top: simple input sketch. Bottom: synthesized animation.

However, *spacetime constraints* suffer from several limitations. Firstly, the complexity of the problem and the large number of unknown usually leads to high computation time, which limits the length of the animation sequences, even if some works focus on the decrease of the complexity [Cohen 92, Liu 02, Fang 03, Safonova 04]. Secondly, the process iterates over the whole sequence, which implies to define all the constraints a priori. Thirdly, as constraints are often nonlinear, especially when dealing with dynamics, users are not guaranteed that the optimization will converge towards an acceptable solution. Since the process finds a solution while ensuring all constraints as much as possible, dynamic laws, which are treated as constraints, may not be entirely satisfied when iterations stop.

As for controllers, designing the optimization process is usually specific to a given task. Even if the results are almost dynamically correct, they still may appear unnatural: the computed motions may not be the ones performed by a real human in the same situation. Actually, the naturalness highly depends on the chosen cost function h, which design is still highly debated (minimizing torques, jerk, etc), and the specified constraints X (ensuring balance, center of mass trajectories, etc). Furthermore, dynamic equations of human motions are highly nonlinear, leading to huge computation time and uncertainties to converge to a desired solution. Optimization is also highly sensitive to the initial state of the process.

I.4.4 Dynamics using databases of motions

Dynamic controllers and spacetime constraints allow the creation of dynamically correct motions. However, resulting motions may suffer from a lack of naturalness. On the contrary, using a set of real motions stored in databases may produce natural looking motions, which may not be always dynamically correct. A solution consists in coupling dynamic simulation with databases of motion capture data.

Using captured motions stored in databases, it is possible to keep the naturalness of the original motions while satisfying as much as possible the different physical constraints. As the different motions present in the databases are intrinsically valid from the mechanical point of view, as they were performed by a real actor, a promising approach consists in being able to compute physically valid transitions between several clips in order to react to external perturbations [Zordan 05, Komura 05, Arikan 05]. These approaches usually simulate an immediate reaction, depending on the intensity of the external perturbations, before interpolating towards a response motion belonging to the database.

Zordan et al. [Zordan 05] proposed a complete system which selects a reasonable clip from a motion capture database for soon after the interaction (the green clip in Figure I.13.a) and simulated the new

motion (shown red in Figure I.13.a) that allows the character to respond to the physical conditions and prepare for its newly determined, upcoming animation.

In the same vein, Arikan et al. [Arikan 05] built a model of natural looking transitions from external perturbations. Using a database of reactions to perturbations, they synthesize reactions to pushes by restoring balance without falling down (Figure I.13.b). As it is not possible to record perturbations from every direction and magnitude, they proposed a response motion deformation method based on an Oracle. Their Oracle is trained by showing users a large set of synthesized reactions. Users labeled the quality of the synthesized reaction and the Oracle updated his predictor model until users mostly agreed with the propositions. Then, during the simulation, the Oracle is able to synthesize automatically a correct reaction to perturbations.

Previous approaches rely on the size of the database to produce natural responses. On the contrary, Komura et al. [Komura 05] focused on reactions using small amount of data. When an external perturbation is applied to the character, it is transformed to an increase in the linear momentum and angular momentum around the center of mass. At the same time, a counteracting motion is searched in the database to be blended into the primary motion. When searching for the counteracting motion, they mainly focus on the moment of inertia of the whole body and the status of the feet. Since it is usually not possible to pre-capture all potential reactive motions, they edit the selected reactive motion using a momentum-based inverse kinematics method: both the momentum and the footsteps are adjusted to deal with impacts of various strengths (Figure I.13.c).

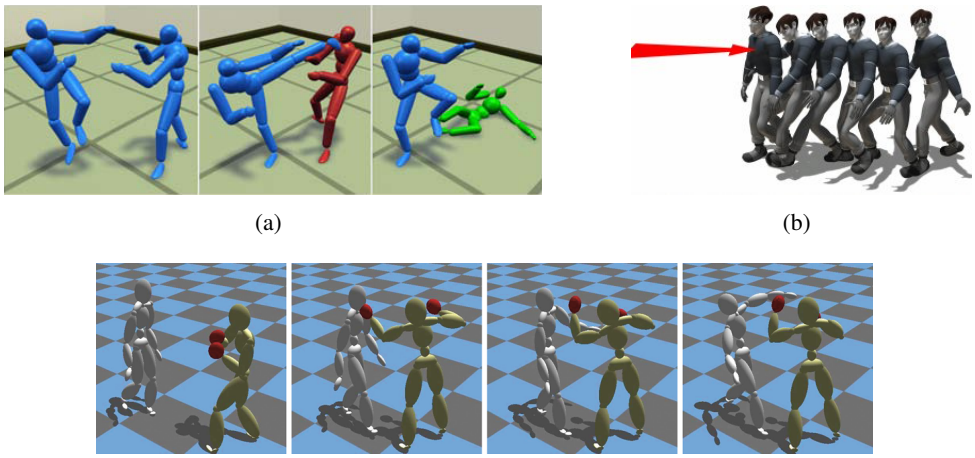

(a) (b)

(c)

Figure I.13: a) Fall [Zordan 05] and b) recovery [Arikan 05] reactions to external perturbations. Reaction to external perturbations using a small database [Komura 05].

Mitake et al [Mitake 09] also worked on reactions to perturbation. They created a Multidimensional Keyframe Set mapping *(Travel distance D, Tilt θ, Behavior B)* to frames of the set. They model the dynamics of their virtual characters with an inverted pendulum and a single rigid body inertia model. When a perturbation occurs, they compute a correct tilt θ of the single rigid body and generate the resulting motion by finding the corresponding reaction in the Multidimensional Keyframe Set. Using this Multidimensional Keyframe Set, they managed to handle recoveries and falls after external perturbations.

However, taking dynamics into account in virtual human motion is not limited to realistic responses to external perturbations. Dynamics is also necessary to ensure the naturalness of sequences combined together to perform a new motion. For the special case of aerial motions, Majkowska et al. [Majkowska 07] presented a dynamic based motion editing technique. By sequencing aerial motions in take-off T_i, aerial A_j and landing L_k clips, they generate new aerials motion by combining different clips, such as a new aerial motion composed as $T_0A_0A_1A_0A_1L_0$. As linear and angular momentum are highly regulated through aerial phases, they carefully select motion clips with a similar angular momentum direction. Then, they retimed motion clips to ensure a constant angular momentum during aerial phases. Through a user perceptual study, they demonstrated that there method is efficient to dynamically correct motions without perturbing the visual perception.

All these methods depend on motion databases to find the best motions that will lead to a dynamically-valid response to external perturbations. Hence, the naturalness of the animation highly depends on the quality and quantity of motions stored in the database. In the same way, computation time depends on the size of the database: too many motions could dramatically increase the search time, which may forbid a real time application, while too small databases will produce unnatural sequences to be compatible with real-time applications

Furthermore, the variety of human motion makes it impossible to store all different reactions to external perturbations. In the case of reactions to pushes, this is even more visible as perturbations can be applied with different locations, directions and intensities. Thus, it is not possible to create a complete reaction database. Moreover, as motions depend on the morphology of the character (a new morphology modifies the different segment masses, inertias and lengths) the change of morphology of the virtual character should also be taken into account during this process, which is not the case. As is it not possible to create an exhaustive database of human motion reactions, another technique to obtain dynamically correct sequences consists in dynamically adapting a unique motion.

I.4.5 Dynamic adaptation

Most of the previous approaches are able to produce dynamically correct sequences but require high computation time or huge databases of captured motions. To solve this problem, it is possible to dynamically correct sequences only when necessary. A common solution consists in filtering the motion to take a set of dynamic constraints into account. Each pose is thus corrected depending on the original pose $q(t)$, a set of original poses $q(t \pm i\Delta t)$ around the current one and previous corrected poses $q_f(t - j\Delta t)$:

$$q_f(t) = filt(q(t), q(t \pm i\Delta t), q_f(t - j\Delta t)) \tag{I.22}$$

where $filt$ is a filtering function and i and j represent pose windows.

A common dynamic constraint to ensure dynamic balance is that the Zero Moment Point (ZMP) remains in the base of support during all contact phases. Tak et al. [Tak 00] presented an offline filter correcting only the sequences where ZMP goes outside the base of support. To ensure dynamic balance, they compute a correct desired ZMP trajectory, always remaining in the base of support. Then, an optimization process corrects unbalanced sequences by minimizing the distance between the actual and the correct ZMP while satisfying a set of constraints. For instance, a limbo walk can be originated from a normal walk by constraining the head below the limbo bar (Figure I.14).

Shin et al. [Shin 03] extended the method by proposing an analytical solution to the ZMP correction. Contact phases are corrected by analytically computing the additional rotation ensuring that ZMP

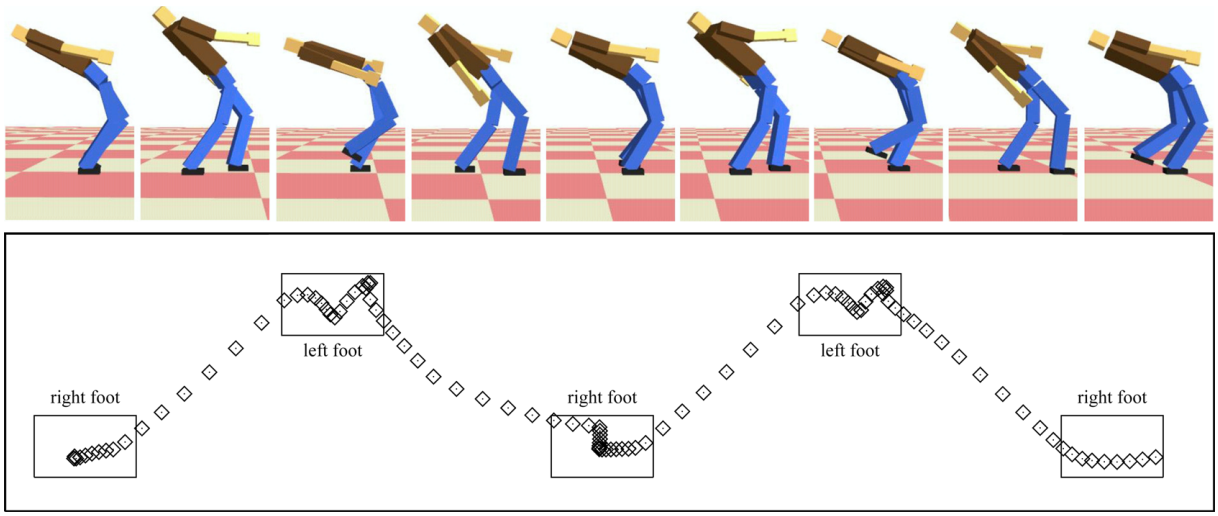

Figure I.14: Corrected ZMP trajectory of a limbo walking [Tak 00].

remains in the base of support, while aerial phases are analytically corrected to ensure a constant angular momentum and a parabolic trajectory of the center of mass. These adjustments are stored in a displacement map, which is filtered before being applied to the original motion.

However, applications where the environment may change at any time, due to user actions or events in the environment, require specific approaches. In these kind of applications, a common technique consists in adapting the motion on the fly to satisfy the new dynamic constraints.

A recent approach, called dynamic filters, consists in filtering motions using frame-based approaches [Yamane 00, Yamane 03, Pollard 01, Tak 05]. Given previous pose(s) $q(t)$, the dynamic filter uses a physical model to predict the next dynamically correct pose $\hat{q}(t + \Delta t)$. Then, this prediction if corrected using the original motion to produce a correct pose $q(t + \Delta t)$ (Figure I.15). This technique makes the assumption that both the current pose $q(t)$ and the original motion are dynamically correct.

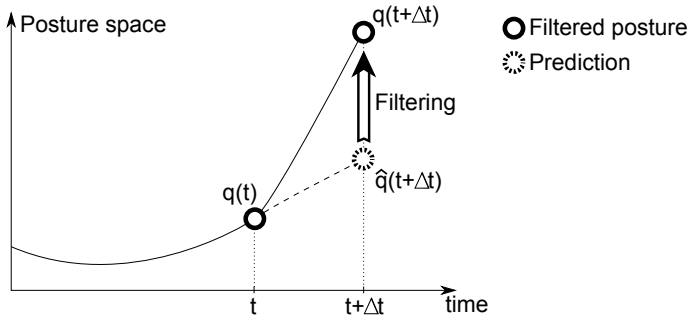

Figure I.15: Dynamic filtering evolution of pose $q(t)$.

However, even if dynamic filters allow real time dynamic corrections, results highly depend on the simplified model chosen to predict the next pose. This choice influences both dynamic correctness

and computation load. Yamane et Nakamura [Yamane 00] presented a model that is simply based on preserving accelerations to prevent dynamically unfeasible accelerations. However, this model can be more complex to increase dynamic correctness. For instance, Pollard and Reitsma [Pollard 01] presented a dynamic filter based on a friction model of contacts between the character and the environment. Their filter discards impossible forces and torques and enforces foot contact with the ground, while allowing the foot to pivot or slide when needed.

Tak. et al [Tak 02, Tak 05] proposed a unified formulation of constraints (constraints on positions, balance, torques or momentums) to handle both kinematics and dynamic corrections and filtered the original motion to satisfy these constraints. However, kinematic constraints depend on positions while dynamic ones depend on velocities and accelerations. They applied Kalman filtering to their problem while considering positions, velocities and accelerations as independent degrees of freedom. Then, they ensure coherence between positions, velocities and accelerations with a least-squares fitting technique. This two-step process (Kalman filtering and least-squares fitting) is applied until convergence.

Although a simple filter is highly generic and computationally efficient, it may however be limited in the dynamic correctness of the produced motions. On the contrary, using a specific predictor increases the dynamic correctness while usually increasing at the same time the computation load. Furthermore, the latter is usually specific to a family of motions and has to be reconfigured for each new application. Finally, a lot of parameters should usually be tuned to obtain natural results.

Provisional conclusion

Thus, different methods have been presented in the literature to handle dynamics in virtual human motions. A first possibility consists in generating motions from high level parameters, such as in the case of controllers. However, it is necessary to design one controller per different task and thus to study the specific motion.

To prevent the tedious design of controllers and increase the naturalness of resulting motions, another approach consist in defining whole joint trajectories thanks to an optimization process. Joint trajectories of a whole motions are then computed while ensuring different kinematic and dynamic constraints. However, this approach is usually highly computational costly.

Thus, approaches using databases of captured motions have been introduced to handle natural reactions to dynamic constraints. If this approach is well suited for reactions to instantaneous perturbations, results however highly depend on the size and the quality of the database of captured motions.

One last approach to handle dynamics consists in correcting a unique motion when mechanical laws are violated. Dynamic filters use a mechanical model to predict dynamically correct poses, but results and computation time highly depend on the quality of the model. An alternative to dynamic filters consist in defining analytical correction methods.

I.5 Conclusion: framework and objectives

As human motion is highly driven by dynamics, taking dynamic equations into account is a key-point towards credible and natural virtual humans. In the last few years, many approaches have been proposed to produce dynamic-based virtual motions. Virtual characters are now more and more capable of expressing natural behaviors.

Many dynamic-based approaches have been proposed in the literature in the past years and it is a very active field of research that will certainly continue in the near future. Most of the last contributions in computer animation are based on designing more and more sophisticated dynamic controllers, especially

for locomotion. Controllers are more and more efficient and robust to produce dynamic-based balanced walking. Controlled characters can perform various walks (forward, backward, side-steps, etc) with different skeleton structures (humanoid, animal, skeleton asymmetries, etc) while keeping balance when subject to perturbations or performing tasks in complex environments (stairs, slippery floor, uphills, downhills, etc). Most of these approaches try to design controllers without using motion capture data. However, in our opinion, most of the results lack of the naturalness of subtle human behavior, which is a key point to produce credible human motions.

On the contrary, motion capture data retails all the subtle details of the actor's motion but requires modifications in order to satisfy the specific constraints of the simulation. Different approaches based on these captured motions also exist in the literature. Approaches depending on databases of captured motions are well fitted to handle reactions to short unpredictable perturbations. However, the naturalness of the results highly depend on the size and quality of the database. Other techniques adapt existing motions to satisfy new dynamic and kinematic constraints, but usually require to tune many parameters specific to a given motion to produce natural motions, especially in interactive applications. These methods may also introduce artifacts when adapting the motion to new constraints.

In this PhD, we focus on the dynamic adaptation of motions subject to continuous external perturbations. One of our most important problem consists in correcting these motions in real-time to deal with interactive applications, while ensuring the naturalness of the resulting motion. Thus, we worked on the adaptation of captured motions to satisfy new dynamic constraints that were not present in the original motion. Our approach lies in the category of *Dynamic adaptation* techniques.

If it is clear that dynamics plays an important role in the naturalness of produced virtual motions, it is still not straightforward to take it into account to produce natural motions. Different hypothesis are often required to dynamically control these motions, such as driving the center of pressure position or ensuring zero angular momentum (to prevent rotation instabilities) during walking. However, as for Inverse Kinematics, an infinite number of solutions might be available to satisfy the given dynamic constraints, while only a subset of these solutions will look natural. Thus, simulating natural motions requires to understand how human motion dynamically behave. This is in particular important to understand how virtual humans should behave under various conditions (perturbations, displacements, interactions with virtual environments, etc) and necessary to obtain virtual characters naturally keeping balance while performing complex tasks. Depending on these dynamic properties, a real human will try to perform actions as comfortably as possible to prevent tiredness, injuries or optimize a given task. Understanding how human actions are related with dynamic parameters will enable us to increase the credibility of virtual humans. Thus, it is necessary to define metrics that will measure and give information about the dynamic correctness of motions.

However, only few works focus on the users' perception of these dynamic properties to evaluate the naturalness of motions. Most of the approaches produce dynamic-based motions without evaluating how users perceive the various dynamic properties. In this PhD, we think that it is necessary to study dynamics to understand how it naturally behaves in human motion, but we also think that it is necessary to study how these dynamic parameters are perceived by users. It could, for instance, help to choose the relevant dynamic parameters of a simulation based on the parameters perceived by external users or save computation time by taking dynamics into account only when it would be perceivable. It is also necessary to evaluate the naturalness of motions produced with dynamic-based techniques.

In this PhD, we focus on the dynamics of virtual humans in order to produce natural adaptations when virtual characters are subject to continuous external perturbations. For instance, this problem can be applied to simulate strong interactions of virtual humans with their environments (such as carrying objects). Hence, we propose a real-time method for dynamic adaptation of virtual motions. Our method is based on two studies: a study on dynamic mechanisms in human motions and a study on users' perception of dynamic properties.

Thus, the next Chapter presents an experiment on human dynamic balance. It studies different criteria presented in the literature to measure human balance and studies the main advantages and limitations of a set of these criteria. The goal is to propose a possible optimum range of utilization depending on the level of dynamics in the studied motions.

Chapter II

Modeling dynamic balance in biological motions

As shown in the previous Chapter, dynamic balance is a key point to enhance the naturalness of virtual human motions. Several fields are interested in understanding and measuring dynamic balance of humanoids. However, a challenging question is to define a relevant criterion to model the balanced/unbalanced state of a character.

This Chapter focuses on studying various criteria proposed in the literature to measure the unbalanced states of characters. The goal is to define to which extend these criteria are able to predict a loss in balance in static and dynamic situations.

II.1 Background

To ensure the dynamic correctness of virtual characters' motions, it is important to satisfy dynamic equations (Section I.4.1) at any time. It requires to define relevant criteria to model the dynamic state of the character. Depending on the level of dynamics, motions can be classified in different categories:

- quasi-static : slow motions with negligible accelerations,
- low dynamic : slow motions with non-negligible accelerations,
- high dynamic : motions with high accelerations.

Depending on these categories, different criteria have been presented in the literature. However, human balance is linked with the surfaces of contact of the character with his environment.

II.1.1 Base of support

One of the main problem with human balance is that humans have small contact surfaces with their environment compared to their global body surface where perturbations can occur. Thus, maintaining balance is highly linked to these contact surfaces, also called base of support (BoS).

On a flat floor, the base of support corresponds to the convex hull of the contact surfaces with the floor. In computer animation, it is usually approximated using a polygon. For instance, Figure II.1 presents the supporting polygon (red) when both foot are on the ground.

Figure II.1: Base of support (red) for a double support stance.

II.1.2 Quasi-static balance: projection of the center of mass

In order to ensure the balance status of a virtual character, the simplest criterion is based on the projection of the center of mass on the ground (Ground Center Of Mass – GCOM). Several authors demonstrated that this criterion is sufficient to analyze balance of human beings in quasi-static situations [Dyson 77, Winter 95]. Under the quasi-static assumption, Equation I.15 is rewritten as:

$$\begin{cases} \mathbf{P} + \mathbf{GRF} + \sum \mathbf{F}_i & = & \mathbf{0} \\ \mathbf{OG} \times \mathbf{P} + \mathbf{OCoP} \times \mathbf{GRF} + \sum \mathbf{OA}_i \times \mathbf{F}_i & = & \mathbf{0} \end{cases} \tag{II.1}$$

If no additional external forces are applied to the character ($\sum \mathbf{F}_i = \mathbf{0}$), we obtain $\mathbf{GRF} = -\mathbf{P}$. The momentum part of expression II.1 expressed in G becomes:

$$\mathbf{GCoP} \times \mathbf{GRF} = \mathbf{0} \tag{II.2}$$

which is possible only if $\mathbf{GRF} = \mathbf{0}$ (meaning no gravity or a zero mass m) or if **GCoP** and **GRF** are collinear. As $\mathbf{GRF} = -\mathbf{P}$ is directed upwards under a normal gravity, CoP is thus the projection of G. As the CoP belongs to the base of support (BoS), by definition (see Section II.1.4.1), *GCOM* has to lie in the base of support to achieve quasi-static balance.

This criterion is widely used in biomechanics and neurosciences to analyze the balance status of normal and pathological subjects according to standardized protocols. To this end, it has also been widely used to adapt the pose of a character.

Hence, to ensure balance of a character under a quasi-static assumption, it is necessary to control the center of mass of the virtual character. To solve this problem, Boulic et al. [Boulic 96] proposed an extension of Inverse Kinematics, called Inverse Kinetics, that integrates the mass distribution information and drives the position of the center of mass under quasi-static assumptions. Baerlocher et al [Baerlocher 00] also proposed to ensure balance while satisfying given momentums of inertia (Figure II.2). Similarly, Kulpa et al. [Kulpa 05a] proposed a real-time algorithm to ensure the quasi-static balance of a humanoid while also satisfying kinematic constraints. (Figure II.3).

II.1.3 Low dynamic balance

Because of the quasi-static assumption, analyzing only the of GCOM is highly limited. Pai and his group [Pai 97, Iqbal 00] demonstrated that this condition is insufficient in dynamical situations, such as

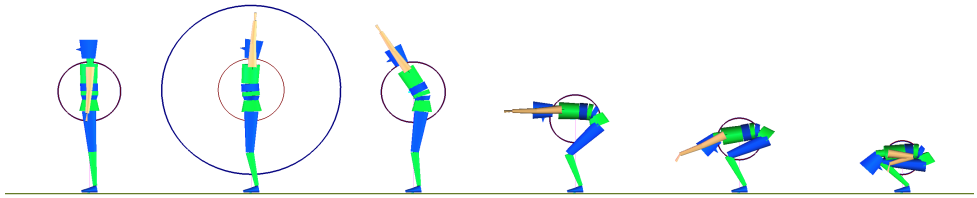

Figure II.2: Lateral view of a simple 2D human figure trying to match prescribed momentums of inertia while keeping balance [Baerlocher 00].

Figure II.3: Adaptation of the pose of a humanoid to satisfy as much as possible kinematic constraints while preserving balance [Kulpa 05a].

low dynamic situations where accelerations are not negligibles. For instance, balance may be impossible to ensure even if the projection of the CoM belongs to the base of support if the CoM velocity is directed outward. The reverse is also possible: even if the CoM projection is outside the base of support, balance may be achieved if the CoM velocity is directed inward.

Based on these assumptions, Hof [Hof 05] proposed to model balance of a humanoid using the Extrapolated Center of Mass (XcoM). It corresponds to an extension of the GCOM that takes velocity into account. Balance is thus defined as maintaining XcoM in the base of support (BoS). Using a simple inverted pendulum model, Equations for dynamic balance are defined as:

$$XcoM = GCOM + \frac{\dot{GCOM}}{\omega_0} \in BoS \qquad \text{with} \qquad \omega_0 = \sqrt{\frac{g}{l}} \tag{II.3}$$

where m and l are respectively the single mass and the stick length of the inverted pendulum model.

However, XcoM models the human as an inverted pendulum, which can be too simple in some situations. Next to the movement of the whole body CoM, which is the only variable in inverted pendulum models, segments can also move with respect to this CoM: accelerations of these segments can give an appreciable contribution to the moment equation [Zatsiorsky 98]. By using these mechanisms, e.g. by bending the hips or by moving the arms, a disbalance with the XcoM outside the BoS can still be restored [Otten 99].

Furthermore, Hof [Hof 05] states that XcoM is valid for both quasi-static and dynamic situations. However, this criterion has only been tested with locomotion and tip-toe walks. Thus, more tests are necessary to validate its relevance in highly dynamic situations (gymnastics, combat sports, sprints, etc).

II.1.4 Highly dynamic motions

In order to deal with highly dynamic motions, it is important to take all dynamic parameters (accelerations and angular momentum) into account. From Equation I.15, forces acting on a humanoid can be separated into two categories: forces exerted by contact or forces transmitted without contact (gravity and inertia forces). Center of Pressure is linked to contact forces while Zero Moment Point is linked to inertia and gravity forces. Let us consider these two variables.

II.1.4.1 Center of Pressure

When considering a system with one segment in contact with the ground, the field of pressure is equivalent to a single resultant force: the Ground Reaction Force. This force is composed of a pressure resultant $\mathbf{R}^p$ (normal to the contact surface) and a friction resultant $\mathbf{R}^f$ (tangential to the contact surface). It is exerted at the point where the resultant momentum of the pressure forces is zero. This point is called the Center of Pressure.

At any point P of the contact surface, the contact force $\mathbf{grf}(P)$ can expressed as:

$$\forall P \in (S), \quad \mathbf{grf}(P) = \mathbf{p}(P) + \mathbf{f}(P) \quad \text{with } \mathbf{p}(P) = k(P).\mathbf{n},\ k(P) \geq 0 \quad \text{and} \quad \mathbf{f}(P) \cdot \mathbf{n} = \mathbf{0} \tag{II.4}$$

where the normal component $\mathbf{p}(P)$ is the local pressure force, the tangential component $\mathbf{f}(P)$ is the local frictional force and $\mathbf{n}$ is a unit vector normal to the contact surface S.

The resultant of these elementary contact forces corresponds to the sum of pressure forces (superscript p) and friction forces (superscript f):

$$\mathbf{GRF} = \int_S \mathbf{grf}(P)dS = \mathbf{R}^p + \mathbf{R}^f, \quad \mathbf{R}^p = K.\mathbf{n},\ K \geq 0 \quad \text{and} \quad \mathbf{R}^f \cdot \mathbf{n} = 0 \tag{II.5}$$

$$\mathbf{R}^p = \int_S \mathbf{p}(P)dS = \Big(\int_S k(P)dS \Big).\mathbf{n} \quad \text{and} \quad \mathbf{R}^f = \int_S \mathbf{f}(P)dS \tag{II.6}$$

Computing the momentum of the **GRF** about any point Q leads to:

$$\mathbf{M}(\mathbf{GRF})_{/Q} = \mathbf{M}(\mathbf{R}^p)_{/Q} + \mathbf{M}(\mathbf{R}^f)_{/Q} \tag{II.7}$$

with:

$$\mathbf{M}(\mathbf{R}^p)_{/Q} = \int_S \mathbf{QP} \times \mathbf{p}(P)dS = \Big(\int_S k(P)\mathbf{QP}dS \Big) \times \mathbf{n} \quad \text{with } \mathbf{M}(\mathbf{R}^p)_{/Q}.\mathbf{n} = 0 \tag{II.8}$$

$$\mathbf{M}(\mathbf{R}^f)_{/Q} = \int_S \mathbf{QP} \times \mathbf{f}(P)dS \quad \text{with } \mathbf{M}(\mathbf{R}^f)_{/Q} \times \mathbf{n} = \mathbf{0} \tag{II.9}$$

Whatever the point Q, the momentum of pressure forces $\mathbf{M}(\mathbf{R}^p)_{/Q}$ is always perpendicular to the normal vector $\mathbf{n}$ (thus tangential to support surface). As the resultant pressure force $\mathbf{R}^p$ is directed along $\mathbf{n}$, an axis Δ^p exists where the momentum $\mathbf{M}(\mathbf{R}^p)_{/Q}$ is null at every point Q of this axis. Hence the CoP is defined as the point at the intersection of Δ^p and the surface S, where $\mathbf{M}(\mathbf{R}^p)_{/CoP} = \mathbf{0}$. Then:

$$\mathbf{M}(\mathbf{GRF})_{/CoP} = \mathbf{M}(\mathbf{R}^f)_{/CoP} \quad \text{and} \quad \mathbf{M}(\mathbf{GRF})_{/CoP} \times \mathbf{n} = \mathbf{0} \tag{II.10}$$

When only one segment is in contact with the ground, the CoP belongs to the contact area of this segment with the ground. If more than one segment are in contact with the same ground surface (for instance two foot on a plane floor), the CoP belongs to the convex hull of the contact surfaces (Figure II.1).

In Biomecanics, CoP is commonly used to estimate the balance status of a subject. For instance, Hof [Hof 05] presented three mechanisms used by humans to keep their balance, using the CoP location. First, humans move their center of pressure inside the base of support to compensate small perturbations. However, it quickly reaches the limit of the base of support. Thus, humans switch to a second strategy to compensate these perturbations: they use counter rotation of segments around the center of mass to restore balance, such has swinging the arms. Then, the last strategy consists in applying external forces (such as holding a bar, handrail, wall, etc) or making a step to enlarge the base of support. These strategies are presented in Figure II.4.

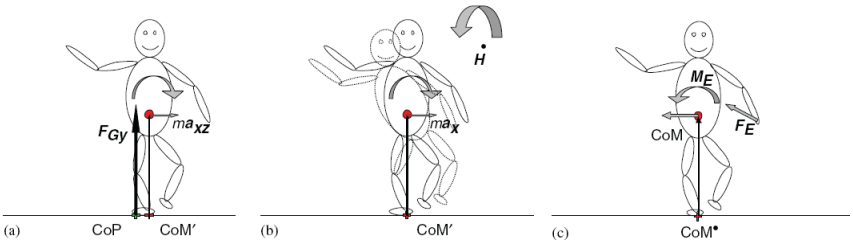

Figure II.4: Illustration of the three mechanisms for balance: a) moving the CoP, b) rotating around the COM, c) applying an external force [Hof 05].

As a forceplate is required to measure the CoP, we usually do not have access to its trajectory in computer animation. For most of captured motions, capturing the CoP trajectory would require to equip a large capture area with forceplaces, which is not possible. To by-pass this problem, the Zero Moment Point (ZMP) is usually computed to obtain the trajectory of the CoP.

II.1.4.2 Zero Moment Point

As presented before, CoP is linked to forces exerted by contact. Respectively, ZMP is linked to forces transmitted without contact (accelerations and inertia). The ZMP concept was first introduced and developed in [Vukobratovic 69, Vukobratovic 90]. It has been exhaustively reviewed and formally related to the CoP in [Goswami 99, Sardain 04, Popovic 05].

By definition, ZMP is the point on the ground where the tipping moment acting on the character, due to gravity and inertia forces, equals zero. The tipping moment is defined as the component of the moment that is tangential to the supporting surface. The resultant force $\mathbf{R}^{g_i}$ of inertia and accelerations and its momentum around any point Q are expressed as:

$$\mathbf{R}^{g_i} = m\mathbf{g} - m\mathbf{a}_G \tag{II.11}$$

$$\mathbf{M}_Q^{g_i} = \mathbf{QG} \times m\mathbf{g} - \mathbf{QG} \times m\mathbf{a}_G - \dot{\mathbf{H}}_G \tag{II.12}$$

where m is the global mass, $\mathbf{g}$ is the acceleration of the gravity, G is the center of mass of the system, $\mathbf{a}_G$ is the acceleration of G and $\dot{\mathbf{H}}_G$ is the derivative of the angular momentum about G.

As defined before, ZMP is the point on the ground where the tipping moment is null. Then, Equation II.12 can be expressed for the point ZMP as:

$$\mathbf{M}_{ZMP}^{g_i} = \mathbf{ZMPG} \times m\mathbf{g} - \mathbf{ZMPG} \times m\mathbf{a}_G - \dot{\mathbf{H}}_G \quad \text{with} \quad \mathbf{M}_{ZMP}^{g_i} \times \mathbf{n} = \mathbf{0} \tag{II.13}$$

It is important to notice that $\mathbf{M}^{g_i}_{ZMP}.\mathbf{n}$ might not be equal to zero. The demonstration for the equivalence of CoP and ZMP definitions is reminded in Appendix A, Section A.2.

In computer animation, simulating virtual humans requires to define simplified models of the character. Depending on computation time or on level of simulated details, different models are commonly used in the literature. However, three main models are predominant [Kajita 09]:

- Inverted pendulum: the virtual human is represented as a particle of mass m located at its center of mass (Figure II.5.a).
- System of particles: the virtual human is represented as a set of particles. Each segment i of the virtual human body is represented by a particle of mass m_i located at the center of mass of the segment (Figure II.5.b).
- Articulated rigid body: the virtual human is represented as a set of rigid segments. Each segment i of the virtual human body is represented by an object with a mass m_i, a center of mass G_i and an inertia matrix I_i. Cylinders are commonly used to represent segments (Figure II.5.c).

ZMP Equations for these three models are reminded in Appendix A, Section A.1.

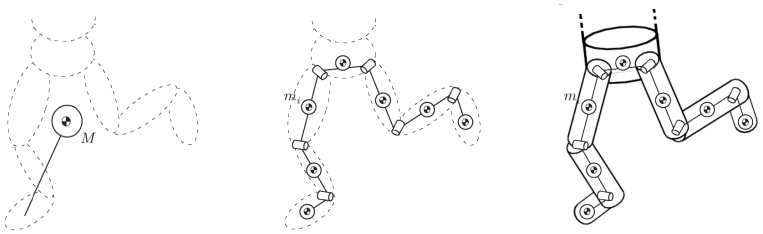

(a) Pendulum model (b) System of particles model (c) Articulated rigid body model

Figure II.5: Three main models commonly used in the literature. The virtual human is represented as a) a particle of mass m located at the center of mass of the character (pendulum model), b) a set of particles (system of particles model) or c) a set of rigid segments (articulated rigid body model). Only the lower body is represented by simplicity.

II.1.4.3 CoP and ZMP limitations

One important limitation of ZMP computation (and CoP definition) is that it is only valid if all the contacts are on the same plane surface [Sardain 04, Hirukawa 06]. If it is not the case, one momentum exists per contact area, each momentum directed along the normal of the corresponding surface. Then, CoP does not necessarily lie on the contact surfaces, and the momentum at the center of pressure is not necessarily null on two axes. However, different works focus on adapting ZMP equations to other contact surfaces [Takenaka 94, Sardain 04].

To replace the ZMP, Hirukawa et al. [Hirukawa 06] proposed to use the polyhedral convex cone of the contact wrench. They show that the humanoid robot is stable if the sum of the gravity and inertia wrench applied to the COM are inside this polyhedral convex cone, corresponding to a sufficient friction to ensure the balance of the robot. They showed that this criterion is equivalent to the ZMP in the case of a flat floor, but it is also more universal as it can handle complex floors (contrary to the ZMP).

Vukobratovic [Vukobratović 04] gave a special review of the ZMP definition, reminding that when the ZMP exists it is always coincident with the CoP. However, in some unstable cases where a robot is turning around the edge of its foot, the momentum at the CoP is not null along the axes tangential to the surface. Then, even if the CoP belongs to the base of support (as by definition it cannot exist elsewhere), there is no point on the contact surface where the momentum is null on both axes tangential to the surface. Nevertheless this case does not happen for real human locomotion, due to the structure and shape of the foot, and is specific to humanoid robots with a rigid sole.

ZMP and CoP are widely used in many domains, including Biomechanics, Computer Animation and Robotics. By definition, these points are restricted to be in the base of support. Then, computing a ZMP or CoP outside the base of support implies that either the motion is dynamically incorrect or that terms were neglected in Equations I.15, such as external torques. Furthermore, ZMP equations make the assumption that the momentum of the GRF at the ZMP position is null on both axes tangential to the surface. However, this assumption does not hold if the humanoid is rotating around one edge of the foot for instance.

II.1.4.4 Foot Rotation Indicator (FRI)

As CoP is required to stay inside the base of support, it is not fitted to measure the balance of a humanoid. To solve this problem, Goswami [Goswami 99] presented the Foot Rotation Indicator. This point measures the foot rotation of a humanoid: "foot rotation is an indication of postural instability and should be carefully treated in dynamically stable motions and avoided altogether in statically stable ones" [Goswami 99]. He used this point to characterize postural instability of the gait during single support phases of the locomotion.

FRI corresponds to "the point on the ground where the net ground reaction force would have to act to keep the foot stationary". To ensure no foot rotation, it must remain within the convex hull of the foot support area. FRI coincides with ZMP when the foot is stationary and differs when non-zero rotational foot accelerations occur. Thus, FRI can be considered as an indicator of the severity of the foot rotational acceleration.

The dynamic equilibrium Equation of the foot can be expressed as:

$$\mathbf{OG_{foot}} \times \mathbf{P_{foot}} + \mathbf{OCoP} \times \mathbf{GRF} + \mathbf{OA_{ankle}} \times \mathbf{F_{ankle}} + \tau_{\mathbf{ankle}} = \dot{\mathbf{H}}_{\mathbf{foot}/O} \tag{II.14}$$

where G_{foot} is the center of mass of the foot, $\mathbf{P_{foot}}$ is the weight force of the foot applied at G_{foot}, A_{ankle} is the position of the joint linking the foot with the shinbone, $\mathbf{F_{ankle}}$ and $\tau_{\mathbf{ankle}}$ are the force and the torque applied by the rest of the body on the foot, and $\dot{\mathbf{H}}_{\mathbf{foot}/O}$ is the derivative of the angular momentum of the foot expressed at the point O. These points are represented in Figure II.6.

Assuming the existence of a point FRI where the momentum of the **GRF** equals $\dot{\mathbf{H}}_{\mathbf{foot}/FRI}$ on the axes tangential to the contact surface, FRI thus corresponds to the point where the GRF should act to prevent the foot for rotating. It is expressed as:

$$\left(\mathbf{FRICoP} \times \mathbf{GRF} = \dot{\mathbf{H}}_{\mathbf{foot}/FRI}\right)_{\perp \mathbf{n}} \tag{II.15}$$

Then, Equation II.14 can then be rewritten on the same axes as:

$$\left(\mathbf{FRIG_{foot}} \times \mathbf{P_{foot}} + \mathbf{FRIA_{ankle}} \times \mathbf{F_{ankle}} + \tau_{\mathbf{ankle}} = 0\right)_{\perp \mathbf{n}} \tag{II.16}$$

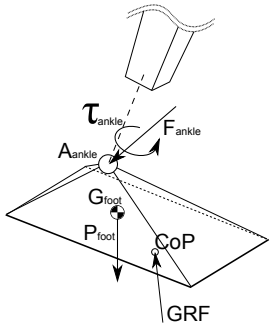

Figure II.6: Sketch of a 3D foot with the different forces and torques applied to the foot, and the forces locations.

Equations II.15 and II.16 are two equivalent physical expressions of the FRI point. If the foot is at rest, then $\dot{\mathbf{H}}_{\mathbf{foot}/FRI} = \mathbf{0}$. From Equation II.15 the only possibility is that FRI is equals to CoP (as GRF is not null on the axis normal to the surface). If $\dot{\mathbf{H}}_{\mathbf{foot}/FRI} \neq 0$, Equations II.15 implies that FRI differs from the CoP location. Equations for FRI computation are reminded in Appendix B.

Goswami [Goswami 99] argued that the distance between the FRI point and the ZMP is useful because it provides us with information about foot rotational dynamics during the single support phase (excluding foot rotations about the vertical axis). However, Popovic et al. [Popovic 05] showed that the difference between the position of ZMP and FRI is not significant in human locomotion (only a few millimeters). Clearly, during the foot-flat phase, one should not expect a large distance between FRI and ZMP because the stance foot does not rotate. However, during the heel-off or powered plantar flexion phase, the foot rolls and undergoes acceleration, and one would therefore expect a more significant FRI–ZMP difference. Thus, they conclude that FRI is not relevant to measure foot rotational accelerations.

To overcome this problem, Popovic et al. [Popovic 05] proposed a modified version, called MFRI, where the momentum due to the foot is used instead of the momentum due to the **GRF** (the MFRI-CoP separation scales much better than the FRI-CoP simply because $\mathbf{GRF} >> \mathbf{P}_{\mathbf{foot}}$):

$$\mathbf{FRICoP} \times \mathbf{P}_{\mathbf{foot}} = \dot{\mathbf{H}}_{\mathbf{foot}/FRI} \tag{II.17}$$

To demonstrate the advantage of MFRI over FRI, they showed the MFRI–ZMP separation distance is higher than those the FRI–ZMP. At the peak foot acceleration of the powered plantar flexion phase of single support of human locomotion, this separation is about 20cm for MFRI–ZMP while about 1cm for FRI–ZMP. Thus, MFRI is more relevant to detect rotational instabilities than FRI.

However, an important limitation of MFRI and FRI is that they are limited to single support phases. Even if most instabilities occur during the single support phase (in locomotion for instance), it is still difficult to extend this criterion for dynamic balance during random tasks. Furthermore, although foot rotation might be an important indicator of a loss of overall postural balance, a lack of foot rotational equilibrium is clearly not always related to overall postural instabilities. For instance, different simple situations exist where the stance foot is rolling but postural stability is perfectly satisfied. In fact, during a large portion of the human gait cycle, the stance foot is not in perfect rotational equilibrium even during the single support phase [Rose 94].

II.1.4.5 Zero Rate of Angular Momentum (ZRAM)

To overcome the limitations of FRI, Goswani et al. [Goswami 04] proposed to evaluate rotational balance through the regulation of angular momentum. To measure this rotational balance, they presented the Zero Rate of Angular Momentum (ZRAM) point. They state that a humanoid robot is stable if the external forces and momentums sum up to a zero centroidal momentum, i.e. $\dot{\mathbf{H}}_G = \mathbf{0}$. Thus, ZRAM corresponds to "the point where the **GRF** would have to act to produce a Zero Rate of Angular Momentum $\dot{\mathbf{H}}_G$". Different authors presented the same criterion under a different name: the Zero Spin Moment of Pressure [Popovic 04] or Centroidal Moment Pivot [Popovic 05].

When no additional external forces are applied on the humanoid, dynamic equations are equivalent to:

$$\mathbf{GCoP} \times \mathbf{GRF} = \dot{\mathbf{H}}_G$$

If **GRF** is parallel to **GCoP**, then $\dot{\mathbf{H}}_G = \mathbf{0}$, i.e. the humanoid is not subject to rotational instabilities. However, if **GRF** is not parallel to **GCoP**, a centroidal moment $\dot{\mathbf{H}}_G \neq \mathbf{0}$ occurs around the center of mass. Thus, ZRAM is defined as the point on the floor where **GRF** is parallel to **ZRAMG**. Then, the rotational stability of the humanoid is defined by the distance $d = \|\mathbf{CoPZRAM}\|$, with $d = 0$ representing the best stable pose. It also means that if ZRAM is in the base of support but is different from CoP then the pose can be slightly rotationally unstable.

With the ZRAM definition, Goswani [Goswami 04] presented different methods to control the balance of a humanoid robot. He extracted three main strategies consisting in:

1. enlarging the base of support such that it encompasses the ZRAM point,
2. moving G with respect to CoP such that **GRF** passes through G in its new location G',
3. changing the **GRF** direction by means of changing the COM acceleration a to a'.

ZRAM has the advantage of being usable whatever the type of surface (Figure II.7), as $\dot{\mathbf{H}}_G$ remains valid for stability quantification. Moreover, compared with FRI, ZRAM is not defined on the basis of physical foot rotation: it is therefore valid during both single and double support phases. On a flat floor, computing ZRAM corresponds to computing ZMP with the pendulum model.

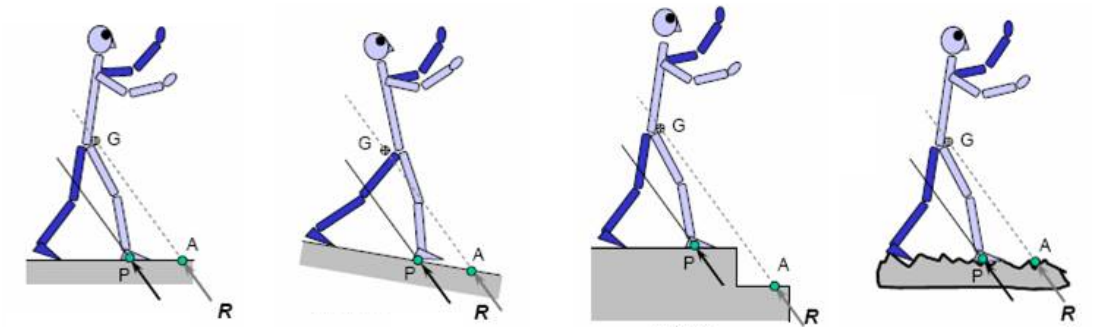

Figure II.7: Representation of the ZRAM (point A) from left to right for: level ground, inclined ground, stairs, uneven ground [Goswami 04]

In relation with the ZRAM concept, other authors in biomechanics studied the behavior of the angular momentum during human walking. If angular momentum is a conserved physical quantity for isolated systems where no external momentums act about the center of mass, there is no reason for this affirmation to hold in the case of human motions interacting with the environment (such as locomotion). However, Herr and Popovic [Herr 04] showed that angular momentum is highly regulated through the locomotion walking cycle, and almost equals to zero.

Then, making the assumption that it is possible to consider a null angular momentum during locomotion, they estimated the GRF and CoP values using this hypothesis and compared it with the corresponding measured values. They found good agreements between captured values and those computed with the null angular momentum hypothesis. Moreover, they showed, for the special case of locomotion, that the centroidal moment pivot (equivalent to ZRAM) never leaves the base of support.

However, their study is only valid for human locomotion staying in specific ranges of velocities and without external perturbations applied to the character. For instance it would not be valid anymore if the character has to suddenly change his speed as it would create a rotational momentum around the center of mass, or if different perturbations occur, such as strong wind or pushes.

Provisional conclusion

This state of the art presented different criteria commonly used in the literature to measure, estimate or simulate the dynamic balance of a person, virtual character or robot. However, each criterion is valid under different assumptions and fitted for a given dynamic level. Based on their different definitions, Table II.1 presents main advantages/drawbacks and proposes a possible range of utilization of each criterion.

Criteria are evaluated using the following parameters:

- Valid for both double and single support phase,
- Computed using rotational angular momentum, i.e. inertias (Appendix C),
- Floor restriction (flat: valid only for flat floor assumptions, all: valid whatever the floor surface),
- Computation time (-: high computation time because of inertias, +: correct computation time, +++: low computation time),
- Position, velocity or acceleration based.

Criterion	bipedal	rotational Ang. Mom.	floor	Computation	Based on	Possible dynamic level range
GCOM	✓	✗	all	+++	positions	quasi-static
XcoM	✓	✗	all	+++	velocities	low dynamics
ZMP pendulum	✓	✗	flat[2]	+++	accelerations	low dynamics
ZMP particles	✓	✗	flat[2]	+	accelerations	high dynamics
ZMP rigid body	✓	✓	flat[2]	-	accelerations	high dynamics
FRI	✗	✓	flat	-	accelerations	low dynamics
ZRAM	✓	✗[1]	all	+++	accelerations	low dynamics

[1] – makes the assumption that $\dot{\mathbf{H}}_G = \mathbf{0}$

[2] – different approaches try to generalize ZMP to non-parallel/flat contact surfaces

Table II.1: Main advantages and drawbacks of criteria for modeling the status of humanoids..

If many criteria have been presented in the literature, few work however focus on comparing the performance of these criteria to model the actual balance status on various type of motions. To our knowledge, the main comparison is the work of Popovic et al. [Popovic 05] which compares ZMP (with an articulated rigid body) to FRI and ZRAM (called Central Moment Pivot in their paper) for the special case of locomotion. They showed that the difference between the position of ZMP and FRI is not significant in human locomotion (only a few millimeters) and that the ZRAM never leaves the ground support base (with a small mean distance between ZRAM and ZMP). However, depending on the type of motions, the different criteria might be more or less efficient to measure/detect unbalanced phases, especially for highly dynamic motions.

II.2 Biomechanical study of various dynamic criteria for human motions

This study aims at evaluating the performance of various criteria to measure the loss of balance of biological motions. We asked subjects to perform motions with various level of dynamics: *Quasi-static*, *Low Dynamics*, *High Dynamics*. A forceplate was carefully synchronized with the motion capture system to capture the CoP trajectory.

Participants had to perform different type of motions. For some motions, they had to try to reach their limits of balance while preventing from loosing balance as much as possible. In this study, we analyze how each criterion behaves when the subject succeeds or fails to maintain balance.

II.2.1 Methods

II.2.1.1 Stimulis and Apparatus

Setup Thirteen naive male participants took part in this experiment (mean age: 22.08 years, SD: 1.54 years; mean weight: 82.92kg, SD: 10.69kg; mean height: 1.83m, SD: 0.07m). All participants were used to practice sports and gave their informed consent prior to the experiment. They were instructed to perform several repetitions of each motion and enough rest was given between each repetition.

Twelve VICON MX40 cameras captured at 150Hz the 3D position of 45 reflecting markers positioned on the user's body (Figure II.8.a and based on [Zatsiorsky 90] for position of markers). Joint centers trajectories were computed using the method of [Ehrig 06]. To ensure the smoothness of velocities and accelerations, the trajectories of the markers were filtered using a 2^{nd}-order butterworth filter with a cut frequency of 5Hz.

To capture the position of the center of pressure and the total Ground Reaction Force, an AMTI OR6 forceplate was carefully synchronized with the motion capture system. CoP and GRF were captured at 600Hz and downsampled according to the frequency of the motion capture system. Furthermore, the forceplace was carefully adjusted to ensure its spatial location relatively to the capture system global coordinate.

Human model A human model was constructed in order to compute the different criteria that have to be tested. It consisted of 14 links: right and left feet, shanks, thighs, hands, forearms, upper arms, along with trunk and head. All segments are modeled as cylinders with a ellipsoid base, which anthropometric parameters (mass, center of mass and inertia) were computed using anthropometric tables of De Leva [De Leva 96]. Each segment length was computed from captured data. This simple representation was chosen because it is commonly used in computer animation [Kajita 09] and because we want

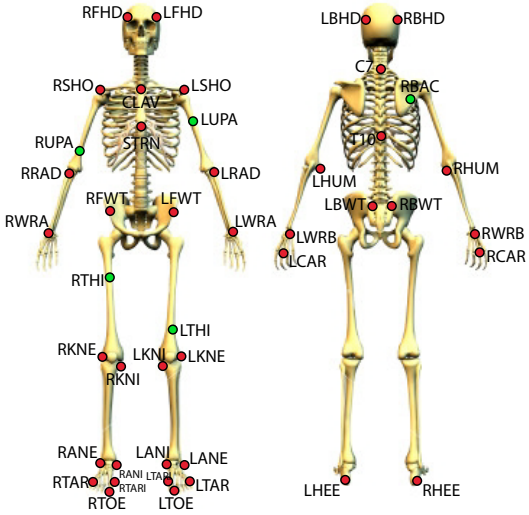

Figure II.8: Placement of the 45 reflecting markers positioned on the user's body (based on [Zatsiorsky 90]).

to study the performance of balance criteria in common applications. Thus, anthropometric parameters correspond to standard average values from De Leva tables and users' global height and weight.

Motions To evaluate the performance of the criteria presented in Section II.1, we asked subjects to perform motions involving dynamic levels: *Quasi-static*, *Low Dynamics*, *High Dynamics*. The different motions in each category are presented in Table II.2. Details of the motions are listed below.

Quasi-static motion

- **Reaching:** both feet are in contact with the ground while trying to reach as much as possible a target slowly moving out of reach. Balance is lost when the subject makes a step to prevent falling. By definition, it is not possible to return to a balance state for quasi-static motions when the GCOM goes outside the base of support.

Low dynamic motions

- **Oscillations:** increasing voluntary oscillations while trying to keep balance. The use of arms to restore balance was forbidden (arms had to stay close to the body, hands placed over the pelvis). The goal is to explore the limits of balance for low dynamic motions. Hence, the subject was asked to increase the oscillations until losing balance.

- **Walking:** walking is defined as a succession of forward unbalanced phases [Alexander 84]. Thus, there exists a time in the locomotion cycle where it is impossible to return back to the previous stance without finishing the step. For this motion, we try to study the behavior of balance criteria just before or after this limit. Subjects were instructed to walk at their preferred speed and to try to stop their motion on the current support when a given signal occurred, without making a new step or putting the foot on the floor.

- **Turning:** walking followed by a sudden turn at 90° or 180° degrees. The goal is to measure if turns are considered as unbalanced phases and how balance criteria behave for this type of motion.

Highly dynamic motions

- **Dynamic oscillations:** increasing voluntary oscillations while trying to keep balance, with possible use of the arms to compensate. The goal is to measure the effect of arm momentum to restore balance, especially as several criteria do not take it into account.

- **Spin around:** subjects had to spin around once or twice (when possible) on one foot.

- **One foot support:** subjects had to stay on one supporting foot while performing voluntary maximal swings with the other leg. The goal is to study how dynamic criteria behave for highly dynamic motions on a single supporting foot.

- **Jog and jump:** jog followed by a vertical jump at the given signal to try to touch a target hung above the forceplate. The limit between the support phases and the flight phases are usually not well measured by dynamic criteria. By adding a constraint on the vertical velocity at the end of the support phase, we want to analyze the behavior of balance criteria compared to simple jogging sequences.

Quasi-static		*High Dynamic*	
	**Reaching:** two feet in contact with the floor while trying to reach a target.		**Dynamic oscillations:** increasing voluntary oscillations using the arms if needed to keep balance.
Low dynamic			**One foot support:** high dynamic motions by swinging a leg.
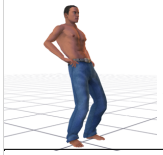	**Oscillations:** increasing voluntary oscillations without using the arms to compensate.		**Spin around:** spin around on one foot once or twice.
	**Walking:** walking at preferred velocity and trying to stop the motion at the signal.	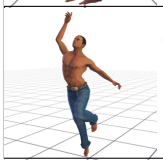	**Jog and jump:** running and jumping at the signal.
	**Turning:** walking at preferred velocity and suddenly turning at 90° and 180°.		

Table II.2: List of motions performed by subjects. A vignette represents each task, using a captured motion applied to a virtual character for display purpose.

II.2.1.2 Procedure

For each motion, we computed the following criteria: GCOM, XcoM, ZMP and FRI. ZMP was computed for the three different human models (Pendulum, Particles, Articulated Rigid Body) presented in Appendix A. ZMPs computed with these models will be referred as ZMP pend., ZMP part. and ZMP arti. in the remaining of this Chapter. We also compared the computed ZMPs respectively with the ground truth CoP obtained from the forceplate, which was synchronized with the motion capture system. As ZMP and CoP are supposed to be identical, computed and measured values should be close. ZRAM was not computed because it corresponds to the ZMP with pendulum model on a flat floor.

In order to study the relevance of each criterion to model balance in various situations, we analyzed

- if they lead to false unbalanced situations (named *false alarms*): the criterion goes outside the base of support while the subject preserves balance.
- if they fail in detecting an unbalanced situation (named *failure*): the criterion remains inside the base of support while the subject has to perform a step to prevent falling.

To measure the occurrence of false alarms, we propose to study the evolution of the distance between each criteria and the base of support, according to the position of the CoP. We assume here that CoP is the golden truth which always remains in the base of support. Its location inside the base of support thus provides relevant information about the risks associated with a loss of balance. For instance, a CoP close to the limits of the base of support is more likely to lead to unbalanced motions. Thus, the CoP location is associated with a dangerousness index ranging from 0 to 1, with 0 corresponding to a CoP at the center of the base of support and 1 corresponding to CoP on the edges.

To define different levels of dangerousness, we arbitrarily divided the base of support into three areas, according to the distance to the middle of the base of support:

0	-	0.5	Safe area where balanced should not be in danger,
0.5	-	0.8	In-between area,
0.8	-	1.0	Dangerous area where the CoP can rapidly reach the limits of the base of support.

For a given area, we can thus evaluate if the studied criterion belongs to the same area than the CoP. We also computed the distance between the criterion and the base of support. This distance is 0 when inside the base of support (BoS) and $dist(criteria, BoS)$ otherwise. $dist(criteria, BoS)$ is defined as the distance between the criteria and the closest point on the base of support.

Figure II.9 shows the smooth distribution of the index value depending on the CoP location and the areas corresponding to the previous parameters. Figure II.10 shows an example of the distance between a criterion and the base of support, according to the CoP location relatively to the different areas.

II.2.2 Results

Popovic et al [Popovic 05] demonstrated that the difference between the position of ZMP and FRI is not significant in human locomotion (only a few millimeters). We have thus checked this statement in our data. To this end, we calculated the distance between these two criteria for all the single support phases of our set of biological captured motions. As FRI depends on rotational angular momentum, ZMP was computed using the articulated rigid body model, as based on the same type of data. Over 143206 frames of single support, the average distance ZMP-FRI was 0.3mm (sd: 0.6mm). For only 8612 frames (6%)

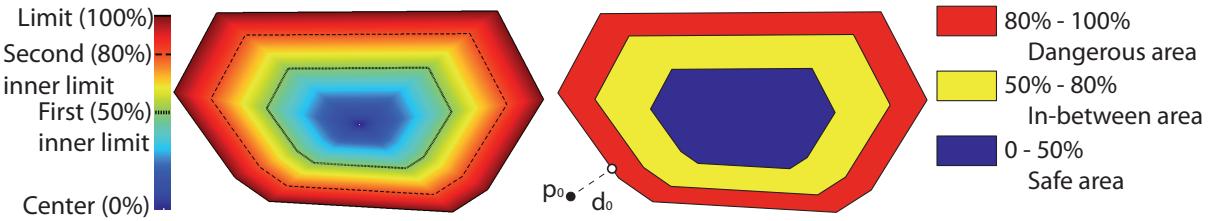

Figure II.9: Base of support with two feet on the floor. Left: distance to the center of the base of support with red being the limit. First and second inner limit represent respectively a distance of 50% and 80% of the distance from the center to the limit. Right: model of the corresponding areas. d_0 represents the distance between a point p_0 and the BoS.

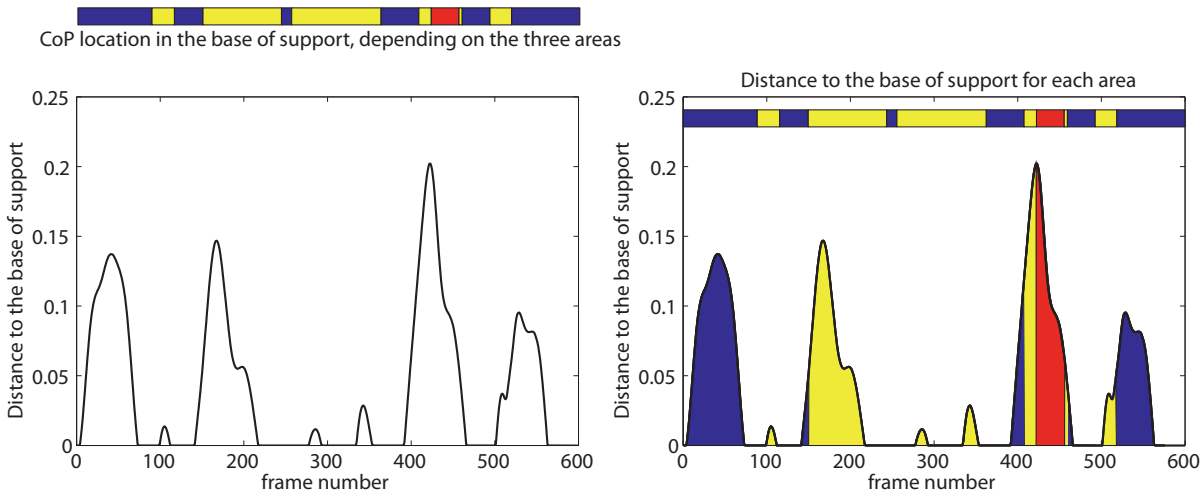

Figure II.10: Left: distance of a criterion to the base of support and location of the CoP in the base of support. Right: distance to the base of support for each area.

the distance was greater than 1mm and for 27 frames (<0.02%) greater than 1cm. Thus, it is in agreement with the results of [Popovic 05] in the special case of locomotion. We have demonstrated here that this statement is also true for other types of motions. Based on these results, we have decided to focus on the other criteria in the remaining of this Chapter.

Let us consider now the results for quasi-static, low dynamic and highly dynamic motions.

II.2.2.1 Quasi-static motions

For reaching motions, participants try to reach a target slowly moving away in front of them, while keeping balance as much as possible. When balance is lost, they make a step to prevent them from falling.

Under quasi-static conditions, GCOM is used to detect unbalance by checking if it goes outside the base of support. Thus, we separated reaching motions into two phases, depending on the position of the

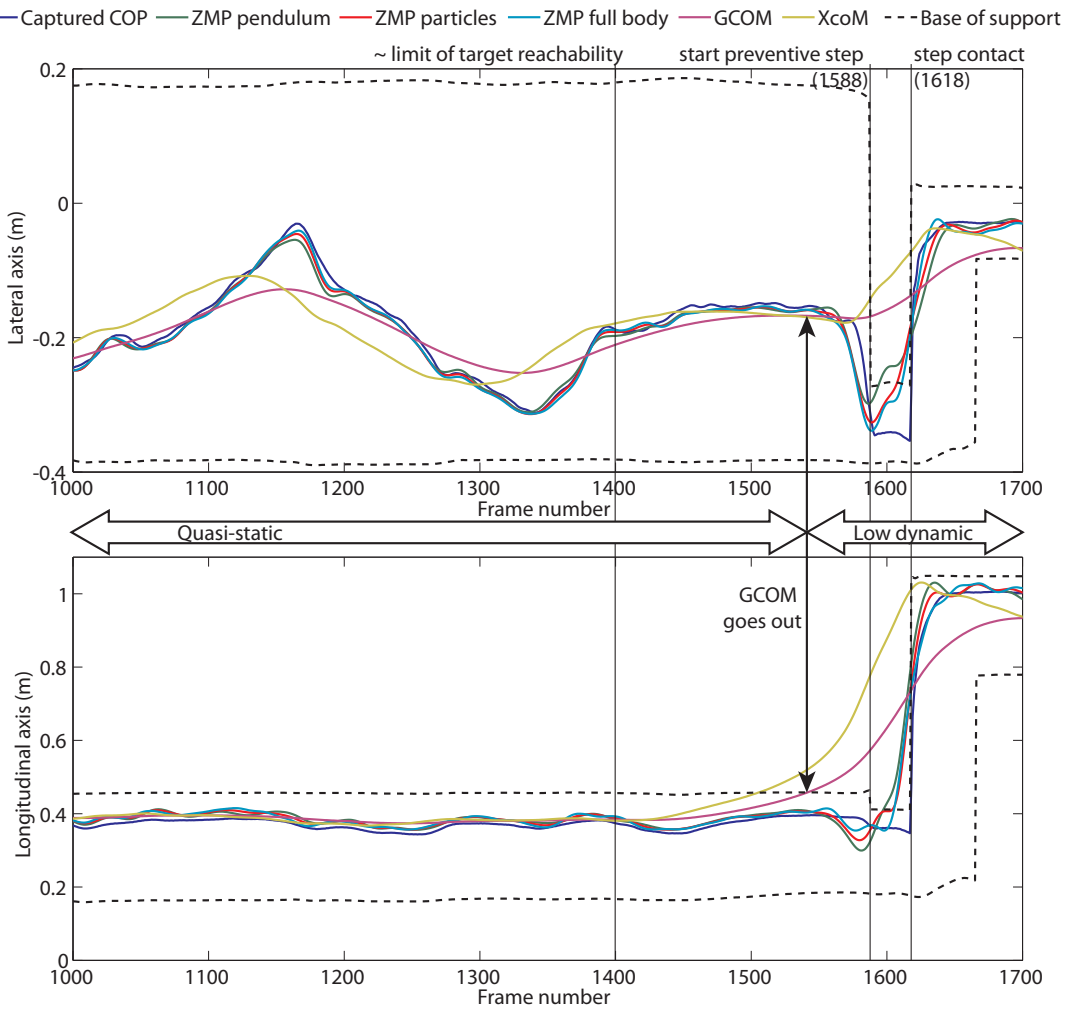

Figure II.11: Trajectories of various criteria for a reaching motion where the target is slowly move out of a reach on the longitudinal axis.

GCOM: a quasi-static phase where accelerations are negligible (before that GCOM goes outside the base of support) and a low dynamic phase where the subject makes a step to prevent from falling (after that, GCOM goes outside the base of support). We consider here that stepping is not quasi-static anymore but mostly corresponds to a low dynamic motion.

Figure II.11 shows a representative example of the trajectories of the different criteria in this case. The subject has his two feet on the floor until frame 1588 (quasi-static phase), then initiates a preventive step (low dynamic phase), which strikes at frame 1618 (start of double support phase).

In the quasi-static phase of these motions, the target is usually close to the participant, which does not endanger balance. Thus, all criteria stay in the base of support. As accelerations are small, all computed criteria (ZMPs, GCOM and XcoM) remain close to the measured CoP trajectory (as shown in Figure II.11 before frame number 1540).

When the target is close to the reaching limit (at frame 1400 in Figure II.11), both GCOM and XcoM start to move away from the CoP, while ZMPs remain close to the CoP trajectory. When GCOM goes outside the base of support, quasi-static balance cannot be recovered anymore and the step is initiated. It corresponds to the end of the quasi-static phase. Before GCOM, XcoM moves outside the base of support and detects the upcoming loss of balance. It then moves in the direction of the future base of support that will enable the subject to restore balance.

Contrary to the previous criteria, ZMPs move outside the base of support during the step (single contact phase), which should not happen as it is restricted to remain in the base of support. However, simplifications in the equations of the ZMPs may introduce errors, especially the choice of the model. Furthermore, ZMPs go outside the base of support during the single contact phase while subjects already started a step to recover balance. Thus, ZMP fails to detect loss of balance in time.

To estimate when these different criteria predict an unbalanced state, we computed parameters based both on the time t_{out} when the criterion goes outside the base of support and the time of the preventive step (take-off t_{start} and landing t_{end} of the foot). These parameters are computed as follows:

- Xcom and GCOM go outside the base of support before the start of the preventive step. To analyze the duration between t_{out} and t_{start}, we compute the mean value of $t_{start} - t_{out}$ for all reaching captured motions.

- ZMPs usually go outside the base of support during the preventive step restoring balance. To evaluate when t_{out} occurs in the single foot sequence, we compute the average value of:

  $$(t_{out} - t_{start})/(t_{end} - t_{start})$$

  It represents the time in the single support phase when ZMPs go outside the base of support relatively to the step duration.

Table II.3 presents these results. It shows that GCOM goes outside the base of support almost 0.61s before the initiation of the preventive step, while XcoM goes outside earlier, 0.84s before the step. For ZMPs, the pendulum model detects an unbalance state earlier than other models. However, all different models used to compute the ZMPs detect an unbalanced state while the step is initiated from a long time (half the duration of the step). Even if the standard deviation is high for the three models, these criteria almost never detect an unbalance state at the beginning of the preventive step. Thus, balance is already lost. One has to notice that this point should always remain in the base of support as it theoretically corresponds to the CoP.

	GCOM	XcoM	ZMP pend.	ZMP part.	ZMP arti.
mean duration	0.61s ± 0.37s	0.84s ± 0.41s	46% ± 28%	61% ± 21%	54% ± 26%

Table II.3: Reaching: For GCOM and XcoM, results present the mean duration between the time t_{out} when the criteria go outside the base of support and the start t_{start} of the preventive step. For ZMPs, results present the time when it goes outside the base of support in the single support phase as a percentage of the preventive step duration.

Table II.4 presents the mean distance of all criteria to the base of support, depending on the CoP location, for quasi-static phases of reaching motions. As GCOM was used to automatically separate reaching motions into a quasi-static and a low dynamic phase, it is not presented in Table II.4. Results show that these criteria do not detect false alarms when the CoP lies in the safe area. Similarly, they almost never detect false alarms for the in-between area (<1% of the number of frames and average distance ~1cm). However, the CoP lies in the dangerous area only in 4% of the total number of frames. In that case, XcoM is often outside (15% of the frames) as it detects the unbalance before GCOM. All ZMPs are outside the base of support in about 10% of the number of frame where the CoP lies in the dangerous area, with a small average distance to the base of support (between 0.4cm and 1.2cm).

		GCOM	XcoM	ZMP pend.	ZMP part.	ZMP arti.	dataset %
Safe area	mean error (cm)	-	-	-	-	-	42% (37301 frames)
	nb frames	-	0	0	0	0	
	% outside	-	0%	0%	0%	0%	
In between area	mean error (cm)	-	1.1 ± 1.18	0.8 ± 1.6	1.2 ± 3.1	1.3 ± 3.0	54% (49179 frames)
	nb frames	-	1682	416	191	315	
	% outside	-	3.5%	0.9%	0.4%	0.7%	
Dangerous area	mean error (cm)	-	1.4 ± 1.8	1.2 ± 0.9	0.4 ± 0.3	0.6 ± 0.4	4% (3580 frames)
	nb frames	-	553	293	339	413	
	% outside	-	15.4%	8.2%	9.5%	11.5%	

Table II.4: Quasi-static reaching: mean distance to the base of support (BoS) for the frames when the corresponding criterion goes outside, for three area representing different levels of unbalanced risks. The column *dataset %* represents the percentage of frames where the CoP lies in the corresponding area. Line *nb frames* presents the number of frames where the CoP lies in the corresponding area and the criterion outside the BoS. Line *% outside* represents the percentage of frame of *dataset %* where CoP is outside the BoS. GCOM is not displayed as quasi-static phases are selected by finding the time when GCOM goes outside the BoS.

We thus have computed the error between the computed ZMPs and the measured CoP for the quasi-static and low-dynamic phases. Mean and sd errors for the three models are presented in Table II.5.

For quasi-static phases, this error is small (mean error ~2cm with ~1cm sd) whatever the model that is used. During the low-dynamic phase where the character is not balanced anymore (after that GCOM goes outside the base of support) both the mean and sd errors increase.

		ZMP pend.	ZMP part.	ZMP arti.
Quasi-static phase	mean error to CoP (cm)	1.9 ± 1.0	1.9 ± 0.9	1.9 ± 1.0
Low dynamic phase	mean error to CoP (cm)	4.5 ± 5.4	3.2 ± 4.3	3.5 ± 4.3

Table II.5: Mean and sd error between measured CoP and ZMP computed with three different models, for both the quasi-static and low dynamic phases of reaching motions.

II.2.2.2 Low dynamic motions

Oscillations without using the arms Participants had to perform increasing voluntary oscillations without having the right to use the arms to balance (arms had to stay close to the body, hands placed over the pelvis). Figure II.12 shows a representative example of the trajectories of the different criteria for the case of an oscillating motion, where the subject is moving from backward to forward (and conversely).

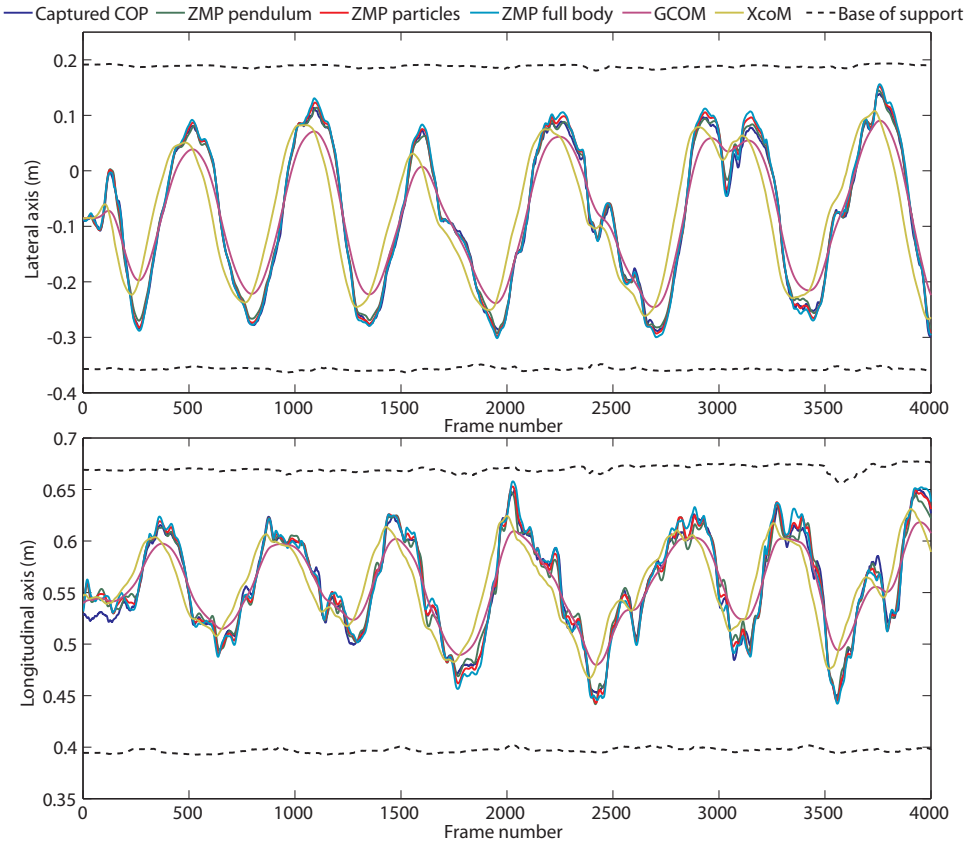

Figure II.12: Trajectories of various criteria for a representative motion where subjects had to perform maximal voluntary oscillations without using the arms to balance.

To study the behavior of the different criteria, we divided the captured motions into two parts: balanced phase, where the subject is balanced, and unbalanced phase, where the subject has to make a step to restore balance. Concerning balanced phases, all criteria have a behavior similar to the CoP trajectory. Still, the studied criteria might move outside the base of support while the subject is balanced. Table II.6 presents the mean distance between the criteria and the base of support according to the CoP location for balanced phases.

When the CoP is close to the center of the base of support (safe area), results show that all these criteria never detect a false loss of balance. Similarly, only a few false alarms are detected in the in-between area (<1% of the number of frames). For the dangerous area (22% of the total number of frames), these criteria reach different level of performance. GCOM and XcoM almost never goes outside the base of support (respectively in 2.6% and 5.4% of the frames in the dangerous area), with a small

average distance to the base of support (respectively 0.3cm and 0.6cm). On the contrary, ZMPs goes outside the base of support respectively in 15.6%, 19.9% and 24.5% of the cases. Thus, ZMPs detects more false alarms than GCOM and XcoM. However, the average distance between ZMPs and the base of support remains small (about 1cm).

		GCOM	XcoM	ZMP pend.	ZMP part.	ZMP arti.	dataset %
Safe area	mean error (cm)	-	0.4 ± 0.2	-	-	-	25% (39528 frames)
	nb frames	0	7	0	0	0	
	% outside	0%	<0.1%	0%	0%	0%	
In between area	mean error (cm)	-	0.5 ± 0.4	0.9 ± 1.1	0.5 ± 0.5	0.6 ± 0.5	53% (83288 frames)
	nb frames	0	205	475	143	607	
	% outside	0%	0.2%	0.6%	0.2%	0.7%	
Dangerous area	mean error (cm)	0.3 ± 0.2	0.6 ± 0.6	1.0± 1.0	0.8 ± 0.7	1.0 ± 0.8	22% (34011 frames)
	nb frames	878	1819	5296	6760	8346	
	% outside	2.6%	5.4%	15.6%	19.9%	24.5%	

Table II.6: Oscillations: mean distance to the base of support (BoS) for the frames when the corresponding criterion goes outside, for three area representing different levels of unbalanced risks. The column *dataset %* represents the percentage of frames where the CoP lies in the corresponding area. *nb frames* presents the number of frames where the CoP lies in the corresponding area and the criterion outside the BoS. *% outside* represents the percentage of frame of *dataset %* where CoP is outside the BoS.

Table II.7 presents the mean and sd error between computed ZMPs and measured CoP for the balanced parts. Results show that computed ZMPs are close to the CoP trajectory (average error ~2cm).

		ZMP pend.	ZMP part.	ZMP arti.
Balanced part	mean error to CoP (cm)	1.9 ± 1.1	1.8 ± 1.0	1.9 ± 1.1

Table II.7: Oscillations: mean CoP–ZMP error.

Walking Walking has been defined as a succession of forward falls corresponding to a transfer between potential and kinetic energy [Alexander 84]. Thus, there exists a time t_{limit} in the locomotion cycle where it is impossible to return back to the previous stance without finishing the step. By studying walking motions, we wished to study the behavior of balance criteria just before and after this limit. Thus, subjects were instructed to walk at their preferred speed and to try to stop on the current support when a given signal occurred, without making a new step or putting the foot on the floor.

However, from the experimental point of view, it is difficult to precisely time the signal to reach this goal. Because of the time of reaction, either the signal was given too early, and it was too easy for the subject to stop, or the signal was given at the limit. In that case, it was not possible to stop at all without finishing the step.

Thus, we finally evaluated the difference between ground truth CoP and measured ZMP at any time, as it was impossible to detect the limit (Table II.8).

		ZMP pend.	ZMP part.	ZMP arti.
Walking	mean error to CoP (cm)	4.9 ± 6.9	4.0 ± 6.3	4.2± 6.3

Table II.8: Mean error for walking between measured CoP and ZMP computed with the different models.

Turning In order to analyze the behavior of the studied criteria while turning, we asked subjects to walk and perform a sudden 90° or 180° turn on the forceplate. However, turns require to capture several steps before and after the turn. With the limitation of the surface of the force plate, we were usually able to capture only one foot on the force plate during 90° turns. However, we still estimate the error between the measured CoP and the computed ZMPs by carefully selecting sequences of motions where the subject is only in contact with the forceplate. This problem did not appear with 180° turns as subjects performed the 180° turn at the end of the force plate (Figure II.13).

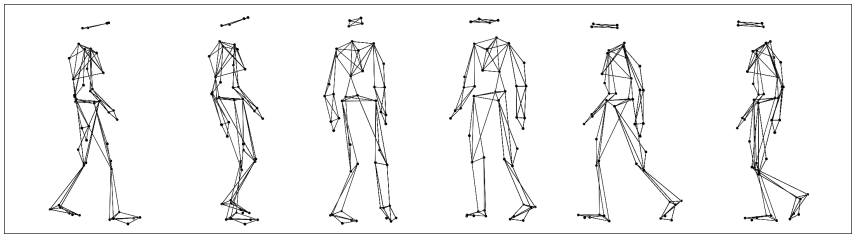

Figure II.13: 180° turning motion.

Table II.9 presents the evolution of the distance between the different criteria and the base of support depending on the CoP location for the 90° turns only. For 180° turns, different strategies were used by participants to perform the wanted task and we failed to automatically compute the support sequences.

During 90° turns, the center of mass of the character follows a curve towards the turning direction (Figure II.14). GCOM, which is the projection of the center of mass, is almost never in the base of support during the single foot sequence, whatever the location of the CoP in the base of support (Table II.9). Furthermore, the average distance to the base of support is important (10~15cm). Similarly, XcoM follows the same behavior; Its average distance to the base of support is however more important, from 14cm (when the CoP is located in the safe area) to 28cm (in-between and dangerous areas). Thus, these criteria consider turning as a highly unbalanced motion.

In the case of ZMPs, results show that CoP pend. is outside the base of support in more than 50% of the total number of frames, while ZMP part. and ZMP arti. are outside in respectively 33% and 38% of the total number of frames. Concurently, Table II.10 presents the mean and sd error between measured CoP and computed ZMPs for 90° and 180° turning motions. Results show that the average error is important between the computed ZMPs and the measured CoP for both 90° and 180° turns. As the average error between the CoP and ZMPs is of the same magnitude than the width of the foot, it is thus difficult to correctly analyze the distance between ZMPs and the base of support.

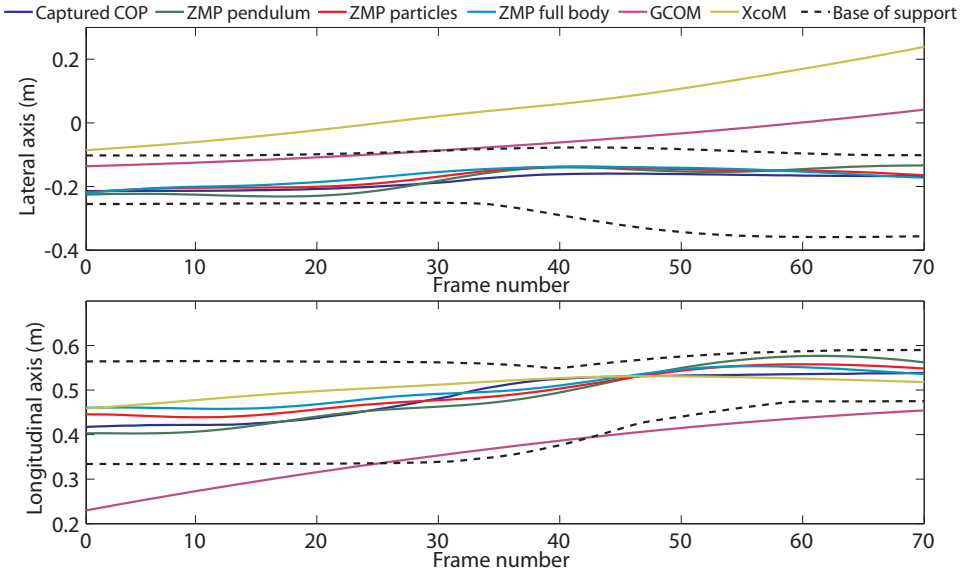

Figure II.14: Trajectories of various criteria for a representative 90° turning motion.

		GCOM	XcoM	ZMP pend.	ZMP part.	ZMP arti.	dataset %
Safe area	mean error (cm)	11.6 ± 5.0	14.4 ± 8.8	1.2 ± 0.9	1.4 ± 1.2	1.9 ± 1.4	25% (1071 frames)
	nb frames	1064	1036	360	135	146	
	% outside	99%	97%	34%	13%	14%	
In between area	mean error (cm)	14.8 ± 7.0	28.0 ± 15.1	2.2 ± 2.0	1.7 ± 1.8	1.6 ± 1.6	57% (2458 frames)
	nb frames	2456	2441	1372	956	1099	
	% outside	~100%	99%	56%	39%	45%	
Dangerous area	mean error (cm)	14.2 ± 7.2	28.5 ± 15.6	2.2 ± 2.1	1.5 ± 1.5	1.2 ± 1.5	18% (753 frames)
	nb frames	750	743	445	322	386	
	% outside	~100%	99%	59%	43%	51%	

Table II.9: 90° turns: mean distance to the base of support (BoS) for the frames when the corresponding criterion goes outside, for three area representing different levels of unbalanced risks. The column *dataset %* represents the percentage of frames where the CoP lies in the corresponding area. *nb frames* presents the number of frames where the CoP lies in the corresponding area and the criterion outside the BoS. *% outside* represents the percentage of frame of *dataset %* where CoP is outside the BoS.

		ZMP pend.	ZMP part.	ZMP arti.
90° turn	mean error to CoP (cm)	5.0 ± 2.6	3.8 ± 2.2	3.9 ± 2.3
180° turn	mean error (cm)	6.0 ± 4.1	4.8 ± 3.3	4.8 ± 3.3

Table II.10: Mean and sd error for 90° and 180° turns between measured CoP and ZMP computed with three different models.

II.2.2.3 High dynamic motions

Dynamic oscillations Subjects had to perform increasing voluntary oscillations while keeping balance as much as possible. Contrary to low dynamic oscillations, they were allowed to use the arms to restore balance. Figure II.15 shows a representative example of the trajectories of the different criteria. From frames 600 to 780 approximatively, the subject managed to keep his balance in an unstable situation by swinging his arms.

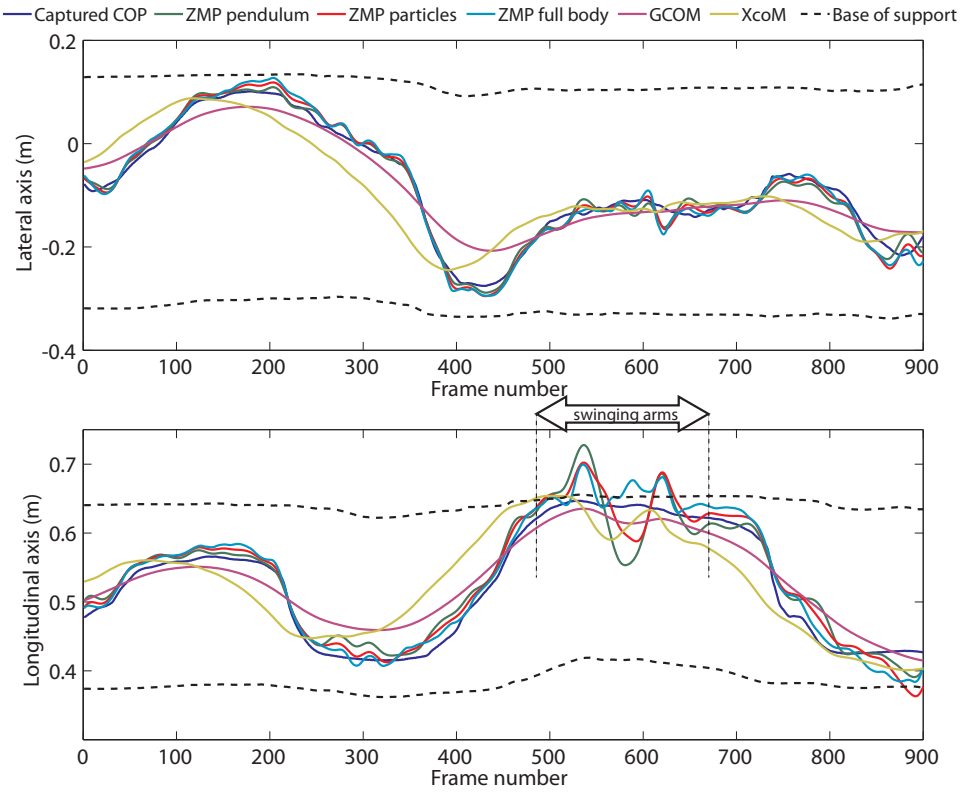

Figure II.15: Trajectories of various criteria for a representative motion where subjects had to perform maximal voluntary oscillations while keeping balance as much as possible. Subjects were allowed to use the arms to restore balance.

We analyzed the distance between each criteria and the base of support according to the CoP location (Table II.11). Results show that the GCOM almost never goes outside the base of support. It only happens in 1.7% of the frames when the CoP lies in the dangerous area (average distance to the BoS: 0.5cm). XcoM occasionally goes outside the base of support when the CoP lies in the in-between or dangerous areas (mean distances to BoS are respectively 0.7cm and 0.9cm). ZMPs goes more often outside the base of support, respectively in 18.6%, 22.2% and 31.5% of the cases. However, the average distance to the base of support is higher for the pendulum model (1.9cm) than for the two others (1.1 and 1.3 cm).

Results also show that the CoP repartition in the three areas is similar for both low dynamic and highly dynamic oscillations (respectively Tables II.6 and II.11). Compared to low dynamic oscillations, results also show that all the criteria go outside the base of support as often for both low and highly dynamic oscillations.

		GCOM	XcoM	ZMP pend.	ZMP part.	ZMP arti.	dataset %
Safe area	mean error (cm)	-	-	0.3 ± 0.2	-	1.5 ± 1.1	23% (40707 frames)
	nb frames	0	0	3	0	5	
	% outside	0%	0%	<0.1%	0%	<0.1%	
In between area	mean error (cm)	-	0.7± 0.6	1.2 ± 1.1	1.0 ± 1.2	1.1 ± 1.5	54% (96220 frames)
	nb frames	0	591	1894	1161	2261	
	% outside	0%	0.6%	2.0%	1.2%	2.3%	
Dangerous area	mean error (cm)	0.5 ± 0.4	0.9 ± 0.7	1.9 ± 2.0	1.1 ± 1.1	1.3 ± 1.1	23% (40480 frames)
	nb frames	686	2068	7518	9008	12769	
	% outside	1.7%	5.1%	18.6%	22.2%	31.5%	

Table II.11: Dynamic oscillations: mean distance to the BoS for the frames when the corresponding criterion goes outside, for three area representing different levels of unbalanced risks. The column *dataset %* represents the percentage of frames where the CoP lies in the corresponding area. *nb frames* presents the number of frames where the CoP lies in the corresponding area and the criterion outside the BoS. *% outside* represents the percentage of frame of *dataset %* where CoP is outside the BoS.

Table II.12 presents the mean and sd error between computed ZMPs and measured CoP. Errors are of the same magnitude for low dynamic and highly dynamic oscillations.

		ZMP pend.	ZMP part.	ZMP arti.
Dynamic oscillations	mean error to CoP (cm)	2.5 ± 1.6	2.2 ± 1.3	2.4 ± 1.3

Table II.12: Mean and sd error between measured CoP and ZMP computed with three different models for high dynamic oscillations.

Spin around Subjects had to perform a full spin. The goal is to evaluate the performance of the studied criteria when subjects turn on their foot as, during spins, the feet slide on the floor. Thus, friction plays an important role in this type of motion. Figure II.16 presents the trajectory of the different criteria for a full balanced spin. The subject starts on two feet (frames 0 to 20), spins around his left foot (frames 20 to 135) and comes back on his two feet (frames 135 to 160). For spinning motins, we will only study the single foot support periods that correspond to spinning.

Table II.13 presents the average distance of the studied criteria to the base of support, according to the CoP location, during the single support phase of full one-spin motions. Results show that GCOM is often outside the base of support during spinning, with an average distance to the base of support ranging from 3cm to 6cm. XcoM goes outside more frequently and farther from the base of support (6~10cm). ZMPs goes outside the base of support in more than 70% of the total number of single support frames, with ZMP arti. obtaining the worth performance (86% of total number of frames outside the base of support).

We also asked subjects to try to perform two-spins motions. Because of the difficulty of this motion, they did not managed to perform it. However, the beginning of the single support phase of two-spins

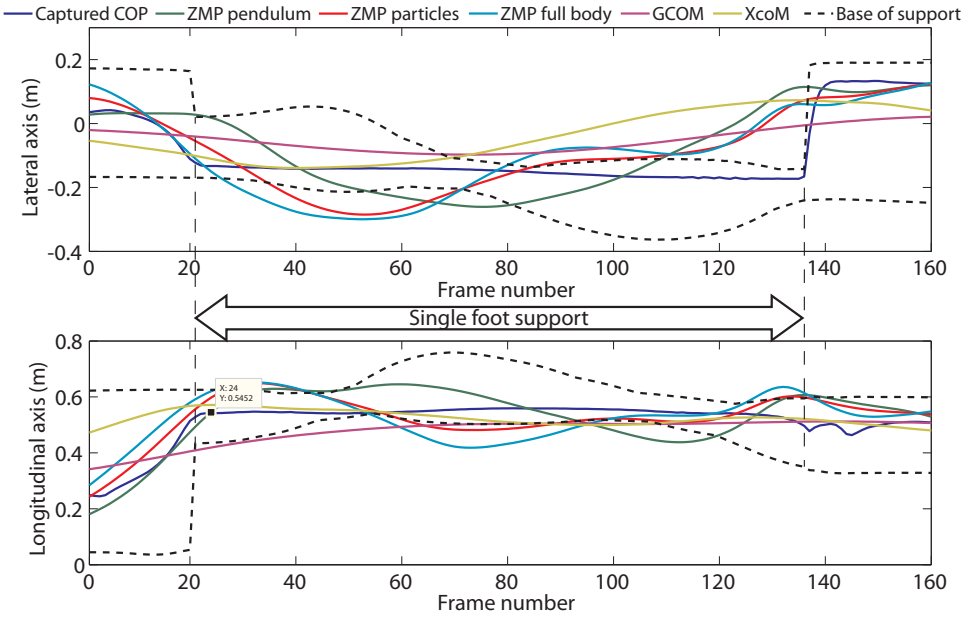

Figure II.16: Trajectories of various criteria for a full balanced spin.

		GCOM	XcoM	ZMP pend.	ZMP part.	ZMP arti.	dataset %
Safe area	mean error (cm)	3.3 ± 4.0	5.8 ± 5.6	4.7 ± 5.4	5.0 ± 4.6	5.8 ± 5.3	14% (1015 frames)
	nb frames	426	735	425	488	648	
	% outside	42.0%	72.4%	41.9%	48.1%	63.8%	
In between area	mean error (cm)	5.7 ± 4.3	8.2 ± 7.6	7.0 ± 6.2	7.1 ± 5.5	8.2 ± 5.3	65% (4640 frames)
	nb frames	3342	3474	3355	3913	4091	
	% outside	72.0%	74.9%	72.3%	84.3%	88.2%	
Dangerous area	mean error (cm)	5.9 ± 3.7	10.5 ± 8.3	8.7 ± 5.7	6.3 ± 4.1	7.7 ± 4.7	21% (1518 frames)
	nb frames	1110	1280	1261	1382	1424	
	% outside	73.1%	84.3%	83.1%	91.0%	93.8%	

Table II.13: One spin: mean distance to the base of support (BoS) for the frames when the corresponding criterion goes outside, for three area representing different levels of unbalanced risks. The column *dataset %* represents the percentage of frames where the CoP lies in the corresponding area. *nb frames* presents the number of frames where the CoP lies in the corresponding area and the criterion outside the BoS. *% outside* represents the percentage of frame of *dataset %* where CoP is outside the BoS.

motions presents high dynamic properties. Thus, two-spins captured trials are still compared with one spin motions to evaluate the difference of error when computing ZMPs.

Table II.14 presents the mean error between measured CoP and ZMPs computed with the three different models for both one-spin and two-spins motions. For these type of motions, ZMP computation is highly different from the ground truth CoP, whatever the chosen model. Furthermore, results show that the average error is always more important for two-spins motions compared to one-spin motions. It

could be explained by the fact that the preparation of second spin increase the unbalance of the overall motion. In both case, the average error between measured CoP and computed ZMPs is always more important than the foot width.

		ZMP pend.	ZMP part.	ZMP arti.
One spin	mean error to CoP (cm)	10.1 ± 6.5	9.6 ± 5.7	11.1 ± 5.9
Two spins	mean error to CoP (cm)	13.6 ± 8.8	15.5 ± 8.3	18.7 ± 9.5

Table II.14: Mean and sd error for one and two spins between measured CoP and ZMP computed with three different models.

One foot support Subjects had to stay on one supporting foot while swinging the other leg in different directions. Figure II.17 shows a representative example of the trajectories of the different criteria. In the first half of the Figure, the subject swings his right leg from frontwards to backwards (and conversely). It shows that all criteria except GCOM regularly go outside the base of support in the longitudinal direction. Respectively, the same behavior can be observed on the lateral axis in the second half of the Figure, as the subject swings his leg from left to right (and conversely).

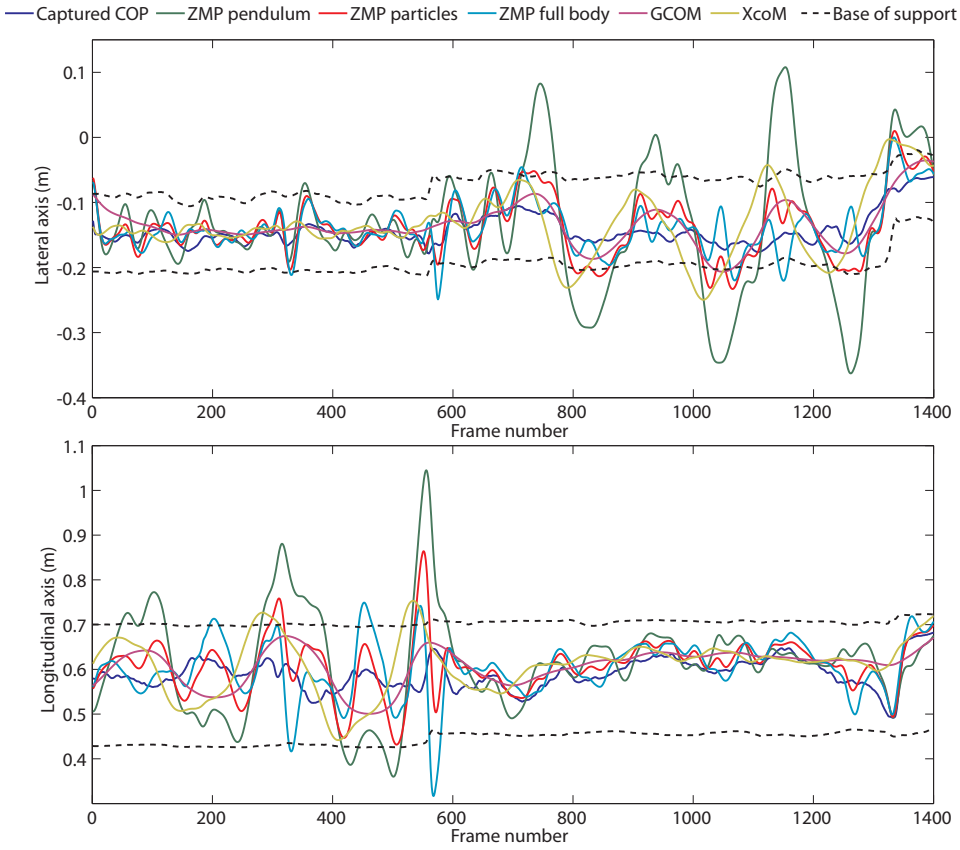

Figure II.17: Trajectories of various criteria for a representative motion where subjects swing one leg in different directions while staying on one foot.

Table II.15 presents the mean distance of the studied criteria to the base of support according to the location of the CoP. Contrary to the previous oscillating motions (both low and highly dynamics ones), GCOM often goes outside the base of support (in 14% of the total number of frames), with a mean distance to the base of support ranging from 0.7cm to 1.4cm depending on the CoP location. XcoM goes more often outside the base of support (in 29% of the total number of frames). Its average distance to the base of support ranges from 1.7cm (safe area) to 2.3 (dangerous area). ZMP part. and ZMP arti. give similar results, going outside the base of support respectively in 28% and 27% of the total number of frames (average distance to the BoS ∼2cm). However, ZMP pend. detects false alarms in 53% of the cases while going usually further away from the base of support (average distance from 4.2cm to 4.9cm).

		GCOM	XcoM	ZMP pend.	ZMP part.	ZMP arti.	dataset %
Safe area	mean error (cm)	0.7 ± 0.7	1.7 ± 1.6	4.2 ± 4.0	1.7 ± 1.9	1.4 ± 1.6	48% (46083 frames)
	nb frames	721	7192	20458	4571	3297	
	% outside	1.6%	15.6%	44.4%	9.9%	7.2%	
In between area	mean error (cm)	1.1 ± 1.0	2.1 ± 2.0	4.8 ± 4.6	1.8 ± 1.7	1.7 ± 1.7	32% (30712 frames)
	nb frames	5069	10982	18305	10133	9973	
	% outside	16.5%	35.8%	59.6%	33.0%	32.5%	
Dangerous area	mean error (cm)	1.4 ± 1.1	2.3 ± 1.8	4.9 ± 4.2	1.9 ± 1.6	2.1 ± 1.8	20% (18916 frames)
	nb frames	7919	9749	12425	11924	12629	
	% outside	41.9%	51.5%	65.7%	63.0%	66.7%	

Table II.15: One foot support: mean distance to the BoS for the frames when the corresponding criterion goes outside, for three area representing different levels of unbalanced risks. The column *dataset %* represents the percentage of frames where the CoP lies in the corresponding area. *nb frames* presents the number of frames where the CoP lies in the corresponding area and the criterion outside the BoS. *% outside* represents the percentage of frame of *dataset %* where CoP is outside the BoS.

Table II.16 presents the mean error between computed ZMPs and measured CoP. Results show that the average error is important. More especially, the pendulum model highly fails to estimate the CoP trajectory (average error around ∼ 7.5cm).

		ZMP pend.	ZMP part.	ZMP arti.
One foot support	mean error to CoP (cm)	7.5 ± 5.0	3.6 ± 2.2	3.5 ± 2.1

Table II.16: Mean and sd error between measured CoP and ZMP computed with three different models for one foot support motions.

Jog and jump By definition, ZMP and CoP are only defined through contact sequences. Thus, the CoP vanishes at the separation between contact and aerial phases.

Let us recall here that subjects had to jump towards a target hung above the force plate when a specific signal occurred. The goal was to impose a vertical velocity constraint that is not present in jogging motions in order to study the effect of this vertical constraint on the balance forecast. Sequences were

carefully selected in order to contain only the last foot contact phase before jumping. It was necessary in order to ensure that the foot is still in contact with the ground. Otherwise, CoP could not be captured and ZMP is not defined anymore because of the absence of contacts.

Figure II.18 presents a representative example of the trajectories of the studied criteria for a jogging and jumping motion where only the right foot is in contact with the ground. Dotted and dashed polygons represent respectively the support polygon of the first and last frames of the sequence. Arrows indicate the direction of the trajectory of the criteria. GCOM goes in the direction of the jog (longitudinal direction). XcoM is almost stable because the velocity of the COM decreases while it moves forwards. During the sequence, the CoP moves from the middle of the base of support of the first frame to the front limit of the base of support of the last frame. However, ZMP trajectories highly differ from the CoP trajectory.

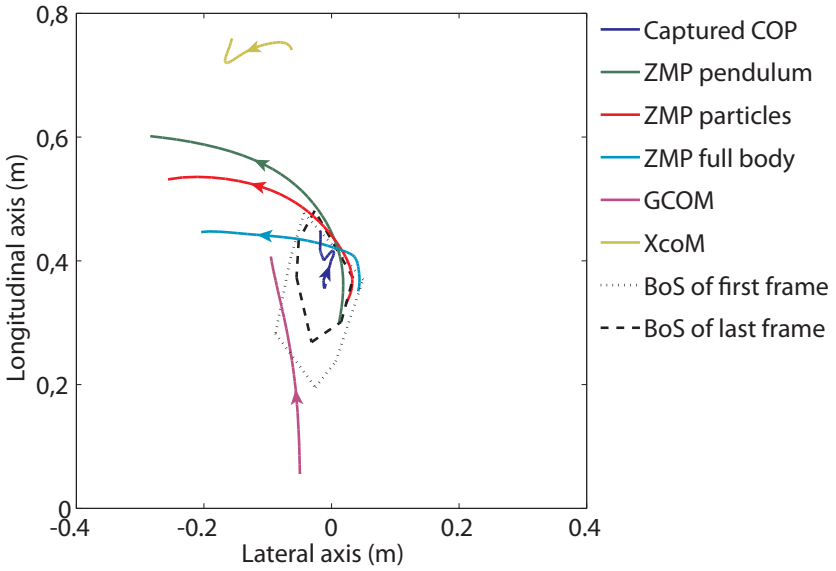

Figure II.18: Trajectories of the studied criteria for a jog and jump sequence (34 frames, 0.23s). Dotted and dashed polygons represent respectively the support polygon of the first and last frames of the sequence. Arrows indicate the direction of the trajectory of the criteria.

Jogging and jumping involve complex foot contacts with the ground. During take-off, the base of support of the foot goes from a full plantar contact to a tip-toe one. Because of the complexity of the contact with the ground, it is almost impossible to accurately represent the base of support. Thus, we did not evaluated the evolution of the distance between the studied criteria and the base of support for these motions. However, Table II.17 presents the average error to the computed base of support in order to give an order of magnitude. We also evaluated the error between measured CoP and computed ZMP for these jogging & jumping motions (Table II.18). Results show that these errors are high whatever the model.

	GCOM	XcoM	ZMP pend.	ZMP part.	ZMP arti.
mean error (cm)	6.2 ± 5.4	34.5 ± 18.8	6.6 ± 8.0	5.0 ± 7.1	4.3 ± 7.8
nb frames	832	1692	991	1044	970
% outside	48.4%	98.4%	57.6%	60.7%	56.4%

Table II.17: Jog & jump: mean distance to the base of support (BoS) for the frames when the corresponding criterion goes outside. The total of frames of jumping motion was 1719. *nb frames* presents the number of frames where the criterion is outside the BoS and *% outside* this percentage relatively to the total number of frames.

		ZMP pend.	ZMP part.	ZMP arti.
Jog & jump	mean error to CoP (cm)	8.5 ± 7.7	7.3 ± 6.9	6.5 ± 7.1

Table II.18: Mean error between measured CoP and ZMP computed with three different models for jog and jump motions.

II.3 Discussion

This Chapter aimed at studying the performance of various criteria to detect the loss of balance of biological motions with different dynamic levels.

For quasi-static motions, it is clear that GCOM going outside the base of support measures the limit of the balance of characters. However, it is not fitted at all to measure the balance of dynamic motions. For instance, it lies outside the base of support during almost all turning motions and regularly during highly dynamic motions.

XcoM could be a good candidate to detect loss of balance. In the case of quasi-static motions, it detects an upcoming loss of balance before the GCOM. During low and highly dynamic oscillations, it lies outside the base of support in less that 2% of the total number of frames with an average distance to the BoS lower than 1cm. However, it almost always lies outside the base of support during turning motions and during most of highly dynamic motions, such as jogging & jumping. Thus, XcoM would consider these motions as highly unbalanced. But for some of these motions the idea of dynamic balance is unclear.

ZMP is certainly the most used criterion in the literature to detect loss of dynamic balance. However, this point is theoretically equal to the center of pressure, which is required to stay inside the base of support. However, we have shown that this is not the case for low and highly dynamic motions, especially when high vertical accelerations occur (such as preparing a jump). In the case of quasi-static motions, we have also shown that this criterion fails to detect the lost of balance in time, going outside the base of support while subjects had already started to recover balance from a long time.

As ZMP and CoP should be equivalent, we also evaluated the error between the ZMP computed with three different models and the ground truth CoP. Figure II.19 reminds the average error for the studied motions. Results show that this error is small for quasi-static motions (~2cm), whatever the model of the virtual human is. Similar results are obtained with both low and highly dynamic oscillating motions.

However, this average error increases up to approximately 5cm for walking and turning motions.

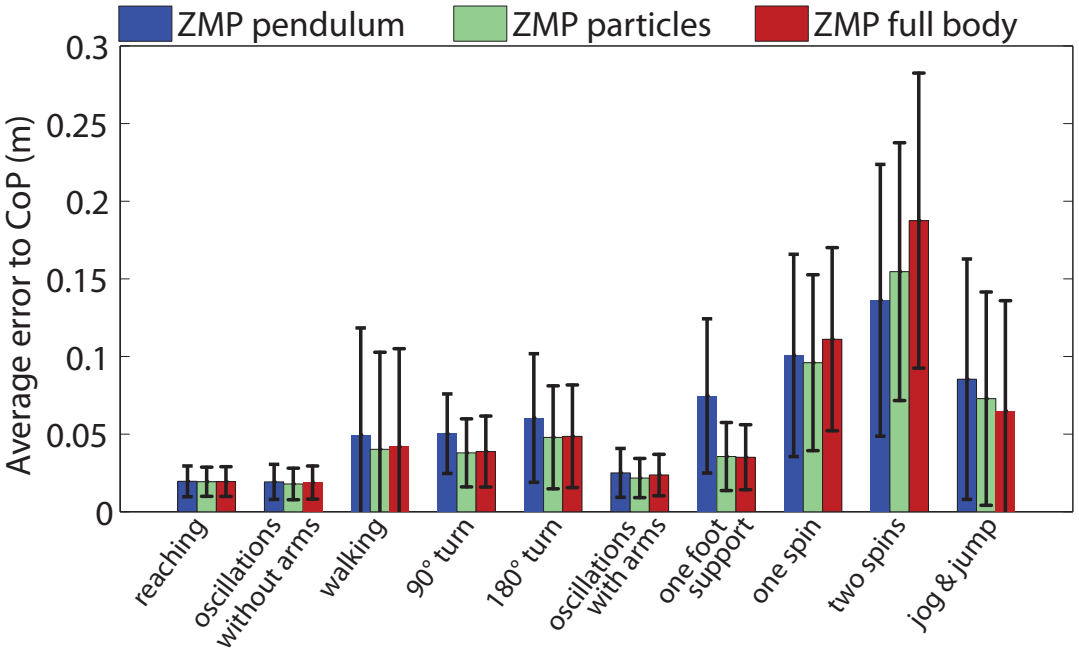

Figure II.19: Error of the computed ZMP to the measured CoP, for three different models of virtual humans: pendulum model (blue), particles model (green) and rigid body model (red).

Results are almost similar with the three models, but ZMP computed with the inverted pendulum model gives the worst results (average error usually 1cm more important than with the two others models). Spins and jumps present even higher average errors ranging from 6.5cm to 15cm. For the specific case of one foot support motions while highly swinging the other leg, the average error using pendulum model is almost twice the average error obtained with the two other models.

Thus, results seem to show that computed ZMPs fail to accurately estimate the CoP trajectory, compared to the ground truth values. However, these results are highly linked with our choices of the anthropometric data of the virtual human. As virtual characters were approximated using the average values from de Leva tables [De Leva 96], anthropometric parameters were approximations of real ones. Furthermore, the choice of the human model (14 links: right and left feet, shanks, thighs, hands, forearms, upper arms, along with trunk and head) also introduces simplifications, such as a rigid one-segment trunk. Thus, further experiments would be required to compare the error between computed ZMP and measured CoP for more precise models. For instance, it would be interesting to evaluate how the results change if the trunk is modeled with a more complex system.

Another interesting point would be to compare these results to ZMP computed with a model where anthropometric parameters were accurately measured. However, this process would be complex and would not represent how ZMP behaves in most of computer animation systems where average anthropometric parameters are used.

We have also shown that the nature of the model used to compute the ZMP may lead to more or less important inaccuracies. Thus, depending on the application, computation of costly models, such as using inertias, could be avoided. In general, the pendulum model, which is the simplest model, gives the worst estimation compared to the ground truth CoP. The only case where results are better for pendulum model is for spinning motions. However, the two other models (system of particles and articulated rigid

	Static	Oscillations	90° turns	Dyn. Oscillations
mean distance (cm)	0.6 ± 0.5	0.3 ± 0.2	2.7 ± 1.2	0.1 ± 0.1
nb frames outside	126 (0.1%)	439 (0.3%)	10 (0.2%)	78 (<0.1%)
total nb frames	102416	156827	4282	177407
	One foot support	One spin	Jump	Global
mean distance (cm)	0.5 ± 0.5	0.4 ± 0.3	2.2 ± 2.2	0.6 ± 0.9
nb frames outside	2081 (2.2%)	150 (2.1%)	235 (13.7%)	3119 (0.6%)
total nb frames	95711	7173	1719	545535

Table II.19: Mean and sd distance between the CoP and BoS, for when CoP is outside, and percentage of times when it is outside.

body) lead to almost similar errors for quasi-static, low dynamic and highly dynamic motions. Because of inertias, these two models do not require the same computation time. In the same time, increasing the complexity of the model do not always improve the accuracy the ZMP computation. Thus, the particle model could be sufficient to compute ZMP for most of the applications.

Our experiments also confirmed that the difference between ZMP and FRI is not significant. For the whole set of single foot sequences of our biological captured motions, the average distance between FRI and ZMP was lower than 1mm. Thus, these results confirm that FRI is not fitted to measure rotational instabilities and are in agreement with the results of [Popovic 05].

In this Chapter, we also presented a method that classifies the position of the CoP in the base of support into three areas, corresponding to three levels of balance dangerousness. We made the assumption that balance is more likely to be endangered when the CoP lies close to the limit of the base of support.

However, these results highly depend on the computation of a correct base of support to evaluate the evolution of the distance to the base of support according to the CoP location. In computer animation, we usually model the base of support using a convex polygon. Thus, edges of the base of support are represented as straight lines and a criterion is binary: inside or outside the base of support. However, humans are made of soft tissues that imply a fuzzy base of support limit, where it is not always easy to keep balance.

As the CoP is required to belongs to the base of support, we evaluated if this constraint is satisfied at any time of our sequences. This evaluation was only done for the sequences which support sequences can be computed accurately enough. Table II.19 presents the percentage of frames where the CoP is actually outside the support polygon and the mean distance of the CoP to this polygon. Results show that the CoP almost never lies outside the base of support for double support motions (<0.3% and <0.5cm). However, this error increases up to 2.7cm for single supporting foot sequences, such as 90° turns, one foot support, jump or spins. This higher error could be explained by the simplification of the base of support compared to the real one. Furthermore, biologocal motions are often subject to important foot deformations, such as when jumping. Thus, it would be necessary to carry-out specific experiments with numerous markers on the feet of subjects to accurately estimate the base of support. Vibrations can also occur on the forceplate and create unstable measures during high dynamic motions such as jumping.

Based on the results of this experiment, one can say that it seems that there is no good criteria to accurately detect loss of balance. Because of the false alarms that are present in almost all motions, it

was not possible to automatically separate motions in balanced and unbalanced phases. Thus, analyzes of this Chapter rely on the fact that all motions where subjects do not make a step to recover are classified as balanced. For those where subjects make a step to recover balance, it is however impossible to automatically detect when balance was lost. The only exception is quasi-static motions where GCOM going outside the base of support prevents from going back to a quasi-static balanced pose.

Furthermore, the notion of limit of balance highly depends on each subject's feelings. For some of the motions studied in this Chapter, subjects had to perform the tasks while trying to keep balance as much as possible. When balance was lost, they were allowed to make a step to prevent from falling. However, the time when subjects feel the need to make a step to recover balance cannot be controlled experimentally. Thus, the limit of the balance status is a subjective condition that highly depends on the subject's feelings. For instance, one of our subject was an inline skater and demonstrated higher balanced skills than other subjects.

II.4 Conclusion

In this Chapter, we presented an experiment analyzing human balance for motions with different levels of dynamics. One of the main goals of this analysis was to measure the actual performance of criteria commonly used in the literature. Our experiments with highly dynamic motions clearly show that none of the tested criteria succeeded in accurately detecting balanced and unbalanced situations. They detected false loss of balance most of the time, while the subject is continuing his motion without any visible need to step or especially act to preserve balance.

Furthermore, as the ZMP is theoretically equivalent to the CoP, computing ZMP outside the base of support seems to be mainly due to inaccuracies linked to the model. For instance, we have shown that ZMP highly differs from CoP when high vertical accelerations occur (such as preparing a jump). Hence, designing a criterion based on detecting when CoP and ZMP go out of the base of support is difficult to justify from the biomechanical point of view. An explanation could be that it actually leads to torques applied to the feet, which should correspond to placing the CoP very close to the border of the base of support.

We have also shown that the nature of the model used to compute the ZMP may lead to more or less important inaccuracies. For instance, the pendulum model clearly fails to capture dynamic properties of motions, especially when the limbs are significantly moving. In the same idea, computing ZMP using a complex inertia-based model do not always increase the accuracy of the result. However, further experiments should be carried-out to evaluate how the results change using more complex systems, such as using more accurate models of the trunk or using accurate anthropometric parameters instead of approximated ones from de Leva tables.

In our opinion, XcoM seems to be a very promising criterion even if it fails, like the other ones, to detect loss of balance with a good accuracy for highly dynamic motions. Moreover, as it is based on velocities instead of accelerations (compared to ZMP), it would be more robust to noise in simulations or measurements. However, it should be extended to deal with highly dynamic motions. An idea could be to replace the inverted pendulum model by a more complex one, as people do for the ZMP.

However, one of the key fundamental question raised by these experiments is to clearly define what balance is in dynamic situations. From the experimental point of view, it is very difficult to determine the time at which the motion stops to be balanced and becomes to be unbalanced. In these experiments, none of the tested criteria succeeded in automatically detecting this time. Thus, specific protocols should be carefully designed to point this problem. This is a key problem that might be studied with a multidis-

ciplinary approach as it rises challenging experimental set-ups. It would be also very important to design a clear criterion to accurately detect the loss of balance in dynamic situations.

Related publications

French conferences

L. Hoyet, F. Multon, K. Mombaur and E. Yoshida (2009): Influence du choix du modèle sur l'estimation du centre de pression à partir du ZMP. Journées Nationales de Robotique Humanoïde, Nantes, Mai 2009.

Posters

L. Hoyet, F. Multon, K. Mombaur, E. Yoshida (2009): Balance in dynamic situations: role of the underlying model. Congrès de la Société de Biomécanique, Toulon, Septembre 2009.

L. Hoyet, F. Multon, K. Mombaur, E. Yoshida (2009): Balance in dynamic situations: role of CoP, XcoM and ground reaction force. ISPGR Satellite Symposium, Pavia, Italie, June 2009.

Chapter III

Perception of dynamic properties in virtual human motions

As shown in the previous Chapter, dynamics is important to simulate virtual humans with natural behaviors. In particular, dynamic balance is a key-point towards credible autonomous characters. However, characters also have to interact with their virtual environment. They may carry or move objects, perform actions with different speeds and forces, or simply navigate through a complex scene.

Animating virtual humans to perform such tasks involves taking many constraints into account, including dealing with the dynamic properties of the environment. It involves using more or less accurate models which computation time is proportional to complexity. Complex models may lead to very accurate simulations while people may not be able to handle and perceive such details in natural motions. A key point is thus to evaluate the perceptual skills of human beings when watching natural motions with physical interactions.

In this Chapter, we propose to evaluate the perceptual capability if human beings to distinguish differences in biological captured motions, especially for lifting motions with different weights (Figure III.1).

III.1 Background

Although Johansson [Johansson 73] have shown that global human motion can be perceived from only a small set of representative points, the problem becomes more complex when the movement is applied on a realistic virtual human. This well known paradox, coined by roboticist Masahiro Mori [Mori 70] as the *Uncanny Valley* (Figure III.2), states that the believability of a human-like character increases with the realism of the avatar, until it is visually too close to a real human still not behaving naturally to be considered as human-like (drop of believability).

Several researchers studied the effect of the quality of the virtual character or of its motion on user believability and their perception of errors. Hodgins et al. [Hodgins 98] showed that subjects are more sensitive to differences between pairs of motions when displayed on a polygonal character rather than a stick figure character. Similarly, Chaminade et al. [Chaminade 07] showed that the ability to discriminate between biological and non-biological motions was impaired when the motions were displayed on cloud point characters rather than polygonal models or even ellipse-made models. Thus, it is easier to perceive differences on complex model of the virtual human. When dealing with errors introduced in virtual

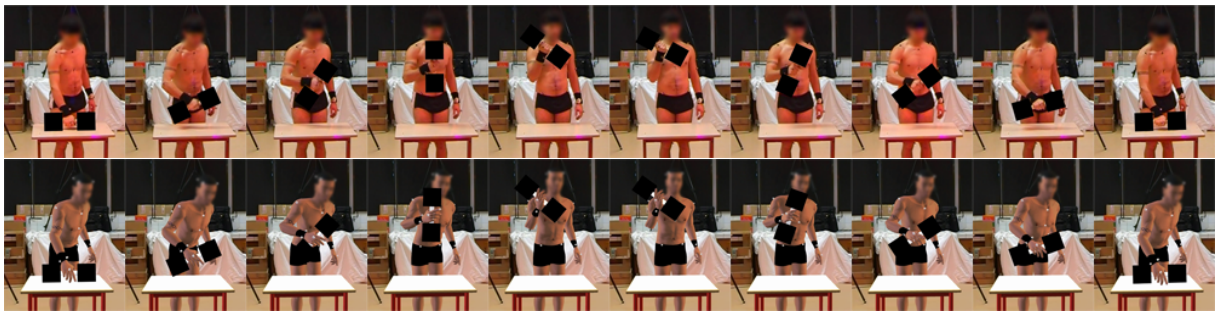

Figure III.1: Actor lifting a 6kg dumbbell: video of a real motion (top) and corresponding captured motion applied to a virtual human (bottom).

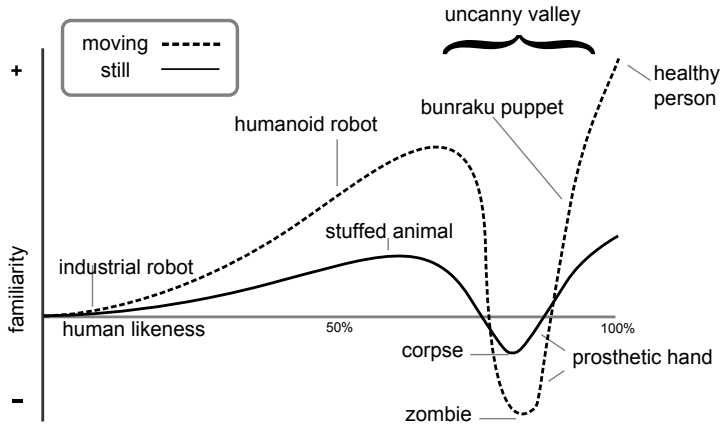

Figure III.2: Uncanny valley: "Hypothesized emotional response of human subjects is plotted against anthropomorphism of a human-like character, following Mori's statements. The uncanny valley is the region of negative emotional response towards robots that seem almost human. Movement amplifies the emotional response." [Mori 70, Wikipedia]

motions, Reitsma and Hodgins [Reitsma 08] demonstrated that errors in ballistic motions are more easily detected on realistic virtual humans than on simple objects such as spheres.

For the study of goalkeeper judgments, Vignais et al. [Vignais 10] showed that the graphical level of details of a virtual handball thrower and ball does not influence the goalkeepers' perception of the final position of the ball, except when the size of the ball is decreased. In their case, goalkeepers take information on the virtual thrower to anticipate the final location of the ball.

However, as more and more applications involve realistic virtual humans, it is important to simulate highly realistic motions. To achieve this goal, most of the current animation techniques rely on reusing motion capture data (such as using displacement maps [Witkin 95]), spacetime optimization [Witkin 88] or motion reorganization (such as using motion graphs [Kovar 02]). These techniques allow to satisfy a set of kinematic constraints linked to the environment and the size of the character. Despite these kinematic constraints, the virtual human is supposed to be subject to mechanical laws, as real humans are (Section I.4.1). Different methods presented in Section I.4 have been pro-

posed in the literature to take dynamics into account in virtual characters' motions, such as dynamic controllers [Hodgins 95, Wooten 96, Yin 07], adding dynamic equations as new constraints to space-time optimization processes [Liu 94, Liu 02, Fang 03], associating accurate passive physical simulation (reacting to external constraints) with a repertoire of prerecorded reactions [Zordan 05, Komura 05] or dynamic filtering motions on-the-fly to satisfy dynamic constraints [Yamane 03, Pollard 01]. All of these techniques could deal with dynamic constraints with different levels of accuracy. A key question is to determine which level of accuracy is required to ensure that a user correctly perceives the motion performed by the virtual human.

To overcome this problem, different authors proposed metrics to evaluate the fidelity or closeness of animations. Some authors built statistical models to automatically assess motion quality based on hand-labeled examples. Reinforcement learning have been used to develop automatic predictors that are able to determine if a motion will be perceived as plausible by users [Arikan 05, Ren 05]. Other works evaluate the physical correctness of interpolated motions and make suggestions for the generation of more natural looking motions [Safonova 05] or propose a dynamic-based metric for transitions generation in motion graphs [Matsunaga 07]. van Basten et al. [van Basten 09] evaluated the performance of three common distance metrics (joint angle, point cloud and Principal Component based metrics) and proposed a set of guidelines for using these distance metrics for motion generation. However, these metrics are still specific to a given problem and no generic means exists to evaluate the correctness or fidelity of virtual human animations. Furthermore, these metrics or predictors cannot quantify the actual sensitivity of the users to evaluate if the motion of a virtual human is appropriate to the current dynamic constraints, such as carrying more or less heavy objects.

O'Sullivan et al. [O'Sullivan 03] evaluated this type of sensibility for the specific case of collision between simple objects. They established non-symmetric thresholds for human sensitivity to dynamic anomalies through psychophysical experiments. They also showed that the tolerance for certain types of errors is significantly higher with the choice of realistic scenarios [Reitsma 09]. Yeh et al. [Yeh 09] took this approach one step further and identified the maximum error tolerance of each phase of physical simulation for complex scenarios.

Reitsma and Pollard [Reitsma 03] evaluated users' sensibility to errors in human motions, for the specific case of ballistic motions. They demonstrated that users are more sensible to changes in horizontal velocity, vertical velocity or gravity through a ballistic motion, especially when displayed on human-like characters. Majkowska et al. [Majkowska 07] generated dynamically-based aerial motions as combinations of existing captured aerial clips and studied users' sensitivity to errors in angular momentum and take-off angle of generated motions. They found that subjects were not sensitive to even significant changes in angular momentum during ballistic motion. For instance, a 25% increase in the angular momentum of the original motion was not perceived by participants. Also, a 30% change in the take-off angle was perceived as physically valid as original motions were.

Most of these previous works focused on establishing if a simulated motion is perceived as natural or not. A complementary problem consists in stating if people perceive dynamic properties of motions simulated on virtual humans. For example, is the user able to recognize a 5kg-lifting motion compared to a 4kg one? The closest work to ours has been performed by Runeson and Frykholm [Runeson 81] who asked subjects to evaluate the mass of a box lifted and carried by an actor represented either normally or with bright patches. Results showed that the mass of the box was well specified in the pattern of the

motion. Indeed, participants were able to linearly estimate the mass of the lifted box, with an average slope of 0.87 and a deviation of 3.8kg. It is then possible to estimate the mass of a box, but with a limited accuracy.

In this work, we focus on the perception of the minimal noticeable difference of lifted masses. On the contrary to the work of Runeson and Frykholm, we focus on small differences between masses. Thus, we propose to address the following problems:

1. From the biomechanical point of view, can we find relevant kinematic parameters that enable us to distinguish lifting motions with different masses? What is the accuracy of such parameters?

2. From the perceptual point of view, can people perceive this difference of weight with the same accuracy when watching videos of an actor's performance?

3. From the perceptual point of view, can humans perceive differences in biological captured motions of virtual humans lifting weights in virtual environments? Is this capacity different compared to watching videos?

With this aim, we captured a set of lifting motions with different masses ranging from 2kg to 10kg with a one-kilogram step. These motions were both captured with a motion capture system and a video camera. Motion capture data is used in the biomechanical study (Section III.2) to automatically distinguish lifting motions based on joint kinematics. Both video and motion capture data are used in the perceptual study (Section III.3). The goal is to compare users' perception of lifted masses through videos of real motions and the corresponding captured motions applied to a virtual character, as shown in Figure III.3.

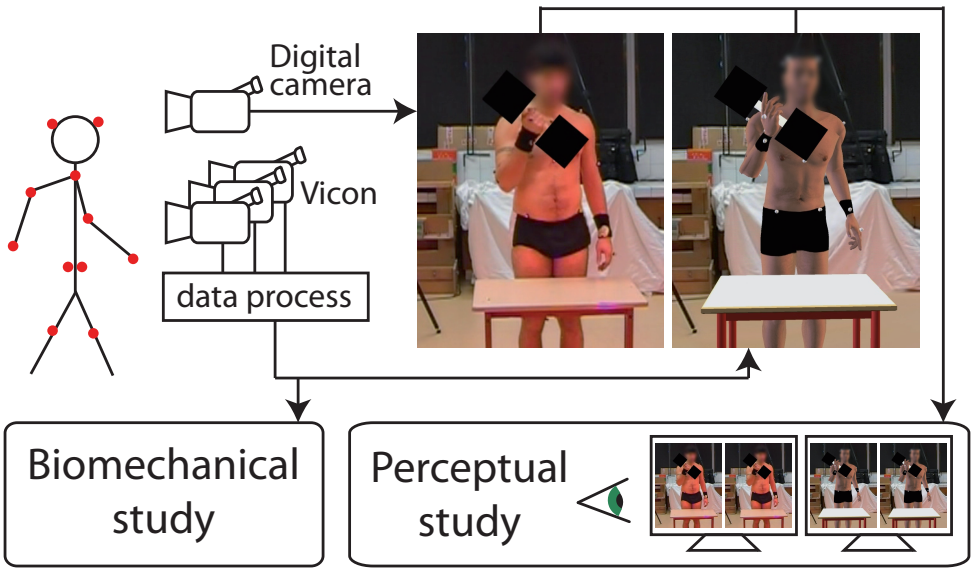

Figure III.3: Framework of the study. Captured motions are used to find if a statistical difference can be observed in joint kinematics of lifting motions associated with different masses. Videos of the actor and captured motions applied to a virtual human are used in the perceptual study.

III.2 Biomechanical study: can we distinguish captured lifting motions using joint kinematics?

This Section studies if significant differences exist in joint kinematics between lifting motions with masses ranging from 2kg to 10kg with a one-kilogram step.

III.2.1 Methods

III.2.1.1 Stimuli and Apparatus

Motion capture To capture these motions, an actor (1.84m, 82kg, 25 years old, normally trained) was asked to lift a dumbbell, carry it during approximately five seconds at shoulder height, then put it back at its original location (Figure III.1). The mass of the dumbbell ranged from 2kg to 10kg by steps of one-kilogram. The subject was asked to perform ten repetitions per weight. To ensure that motions were not affected by tiredness, weights were randomly organized and enough time of rest was given between successive capture sets. As the subject was carrying various weights, a training period was introduced before the ten repetitions. Twelve VICON MX40 cameras captured at 160Hz the 3D positions of 45 reflecting markers placed on the user's body (See [Zatsiorsky 90] and Figure II.8 for position of markers). For the experiments reported in this Section, the actor gave his informed consent prior to the experiment.

Motion selection To ensure that motions were compared on the same basis, we automatically extracted all the parts of the captured motions when the dumbbell was lifted. A lifting motions is cut into two parts: a *lifting* and a *dropping* part. These two parts start and end with a null velocity of the hand. The *lifting* part starts when the dumbbell leaves the table and ends when the dumbbell starts to be held at shoulder height with a minimum velocity. The *dropping* part starts with the dumbbell being dropped down and ends when it touches back the table. As the duration of the part when the character holds the dumbbell at shoulder height can vary, it was removed from the selection.

III.2.1.2 Procedure

To determine if it is possible to observe a significant difference in joint kinematics of lifting motions with different masses, we set up a statistical analysis. The goal is to compare the relevance of a set of criteria with real human perception. Thus, we decided to consider joint positions and velocity and to test if significant differences exist for these criteria for the hand, the elbow and the shoulder. Other criteria could have been studied, such as torques or angular momentum. However, as the final goal is to discriminate perceptual skills in lifting motions, we focused on the kinematic properties of the lifting arm. Indeed, the remaining dynamic parameters cannot be directly perceived by the subject.

The different studied criteria will be referenced as

Position-based	Velocity-based
p_h: hand position	v_h: hand velocity
p_e: elbow position	v_e: elbow velocity
p_s: shoulder position	v_s: shoulder velocity

As the same lifting motion can be performed with different manners, the comparison of raw trajectories is not possible: the dumbbell is not always exactly at the same position, the task duration varies and the amplitude of the motion differs between repetitions. Thus, postprocessing of the 3D trajectories is

needed before comparison. Each 3D trajectory $traj$ is first centered to have an average value equals to zero (Figure III.4.a). They are also time-warped to homogenize durations (Figure III.4.b). Starting and ending points are then set to the average starting and ending values of all the repetitions of the given mass (Figure III.4.c). This is done by adding an offset to the starting and ending points. This offset is then linearly interpolated and added to the trajectory to preserve its continuity.

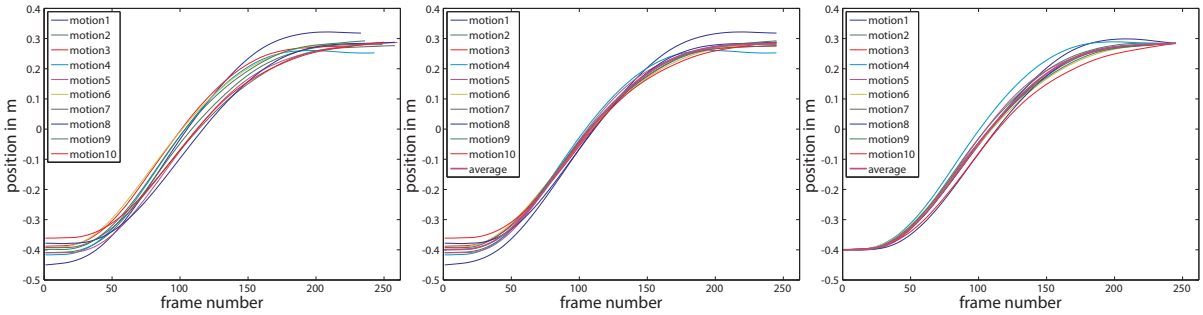

(a) (b) (c)

Figure III.4: Postprocessing process. Figure shows trajectories of the position of the hand for all 6kg lifting motions (lifting part only). a) Firstly, trajectories are centered to have an average value equals to zero. b) Secondly, trajectories are time-warped to obtain trajectories with the same duration. c) Finally, starting and ending points are set to the average starting and ending values of all the repetitions of the given mass.

Thus, the difference between two 3D trajectories $traj_1$ and $traj_2$ is computed using the Euclidean RMS distance $dist$:

$$dist(traj_1, traj_2) = \left\| \sqrt{\frac{1}{N} \sum_{i=1}^{N} (traj_1(i) - traj_2(i))^2} \right\| \tag{III.1}$$

where $\|.\|$ corresponds to the euclidean norm. Here, we do not use Dynamic Time Warping as it would discard the mass-dependent velocity adaptation.

For criterion $c_k \in \{p_h, p_e, p_s, v_h, v_e, v_s\}$, we evaluate the best representative motion of the set of motions associated with the same mass m_i using Equation III.2. This reference motion is called $ref_{m_i}(c_k)$. It corresponds to the motion with the minimum distance to the theoretical average motion for the mass m_i. Two outliers out of ten motions per set were discarded.

$$ref_{m_i}(c_k) = \min_{traj \in motion\_set_{m_i}} dist(traj, avg_{m_i}(c_k)) \tag{III.2}$$

where $motion\_set_{m_i}$ is the set of all repetitions associated with the same lifted mass m_i and $avg_{m_i}(c_k)$ is the average trajectory of all repetitions associated with lifted mass m_i for the criterion c_k.

For each criteria c_k, we tested if a statistical difference exists between each pair of two motion sets associated with two different masses. For a given mass m_i, criterion c_k finds a significant difference if:

$$\forall m_j \in [2..10], j \neq i, dist_{c_k}(motion\_set_{m_j}, ref_{m_i}(c_k)) \neq^{?} dist_{c_k}(motion\_set_{m_i}, ref_{m_i}(c_k))$$

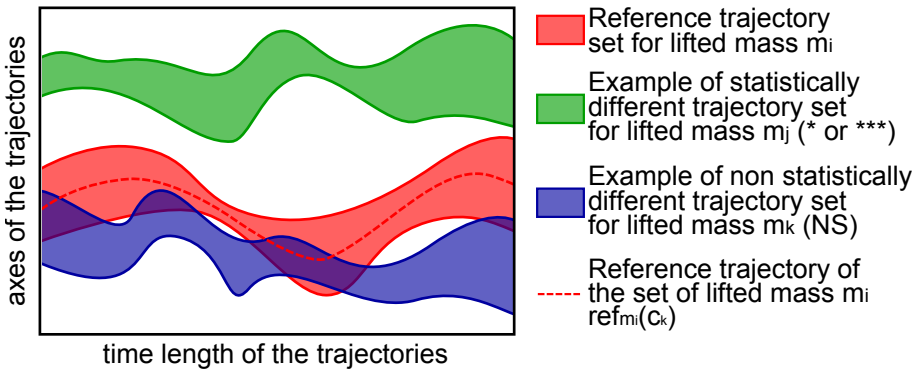

Figure III.5: Example of possible trajectory sets j with ($*$ or $***$ in green) or without (NS in blue) a statistical difference with the reference i (red). A statistical difference usually represents non-overlapping trajectory sets.

where $dist_{c_k}(motion\_set_{m_j}, ref_{m_i}(c_k))$ computes the distance of every trajectory belonging to $motion\_set_{m_j}$ associated with a lifted mass m_j to the trajectory $ref_{m_i}(c_k)$ (using Equation III.1). $\neq^?$ represents the test of a significant difference between computed distances. Thus, a significant difference exists for criterion c_k if the previous test holds for each mass $m_i \in [2..10]$. The accuracy of a criterion is then the percentage of significant differences detected between the motion sets of the two masses.

III.2.2 Results

For each criterion c_k, we ran a one-way ANOVA for each lifted mass $m_i \in [2..10]$ using Bonferroni t-test. Results are presented in Table III.1. Cell(i,j) contains an $*$ ($p < 0.05$) if there is a significant difference, $***$ if $p < 0.001$ and NS if no significant differences were found between reference mass m_i and mass m_j. An ANOVA on rank was used when the equal variance test failed (represented by a † in the first column). A significant difference between m_i and m_j represents the fact that trajectories are significantly different between lifted mass m_i and m_j based on criterion c_k. One has to notice here that if a difference is detected between motions lifting masses m_i or m_j, it is still not possible to determine which mass is the heaviest (examples in Figure III.5).

For position-based criteria, ANOVAs detect significant differences respectively in 59.7% (p_h), 65.3% (p_e) and 59.7% (p_s) of the cases for the hand, elbow and shoudler. Thus, position based criteria are not accurate enough to detect a difference between motions associated with different masses with a good reproductibility. Figure III.6 plots the trajectories of the hand for all the repetition of each lifted mass. It visually appears that there are few differences between trajectories associated with lifting motions with different masses, which is confirmed by the statistical analyzis.

We thus evaluate the same statistical values but with velocities instead of positions. Results showed significant differences in 83.3% (v_h), 86.1% (v_e) and 62.5% (v_s) of the cases for the hand, elbow and shoulder respectively. One has to notice that velocity of the shoulder is less relevant to discriminate lifting motions compared to the velociy of the hand and the elbow. Hence, the velocity of the hand and the elbow seem to be good candidates to discriminate motions associated with different masses. These criteria find significant differences in more than 80% of the cases, even for a one-kilogram difference in the mass lifted by the subject.

(a) Criterion p_h : hand position — 29 *NS* / 72 (40.3%)

	2	3	4	5	6	7	8	9	10	F(8,62) / H(8)
2										3.468
3										6.759
4										14.131
5										11.995
6										5.123
7										10.871
8										7.205
9										7.594
10										9.539

(b) Criterion p_e : elbow position — 25 *NS* / 72 (34.7%)

	2	3	4	5	6	7	8	9	10	F(8,62) / H(8)
2†										53.818
3										43.556
4										31.690
5										9.846
6†										60.073
7†										45.888
8										27.981
9										15.252
10										20.725

(c) Criterion p_s : shoulder position — 29 *NS* / 72 (40.3%)

	2	3	4	5	6	7	8	9	10	F(8,62) / H(8)
2										33.014
3†										56.490
4										8.436
5†										44.134
6†										51.114
7										12.302
8										20.806
9										13.186
10										21.214

(d) Criterion v_h : hand velocity — 12 *NS* / 72 (16.7%)

	2	3	4	5	6	7	8	9	10	F(8,62) / H(8)
2										24.840
3										28.929
4										17.939
5										20.308
6										26.011
7										36.074
8										21.521
9										11.839
10										20.147

(e) Criterion v_e : elbow velocity — 10 *NS* / 72 (13.9%)

	2	3	4	5	6	7	8	9	10	F(8,62) / H(8)
2										21.625
3										20.731
4										24.135
5										23.983
6†										36.450
7										10.906
8										7.932
9										11.964
10										12.582

(f) Criterion v_s : shoulder velocity — 27 *NS* / 72 (37.5%)

	2	3	4	5	6	7	8	9	10	F(8,62) / H(8)
2										18.844
3†										38.914
4										14.787
5†										46.349
6										16.613
7										11.316
8†										46.101
9										5.990
10										10.901

NS (no significant differences)
unadjusted $p < 0.05$ for ANOVA on ranks
$*$ ($p < 0.05$)
$***$ ($p < 0.001$)

Table III.1: One way ANOVA statistical differences for position and velocity based criteria. († represents data where ANOVA on rank was used in case of failure of the equal variance test.). In all cases, we obtained F(8,62) or H(8) with p≤0.001.

III.2.3 Provisional conclusion

Regarding the results of this first study, it is possible to measure significant differences in joint trajectories of lifting motions with different masses, even with a one-kilogram difference. Among the different studied criteria, hand and elbow velocities give the best results. These criteria enable us to distinguish joint trajectories of lifting motions in more than 80% of the cases. This result is in agreement with the results obtained by Bingham [Bingham 87] for a one degree of freedom lifting curl. He suggested that the drop of velocity occurring around half amplitude of the lifting curl could be a source of discrimination between masses.

Even if kinematic data enabled us to discriminate lifting motions with a one-kilogram difference thanks to statistical analyzes, we now wish to analyze is such a small difference can be perceived by people.

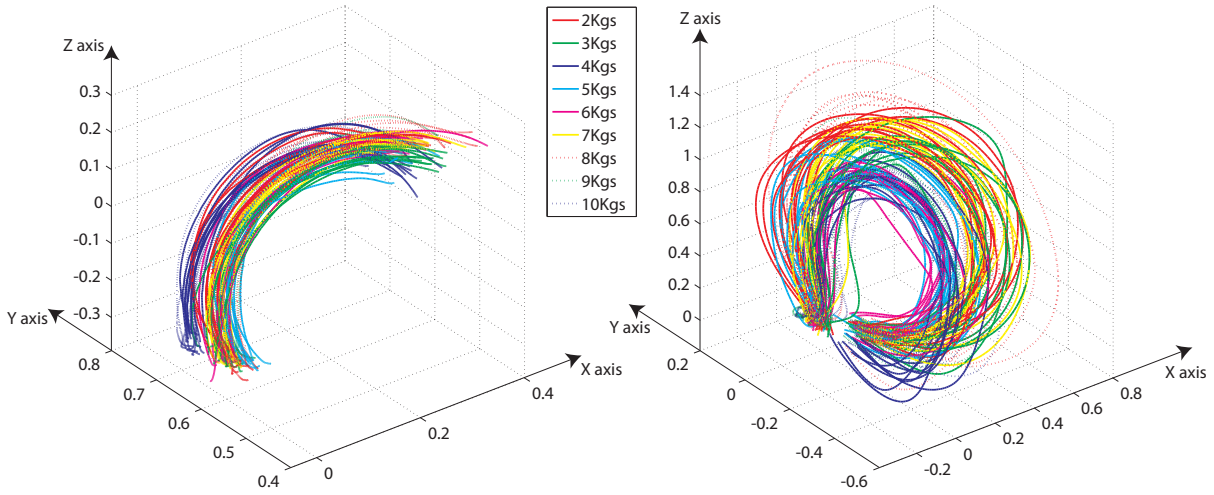

Figure III.6: Hand trajectories (left) and hand velocities (right) for every motion associated with each lifted mass.

III.3 Perceptual study: can humans perceive differences in biological captured motions in virtual environments

A key question consists in knowing if human beings are able to correctly estimate biological motions subject to various dynamic constraints. This experiment focuses on the perception of lifting motions in two situations: using videos of real motions and corresponding captured motions applied to a virtual human.

III.3.1 Method

Eighteen naive participants (15 males, 3 females) took part in this experiment (mean age: 26.83 years, SD: 5.77 years). All participants had normal or corrected-to-normal vision. The pool of participants was composed of a mix of master students (computer sciences or biomechanics), casual gamers, or subjects familiar and unfamiliar with computer animation. Participants gave their informed consent prior to the experiment.

They were exposed to pairs of lifting motions and had to estimate which motion corresponded to the heaviest lifted mass, using a 2-AFC (Alternated Forced Choice) protocol. Each pair was composed of either videos of real motions or captured motions applied to a virtual character. Three conditions were set up:

1. A **real condition** consisted in comparing pairs of videos, to evaluate if participants can perceive differences of weights through videos as accurately as a kinematic criterion does.

2. A **virtual condition** consisted in comparing pairs of computer animation sequences. This condition aims at studying if the perception performance when watching computer animation sequences is similar to watching the corresponding real videos.

3. A **real×virtual condition** consisted in comparing computer animation sequences with videos of real motions. The goal of this condition is to evaluate if users were able to correctly evaluate a video with a set of computer animation sequences.. In this last condition, each pair was composed of one video and one computer animation sequence.

To study the perception of lifted mass differences, each pair was composed of a 6kg reference lifting motion and a motion with another mass.

To eliminate a possible sequential bias, participants were separated into two groups:

1. **real condition** first (video), **virtual condition** second (computer animation sequences), **real× virtual** last

2. **virtual condition** (computer animation sequences) first, **real condition** second (videos), **real× virtual** last

Last condition was always **real× virtual**. Thus, all subjects had to participate to all the situations but in two possible orders.

III.3.1.1 Stimuli and Apparatus

Setup Participants were comfortably seated in front of a 20inches desktop screen with a resolution of 1,600×1,200 pixels. They were instructed to sit at their preferred distance to the screen, on which the motions were displayed. The visual stimulus consisted of the display of lifting motions associated with different masses, either with videos or computer animation sequences with a virtual human (Figure III.1). The experiment runs on a standard computer, (2.66GHz Dualcore processor, 2Go RAM, NVidia Quadro FX 3500). The videos of the real motions were displayed at 25fps (capture frame rate of the camera) and the virtual motions were displayed in real-time (120Hz). Each real motion (video) corresponds to a unique captured motion. In order to eliminate the cues provided by the dumbbell and actor's facial expressions, dumbbell and actor's head were masked in both video and computer animation sequences.

Displayed motions Among all captured motions, it was necessary to select one representative motion for each lifted mass. The biomechanical study demonstrated that it is possible to discriminate captured lifting motions using hand or elbow velocities. For the reference lifting motion of 6kg, the equal variance test prior to the ANOVA failed for the elbow velocity criterion (Table III.1). As both hand and elbow velocities give almost similar discrimination results, we automatically selected motions used in this experiment (videos and corresponding virtual motions) using the criterion *hand velocity* (v_h). These motions are those referred as $ref_{m_i}(v_h)$, with $m_i = 2..10kg$. The VICON MX40 motion capture system was synchronized with a camera (25Hz capture rate, resolution of 720×576 pixel). The camera was placed at eye's height, far enough from the scene to capture the actor from head to mid-calf.

III.3.1.2 Procedure and experimental design

Each participant performed 500 trials, consisting of

- **real condition** (160 trials): the 6kg reference video is compared to videos where the lifted mass is 2, 3, 4, 5, 7, 8, 9 or 10kg.

- **virtual condition** (160 trials): the 6kg reference computer animation sequence is compared to computer animation sequences where the character lifts a mass of 2, 3, 4, 5, 7, 8, 9 or 10kg.

- **real×virtual condition** (180 trials): the 6kg reference video is compared to computer animation sequences where the character lifts a mass of 2, 3, 4, 5, 6, 7, 8, 9 or 10kg. Thus, the real 6kg reference is thus also compared to its corresponding 6kg virtual motion.

For each condition, each pair comparing the 6kg reference with another mass is repeated 20 times. All pairs are randomly organized. After each trial, participants clicked on a button to indicate which motion seemed to be carrying the heaviest mass. They also gave a confidence mark concerning their answer from 1 (not sure at all) to 7 (totally sure) on the Likert scale.

Participants visualized examples of the task before each session, but we did not provided any information about the lifted masses or the examples. Then, they started the session when ready. Each motion of a pair was successively displayed on the screen. Participants were allowed to give their answer after the end of the second motion. A break was set up every 15 minutes. Participants were given as much time of rest as needed, and some refreshments were offered.

After each session, participants were asked to fill-in an intermediate questionnaire, as well as a final one after the last session. These questionnaires are presented in Appendix D. They focused on the cues used by participants to differentiate lifting motions. Intermediate questionnaires ask information about the different strategies and cues used to differentiate lifting motion for the specific condition of the session. Then, the final questionnaire covers the differences/similarities of strategies between the different conditions. It also deals with participant's feeling of the naturalness of the simulation and the difficulty of the task.

III.3.2 Results of the real and virtual conditions

Performance Participants were separated into two groups corresponding to the two possible condition orders. No significant difference appear between groups using a Two Way RM ANOVA (Bonferroni t-test with $p < 0.05$) on the effect of the group ($F(1,2)=1.520$, $p = 0.235$ for real condition results and $F(1,2)=1.112$, $p = 0.307$ for virtual condition results). Thus, it seems that the order of the conditions (real then virtual or virtual then real) does not affect the performance.

Figure III.7 presents the percentage of times when each compared mass $m_j \in [2..10], j \neq 6kg$ is considered heavier than the 6kg reference mass for real (blue bars) and virtual (green bars) conditions.

For the real condition based on videos, light masses (2kg and 3kg) present high discrimination performances when compared to the 6kg reference (considered lighter in 97.5% and 95.28% of the cases). The 10kg mass is estimated heavier than 6kg in 75% of the cases, while the 4kg mass, closer to the reference, is still correcly estimated in 71% of the cases. Results for other masses are more difficult to interpret. The 5kg mass is considered mainly heavier than the reference, while masses of 7kg and 8kg are considered lighter than the reference in more than 70% of the cases. The 9kg mass is considered slightly heavier than the 6kg reference (58%). Furthermore, standard deviations are globally high. It seems to demonstrate the difficulty for the subjects to correctly order lifting motions between 5kg and 8kg. Let us consider now if there exist differences between the real and the virtual conditions.

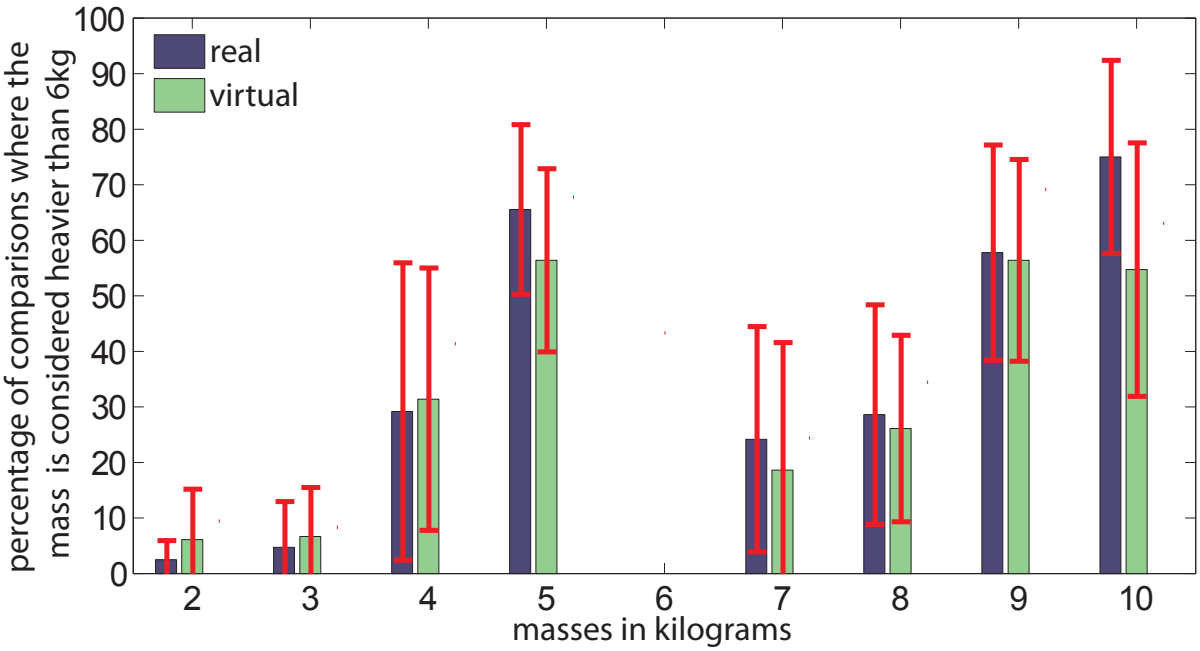

Figure III.7: Discrimination results: percentage of comparisons where compared mass $m_j \in [2..10]$, $j \neq 6kg$ is considered heavier than the reference mass of 6kg for real (blue bars) and virtual (green bars) conditions

To study the effect of the condition (real versus virtual) on the mass perception, we ran a Two Way ANOVA with Repeated Measures using Bonferroni t-test ($p < 0.05$) on the effect of the condition. No significant differences were found between the real and virtual conditions (F(1,2)=4.214, $p = 0.056$). This suggests that users tend to perceive differences between lifting motions in real and virtual environments with similar accuracy and performance.

With a post-hoc Bonferroni t-test ($p < 0.05$) on the effect of the condition on each mass, significant differences were only found for 10kg (Table III.2). The discrimination performance of 10kg relatively to 6kg is higher for the real condition than for the virtual one. This suggests that there are still potentially small differences between videos and captured motions, but they do not really interfere with the global performance of users.

	2	3	4	5	7	8	9	10
real vs virtual	*NS*	*NS*	*NS*	*NS*	*NS*	*NS*	*NS*	*

Table III.2: Results of ANOVA concerning the effect of real and virtual conditions for each mass. Results show that significant differences exist between real and virtual conditions only for 10kg.

To determine if there exists a minimum difference for mass perception, we ran a psychophysical analysis for computing just noticeable differences (JND) [Gescheider 85] using the Matlab Toolbox PsiGniFit. However, it was not possible to extract correct information and to compute JND due to the shape of the resulting fitted psychometric curves. This is certainly due to the sampling of the manipulation

masses (one-kilogram step) as results show that subjects are unable to discriminate 5kg to 8kg lifting motions compared to lifting 6kg.

According to the results of the experiment, it seems that the perception of lifting motions is very close in real and virtual environments. However, human beings are globally not able to accurately perceive small differences on lifting motions for a mass scale ranging from 2kg to 10kg. Results presented in Figure III.7 tend to show that a difference is perceived when comparing the 6kg reference with masses under 4kg and above 9kg. It corresponds to a difference of 50% of the reference mass for our special case, with a possible non-symmetric difference between comparisons with lighter and heavier masses. Under this threshold (approximated JND), it seems that humans are not able to accurately estimate which motion is associated with the heaviest mass. However, if this threshold seems correct for light masses compared with 6kg, it might be underestimated for heavier masses.

Questionnaire Some questions included in the questionnaire were related to the cues used by the subjects. Participants had to select criteria that they used for comparing motions (Table III.3). Results show that participants mainly used velocity over position-based cues. Some subjects specifically reported to have especially used "velocity at the beginning of the lifting" and "velocity just before putting the dumbbell back on the table". Many participants also reported to have used shoulder velocity to compare motions. However, our experiment demonstrated that this criterion failed to distinguish joint kinematics for lifting motions with different masses (Section III.2). Three participants did not answer these specific questions and were not able to tell which criterion they had used.

	Position	Velocity
Hand	2	6
Elbow	3	7
Shoulder	4	9

Table III.3: Questionnaire results: cues used by participants to discriminate lifting motions (Multiple answers were possible).

Participants also reported to have used other cues such as muscle contractions for discriminating real lifting motions. Some participants changed their strategy between real and virtual conditions "because for virtual humans you do not see muscles contractions" or "in videos of real motions you can observe muscle contractions". One participant "expected to see muscle contractions on the virtual human". Many participants also reported to have used a more global strategy for comparing virtual motions: "global pose of the virtual human", "motion of the shoulders", "balance of the virtual character" or "the motion of the lifting hand". The fingers of the avatar were not animated and two participants reported that "the hand was static" or "I was a little bit disturbed by the hand not completely grasping the dumbbell". One participant reported: "I noticed that the fingers were not completely around the dumbbell bar, but it did not matter".

Naturalness of the animations was also a key point of the comments. Participants felt that animations were similar to real motions: "similarities in the way of lifting the dumbbell" or "the virtual human modifies its posture to ensure balance when lifting a weight". However, many participants reported that virtual motions seemed lifting lighter masses: "virtual motions seem to give a lighter feeling of the mass" or "the absence of muscle contractions makes the virtual character more rigid and gives the feeling that the virtual mass is lighter".

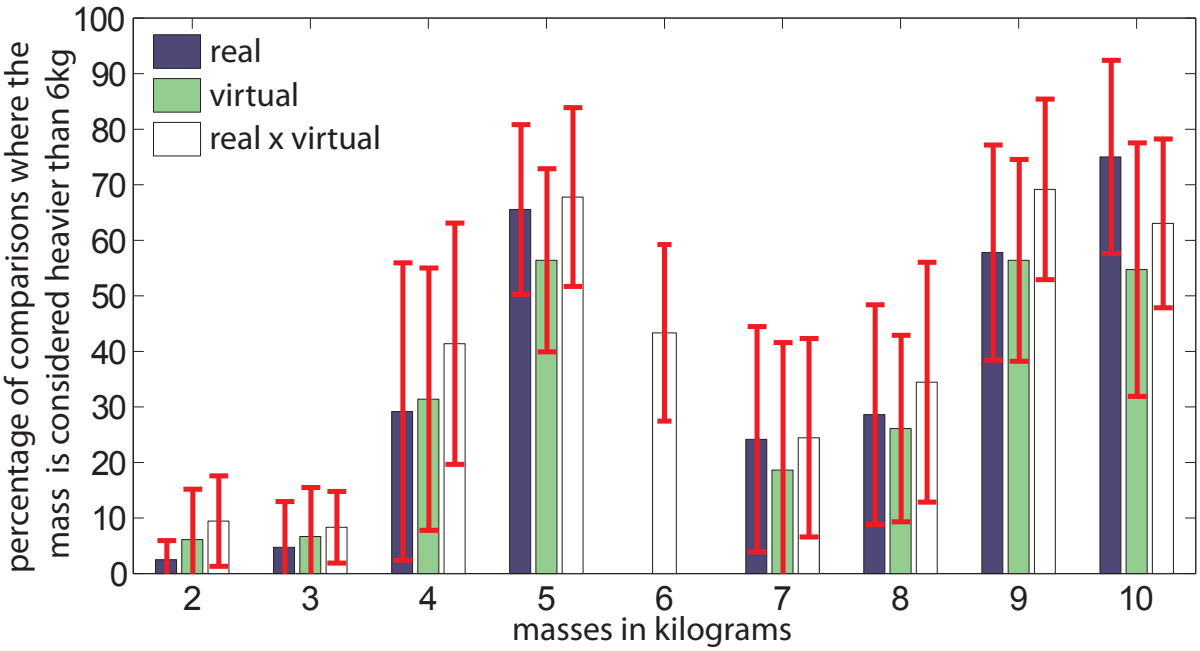

Figure III.8: Discrimination results: percentage of comparisons where compared mass $m_j \in [2..10]$, $j \neq 6kg$ is considered heavier than the reference mass of 6kg for real (blue bars), virtual (green bars) and real×virtual (white bars) conditions

The similarity of the avatar with the real subject was also addressed by comments, such as "the avatar was really similar to the subject". Only one participant had the felling that "the morphology of the real and virtual humans were different and gave the feeling that weights were heavier for real motions".

The overall perception was that "comparisons were more difficult between virtual motions than between videos". One subject reported that "comparisons are really difficult in 60% of the cases and quite easy in 30%, but almost never in between". This comment represents the global performance of subjects well.

III.3.3 Results of the real×virtual condition

In this Section, we aim at estimating how computer animation sequences with a virtual character are perceived when compared to videos of real motions. We thus set up an additional experiment consisting in comparing computer animation sequences to videos. Results of this experiment are plotted on Figure III.8 (white bars), with the results of real and virtual experiments as a reminder. It presents the percentage of comparisons where each mass $m_j \in [2..10]$ is considered heavier than the reference mass of 6kg for the three conditions. For the real×virtual condition, the reference 6kg motion is always a real video and is compared to computer animation sequences with a virtual human.

To evaluate if the performance is impaired when comparing concurrently computer animation sequences and videos, we ran a Two Way ANOVA with Repeated Measures using Bonferroni t-test ($p < 0.05$) on the effect of the real×virtual condition relatively to the two other (real and virtual conditions). No

significant differences were found between the real×virtual and real conditions (F(1,2)=4.349, p = 0.052). However, we found a significant difference between the real×virtual and virtual conditions (F(1,2)=8,645, p = 0.009).

Table III.4 presents the result of post-hoc Bonferroni t-tests ($p < 0.05$) on the effect of the condition on each mass, for real×virtual condition relatively to real or virtual conditions. Significant differences were only found for 4kg, 9kg and 10kg between real×virtual and real conditions. Similarly, significant differences were only found for 4kg, 5kg and 9kg between real×virtual and virtual conditions.

	2	3	4	5	7	8	9	10
real×virtual vs real	*NS*	*NS*	*	*NS*	*NS*	*NS*	*	*
real×virtual vs virtual	*NS*	*NS*	*	*	*NS*	*NS*	*	*NS*

Table III.4: Results of ANOVA concerning the effect of real×virtual vs (real or virtual) conditions for each mass. Results show that significant differences exist between real×virtual condition and the other conditions in some cases.

Furthermore, the comparison of the real and virtual 6kg motions shows that the real motion is considered heavier than the virtual motions in 57% of the cases. However, the standard deviation is 15.9%. Thus, it seems that real and virtual motions are mostly considered as similar, but this result is difficult to validate. We can just conclude that computer animation sequences did not lead to completely different perceptual performances.

Regarding the results of the real×virtual condition, it seems that the performance when comparing real and virtual lifting motions together is similar to the performance when comparing them separately. However, it is difficult to estimate if comparisons of real motions with virtual motions is a natural task.

III.4 General discussion

This Chapter presented a two-steps study to evaluate if human beings are able to distinguish differences in natural lifting motions with various masses in virtual environments.

The first experiment of Section III.2 showed that kinematic data (mainly hand and elbow velocities) enable us to distinguish lifting motions with different masses with only a one-kilogram difference. However, statistical analysis only demonstrates evidence of differences between these motions, but it does not help to determine which motion is associated with the heaviest mass. Furthermore, it is clear that the relevant kinematic data for a lifting motion may be inappropriate for other types of motions, such as pushing, pulling, boxing, etc. The biomechanical study (see Section III.2) used in this work could be reconducted for any new studied motion to determine the relevant kinematic parameters if they exist. However, it provides us with the idea that kinematic data can convey dynamic information with at least a 10N accuracy.

To improve our method, other parameters should also be investigated. For instance, the choice of the actor highly influences the captured motions, especially when heavy masses are implied. Different motor strategies are also available to perform lifting motions depending on the lifted mass. Thus, the performance of the statistical analysis requires to be validated thanks to specific biomechanical analyzes and experiments. An interesting future lead would also be to express the different studied masses according to the maximal lifting performance of actors.

Concerning the velocity profile of lifting motions, Figure III.9.a presents the evolution of the hand velocity for the lifting part of the motions referred as *references* $ref(m_i)$ in the previous experiments. It

appears that the peak of the velocity profile is continuously shifted according to the increase of the mass, until a given threshold. When this threshold is reached, we observe a complete change of strategy on the velocity profile.

To study the shift of the velocity profile, we analyzed both the average maximal velocity and the average time delay introduced by the increase of the mass. Figure III.9.c presents the average maximal velocity for lifting and the average minimal velocity for dropping. For comparison, Figure III.9.d plots the average maximal acceleration and deceleration. As in Figure III.9.a, we observe that the average velocities and accelerations decrease according to the increase of the mass, until a given threshold. Then, a change of strategy occurs. Figure III.9.b also presents the average time delay before lifting according to the lifted mass. Thus, these results seem to show that actors can suddenly change their strategy when the mass parameter changes.

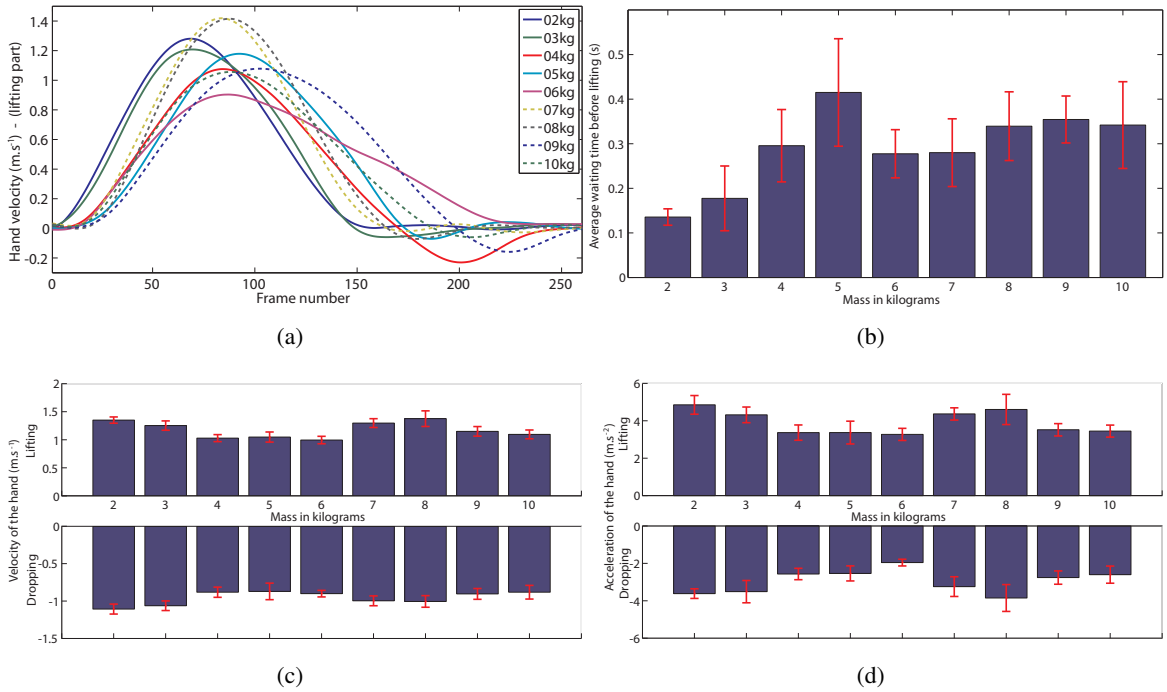

Figure III.9: a) Hand velocity for the lifting part of the reference motions. b) Average time delay at the beginning of lifting according to the lifted mass. c) Average maximal velocity for the lifting parts (up) and average minimal velocity for the dropping parts (down). d) Average maximal acceleration for the lifting parts (up) and average maximal deceleration for the dropping parts (down).

The experiment described in Section III.3 compared the perception of lifting motions in videos or computer animation sequences with virtual humans. Participants reached very close levels of accuracy for both conditions, which seems to show that human beings are able to compare real and virtual motions with the same accuracy. However, it seems that the discrimination performance of the 10kg motion is still slightly higher for video than for the corresponding computer animation sequences. In this experiment, we only used a fully detailed character to perform virtual motions. To evaluate the effect of the virtual human representation on the performance of participants, it would be interesting to compare the perception of virtual motions using more or less complex characters (point light display, stick figure or fully textured character) with different morphologies.

However, our results also show that subjects are not able to perceive a one-kilogram difference as accurately as biomechanical criteria perceive differences in joint kinematics. Indeed, it seems that subjects perceived only a difference of at least half the mass of our reference motion.

The current study also showed that velocity-based criteria appear to be good candidates to distinguish lifting motions. However, one may wonder if these criteria are in agreement with the cues used by users to visually compare lifting motions. The questionnaires filled by participants (Section III.3.2, Table III.3) show that they mainly used velocity over position-based cues. They reported to have mainly used the velocity at the beginning of the lifting and just before putting the dumbbell back on the table. However, contrary to results obtained in the biomechanical study showing that shoulder velocity does not manage to distinguish motions with different masses, many participants reported to have used this criterion to compare the lifted masses. Some information not linked with joint kinematics of the shoulder could thus be used by participants to perceive dynamic properties.

Furthermore, many participants reported to have used other cues, such as muscle contractions, for discriminating real lifting motions. This information is not delivered in the virtual environment. In the same way, they reported that many details were erased in the virtual environment, forcing them to focus on other relevant dynamic cues. Thus, the process transforming capture data in virtual 3D motions could work as a low-pass filter keeping only some of the relevant kinematic information. Despite this filter, the performance of participants in the virtual environment was rather close to the one obtained with the video.

Discrimination of masses close to the reference of 6kg are difficult to analyze and present high standard deviations. It is not possible to correctly fit a psychometric function on the data to evaluate the Just Noticeable Difference (JND). Different participants achieve different levels of accuracy, some being better in estimating differences with lighter or heavier weights. The difficulty may also come from the selected motions. However, variability of the natural human motion makes it impossible to ensure an exact reproductivity of successive lifting motions for the same mass, and even two identical lifting strategies when lifting different masses.

Globally, our results showed that the process of applying motion capture data to a virtual human does not seem to impair the perception of users. It suggests that motion capture data still convey the important dynamic properties captured on the real actor.

III.5 Conclusion

In this Chapter, we showed that it is possible to distinguish captured motions associated with different lifted masses using criteria based on joint kinematics. Furthermore, the performance of human perception seems very similar in real and virtual environments. Participants were able to compare almost as accurately videos of real lifting motions and computer animation sequences using motion capture data. Somehow, it shows that dynamic properties of natural motions are preserved during the animation process (from motion capture to adaptation to the virtual human's skeleton). However, human perception does not globally reach the accuracy obtained with a well chosen biomechanical criterion.

One of the main goals of this study is to provide animators with a better knowledge on the sensitivity of human beings to perceive motions of a virtual human. Results tend to suggest that there is no need to design motions with a one-kilogram resolution as this is not perceived by an external user. VE designers could thus design only limited sets of motions without decreasing the realism of scenarios. In the same way, if the animation is based on dynamic solvers, it would be possible to run the solver only when the

difference of mass is distinguishable.

However, this work is a first step in the acquisition of knowledge about the perception of dynamic properties. It would be interesting to further extend the lifted mass scale to obtain better knowledge about the minimum perceived mass in virtual environments. Different questions also arise about the scalability of mass perception. Should the minimum perception mass be expressed as a relative or an absolute value of the reference mass? Is this minimum perception mass linear when increasing the presented weights, as the estimation of the mass of the box in Runeson's works [Runeson 81] was? How does the muscular skills of the subject influence the perception of the lifted mass? Furthermore, motion capture data showed that changes in motor strategies occur according to the lifted mass. It would be interesting to evaluate if similar changes in motor strategies occur in other motions. Another lead concerns future studies of other highly dynamic motions, such as sport performances.

Related publications

International conferences

L. Hoyet, F. Multon, T. Komura and A. Lecuyer (2010): Can We Distinguish Biological Motions of Virtual Humans? Perceptual Study With Captured Motions of Weight Lifting. Proceedings of ACM Virtual Reality and Software Technology VRST 2010, pages 87-90, 22-24 November, Hong-Kong, 2010.

L. Hoyet, F. Multon, T. Komura and A. Lecuyer (2010): Perception based real-time dynamic adaptation of human motions. Lecture Notes in Computer Science, MIG2010 special issue, Volume 6459/2010, pages 266-277, 2010.

Chapter IV

Perception based real-time dynamic adaptation of human motions

As virtual humans are more and more used to populate virtual environments, realistic interactions with virtual environments is a key issue toward credible autonomous virtual character. In these environments, characters may carry or move objects, perform actions with different speeds and forces, or simply navigate through a complex scene while being subject to different constraints. As human motion is subject to physical laws, it is necessary to develop algorithms to make virtual characters behave in a dynamically correct way.

In such applications, users often interact in real-time with the simulation to control different parameters, such as driving the character in order to catch an object, applying perturbations, or modifying different parameters of the environment (gravity, stronger wind, etc). To satisfy the real-time constraints of the application, a key point lies in computation time to solve dynamics. Application designers have to deal with the compromise between accuracy and computation time.

However, more than naturalness, the way a motion is perceived by a user is the key point in many applications. A paradox is that some animations may look natural while the physical laws are not completely satisfied, such as animating cartoon characters. In the last Chapter, we have evaluated the sensitivity of users to perceive the physical properties of the virtual environment for a specific case. We also showed that the velocity profile seems to convey relevant information about the dynamic status of the motion.

In this Chapter, we describe how to use this knowledge to develop an efficient method to adapt the motion of virtual humans subject to various physical perturbations. It presents a perception based technique for real-time adaptation of dynamic motions of virtual humans when the dynamic properties of the captured motion are modified to satisfy new constraint. This method does not intend to dynamically transform a pushing motion into a dynamically correct punching or kicking motion but explores the possibility of adapting the current motion to a close situation (pushing a heavier object, lifting a lighter box, pulling with two hands because of the mass of the object, etc). We demonstrate the power of our approach on the adaptation of various motions subject to new dynamic constraints. Furthermore, we demonstrate that it is a highly real-time approach, being able to handle the dynamic of numerous characters at the same time.

IV.1 Background

Various approaches have been proposed in the literature to take dynamics into account for the animation of virtual humans. These approaches have been reviewed in Chapter I (Section I.4). To summarize, they are mainly divided into the following categories: dynamic **controllers**, **spacetime constraints optimization**, dynamics using **databases of motion capture data** and **dynamic adaptation**.

Controllers are usually associated with a dynamical model that enables the controller to compute the appropriate forces to drive the system to the desired state [Raibert 91, Hodgins 95, Wooten 96, van de Panne 94, Laszlo 96, Wooten 00, Faloutsos 01a, Faloutsos 01b, Zordan 02, Yin 07, Macchietto 09, Coros 10, de Lasa 10, Mordatch 10, Wang 10, Wu 10]. However, controllers are specific to a motion, or a family of motions, and are designed using the knowledge on this specific motion. Thus, it is necessary to design a new controller for each specific motion. Furthermore, resulting motions are not always natural looking, even if dynamically correct.

Spacetime constraints optimization has been introduced to increase the naturalness of generated motions. This process computes the whole trajectories of the motion based on dynamic constraints introduced in an objective function (prevent foot penetration, minimize energy or joint torques, etc) [Liu 94, Liu 02, Fang 03, Safonova 04, Liu 05]. However, this approach implies to compute the whole motion, which is not compatible with interactive applications.

Thus, Motion capture databases have been introduced to benefit from the naturalness of capture motion data. Different approaches have been proposed, mainly to produce dynamically correct sequences using a repository of pre-captured motions, such as reactions to unexpected perturbations [Zordan 05, Komura 05, Arikan 05, Mitake 09]. However, both the resulting animation and computation time highly depend on the number and diversity of motions in the database. Furthermore, if no correct motion exist in the database, a wrong reaction can be selected.

To solve this problem, a solution consists in adapting a unique motion subject to dynamic constraints that were not present in the original motion (dynamic adaptation approaches). The main approach, called dynamic filters [Yamane 00, Yamane 03], predicts a dynamically correct posture (using a Kalman filter) to eliminate unfeasible poses. However, many parameters have to be tuned and the quality of the resulting motion depends on the predictive model.

In this Chapter, we focus on the adaptation of a unique motion subject to new external perturbations. Our goal is to be able to easily adapt a motion to various situations without using pre-captured reactions or learning. Furthermore, we focus on reaction to continuous external perturbations that a virtual character has to compensate (not undergo). For instance, a virtual character who is turning should bend in the center of the curvature to compensate centrifugal forces and not passively fall due to these forces.

Different approaches focused on taking continuous perturbations into account, especially for pushing or walking against the wind. For instance, Ko and Badler [Ko 96] used inverse dynamics to compute the joint torques of a kinematically-generated locomotion. The resulting torques are then used to ensure that the ZMP remains inside the base of support by rotating the pelvis by a magnitude proportional to the balance error (user-defined parameters). Furthermore, a balance comfort module ensures that joint stress is kept within empirical strength data by driving the high-level parameters of the kinematic locomotion generator.

Similarly to our problematic, Aydin and Nakajima [Aydin 99a, Aydin 99b] addressed the problem of positioning articulated characters using dynamic constraints with an emphasis on balancing. In their method, each joint contributes to the control of the character in proportion to its influence on balance.

However, the inverse dynamic computation at each joint prevents real-time animation of numerous characters.

All the above methods aim at generating an almost physically-valid motion which requires high computation time and sometimes complex dynamic models. However, previous Chapter demonstrated that users do not accurately perceive small differences in dynamic properties, which was also demonstrated on other experiments in [O'Sullivan 03, Reitsma 09, Majkowska 07, Yeh 09].

Using this knowledge, we present a perception based method for producing dynamically-like motions with only few computation time and complexity. It is based on rough physical approximations and biomechanical knowledge to adapt the motion according to external forces. For instance, we adapt pushing and pulling motions to handle heavier or lighter interactions.

Furthermore, when real humans interact with their environment, they naturally prepare themselves for the upcoming action to perform. For instance, humans decrease their step length before starting climbing stairs [Laurent 88], look towards the direction where they want to go before turning [Hicheur 05a, Hicheur 05b], etc. Thus, virtual character have to anticipate their upcoming actions especially they are subject to physical interactions with the environment.

The framework of our method is presented in Figure IV.1.

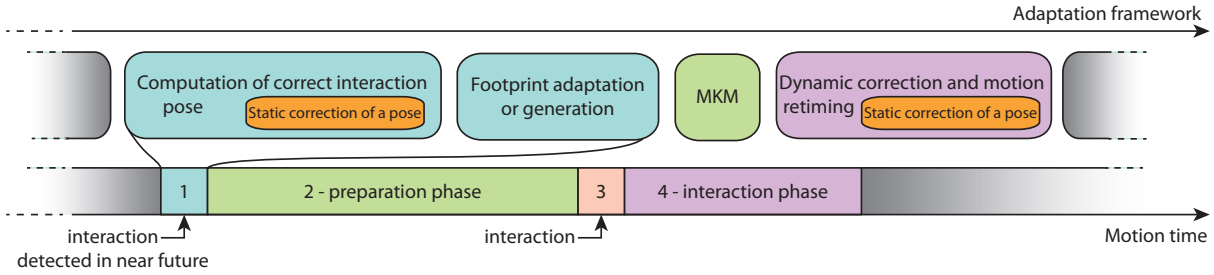

Figure IV.1: Framework of the method. When an interaction is detected in a near future (1 - blue frame), the system adapts the pose (3 - pink frame) depending on the additional external forces assuming zero acceleration. This adaptation may require adapting the footprints at interaction time leading to replanning the foot sequence prior to the interaction time (2 - green sequence). After the beginning of the interaction, poses are corrected in real-time according to the external forces (4 - purple sequence).

IV.2 Real-time dynamic adaptation of human motions

If we consider the global system of the virtual human, Newton laws give:

$$\begin{cases} \mathbf{P} + \mathbf{GRF} + \sum_j \mathbf{F}_j & = & m\mathbf{a} \\ \mathbf{OG} \times \mathbf{P} + \mathbf{OCoP} \times \mathbf{GRF} + \sum_j \mathbf{OA_j} \times \mathbf{F}_j & = & \dot{\mathbf{H}}_{\mathbf{O}} \end{cases} \tag{IV.1}$$

where $\mathbf{P} = m\mathbf{g}$ is the weight force acting on the character applied at its center of mass G, $\mathbf{GRF}$ is the ground reaction force applied at the position of the center of pressure CoP, $\mathbf{a}$ is the acceleration of G and $\dot{\mathbf{H}}_{\mathbf{O}}$ is the derivative of the angular momentum of the character computed at O. The character is also

subject to j external forces $\mathbf{F_j}$ applied respectively at the position A_j . We assume here that the original motion did not involved dealing with such forces. Thus, adding forces $\mathbf{F_j}$ involves changes in all the other terms to satisfy this equation. If the virtual human has to push a 40kg-object 1m far from his center of mass, $\mathbf{OA}_j \times \mathbf{F}_j$ is almost 400Nm which is very important.

To avoid solving nonlinear differential equations we propose to divide the solving process into three steps

1. solving the system in the static situation (static correction of a pose, Section IV.2.1),
2. adapting the motion performed before the interaction, named the preparation phase (Section IV.2.2),
3. adapting the velocity profile of the interaction phase (Section IV.2.3), as it has been identified to be relevant in the previous experiment of Chapter III.

IV.2.1 Static correction of a pose

Assuming that the terms involving acceleration can be ignored, Newton's equations become:

$$\left\{ \begin{array}{rcl} \mathbf{P} + \mathbf{GRF} + \sum_j \mathbf{F}_j & = & \mathbf{0} \\ \mathbf{OG} \times \mathbf{P} + \mathbf{OCoP} \times \mathbf{GRF} + \sum_j \mathbf{OA_j} \times \mathbf{F}_j & = & \mathbf{0} \end{array} \right. \tag{IV.2}$$

This assumption is wrong, especially for highly dynamic motions. We thus assume that:

- it might be sometimes neglected as the error may be lower than the perceptual accuracy of the user,
- it will be partially compensated by the next step (motion retiming).

Based on this assumption, the system is much simpler to solve. However it remains an infinity of solutions (i.e. pose adaptations) that satisfy the above equations. Only some of them may look natural. To select one of these natural solutions, we apply some knowledge provided in biomechanics and neurosciences.

Given a pose q subjects to additional external forces $\mathbf{F}_j$ which were not present in the original motion, it is possible to correct q to ensure static balance using the above Equation IV.2. Biomechanical knowledge is used to guide this process to a natural solution.

Hof [Hof 07] has identified three strategies to naturally maintain balance. First, humans move their center of pressure inside the base of support to compensate small perturbations. However, the center of pressure quickly reaches the limit of the base of support. Thus, humans switch to a second strategy to compensate these perturbations: they use counter rotation of segments around the ankle to compensate stronger perturbations (ankle strategy). Then, the last strategy consists in applying external forces (such as holding a bar) or changing the base of support for higher unbalanced situations. In the method proposed in this Chapter, we propose to successively apply these strategies to mimic the natural behavior of humans to maintain balance.

When the CoP runs out of the base of support, the first strategy consists in correcting the pose by rotating the body around the ankle. Using the second part of Equation IV.2, we compute the static error $\mathbf{C}$ introduced by the additional forces F_j on the pose q:

$$C = \mathbf{OG} \times \mathbf{P} + \mathbf{OCoP} \times \mathbf{GRF} + \sum_j \mathbf{OA_j} \times \mathbf{F}_j \tag{IV.3}$$

Regarding Equation IV.2, $\mathbf{C}$ should be null if the pose is statically balanced. As we do not have access to a captured value of the CoP, we compute the CoP trajectory of the original motion thanks to Equation IV.2 considering no additional external forces. However, when new forces $\mathbf{F}_j$ are applied on a pose, this equation is not verified anymore. An additional angular momentum is introduced by each force $\mathbf{F}_j$. In that case, we search for the ankle rotation θ_{ankle} that ensures a null value of $\mathbf{C}$. The relation between $\mathbf{C}$ and θ_{ankle} can be linearized using the Jacobian matrix $\mathbf{J}$:

$$\Delta\mathbf{C} = \mathbf{J}\Delta\theta_{ankle} \tag{IV.4}$$

By inversing Equation IV.4, it is possible to compute a linear approximation of θ_{ankle}. However, as dynamic equations are not linear, it is necessary to iterate around the solution until convergence. In most of the cases, few iterations are sufficient to obtain θ_{ankle} which leads to a negligible value of $\mathbf{C}$. This corresponds to the computation of the static configuration satisfying as much as possible the static CoP position of the original motion.

Figure IV.2 shows examples of pose correction obtained with this process. The green character represents the original captured motion "pushing nothing", i.e. without external forces, while the textured character corresponds to a static correction with additional external forces (pushing respectively 90N, 180N and 235N). In these examples, as the virtual human was pushing with its two arms, half of the additional external force was applied on each hand.

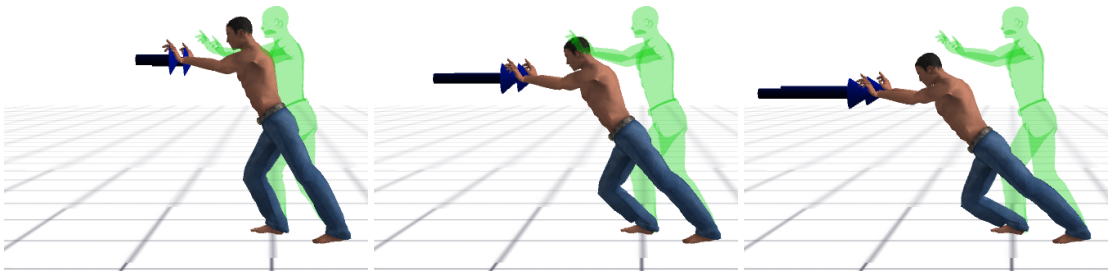

(a) (b) (c)

Figure IV.2: Green character: original pose where the character is pushing nothing (0kg). Textured character: adapted pose using the static solver pushing an external force of a) 90N, b) 180N and c) 235N.

IV.2.2 Preparation to the interaction phase

The preparatory phase to a new upcoming dynamic constraint is divided into two steps. Detecting a new constraint in a near future corresponds to an upcoming event that may modify the character's actions.

1. When a constraint is detected at the time of interaction t_i, our solver starts by computing a correct static interaction pose ensuring balance with the given forces at t_i (first step). It is computed using the method presented in Section IV.2.1. In this step, the configuration of the pose is modified to take the new dynamic constraints into account and the base of support may be modified to ensure balance.

2. Thus, as the position of the foot may be adapted, it is necessary to compute a new footprint sequence to reach the wanted configuration (second step). Once the new footprints are computed, the preparatory motion is then adapted to reach the preparatory pose while verifying the footprints.

IV.2.2.1 Step 1: Computation of a correct interaction pose

When a constraint is detected at the time of interaction t_i (Figure IV.3.a), our solver starts by computing a correct static pose ensuring balance with the given forces at t_i (Figures IV.3.b and IV.3.c). This pose corresponds to a state where the character starts to be ready for the upcoming constraints. It is computed using the method presented in Section IV.2.1. After observing several behaviors during motion capture sessions, we have observed that the supporting foot is generally close to the projection of the center of mass on the ground at the interaction time. Although this assumption should be validated thanks to specific biomechanical analyzes and experiments, we used this empirical knowledge to adapt the base of support. Hence, the static pose at t_i is also modified to ensure that the supporting foot remains close to the projection on the ground of the center of mass, to support the character and maintain balance (Figure IV.3.d). This is performed by simply changing the support foot location and applying inverse kinematics to compute the new configuration [Kulpa 05b].

In the top example of Figure IV.3, a minimal additional force f is required to move the cupboard. f is, by definition, perpendicular to the gravity and its norm equals to $k_s * m_{obj} * g$, where m_{obj} is the mass of the object and k_s is the static friction coefficient depending on the object/floor contact materials. Then, as the virtual human pushes with two arms in these examples, half of the force f is applied on each hand, in the direction of the wanted displacement (Y axis in this example). Thus, in examples of Figure IV.2, the force applied on each hand is $F_{hand} = [\quad 0 \quad 0.5 * k_s * m_{obj} * g \quad 0 \quad]$, with k_s sets to 0.3.

(a) (b) (c) (d)

Figure IV.3: Step 1 correction for pushing an object of 80kg with both hands (upper line) or pulling with a force of 200N (bottom line). a) The pose at the future time of interaction. b) Static correction to additional external perturbations using the method presented in Section IV.2.1. c) Adjustment depending on the original contact location. d) The supporting leg is placed below the center of mass to enlarge the base of support.

IV.2.2.2 Step 2: Footprint adaptation or generation

As the pose at interaction time t_i is different than the one corresponding to the original motion capture data, the sequence of footprints has to be adapted. It is necessary to compute the new footprint sequence to reach the wanted configuration. Two cases can occur:

1. Several steps exist between the current time and the time of interaction t_i (i.e. the motion involves displacements): it is possible to modify the existing footprints to reach the required configuration (**Footprint adaptation**),

2. There is no displacement or the location of the next interaction is too close to the current position: it is necessary to generate new steps to reach the required configuration (**Footprint generation**).

Footprint adaptation When several steps exist in the original sequence between the current simulation time and t_i, it is possible to modify these existing footprints to reach the wanted configuration. Laurent and Thomson [Laurent 88] showed that humans generally adapt their three last steps prior to a new situation (climbing stairs, stopping, etc). In the same way, our method proposes to modify the three last steps of the original preparatory sequence to reach the wanted footprint configuration. We also offer the possibility to tune this value to adapt these last steps according to wishes of the user.

However, in some cases, we do not have access to the required number of steps to prepare the interaction. It could for instance happen if the constraint is activated by a user at the last time. In that case, n is set to the maximum number steps that can be corrected ($n < 3$).

For each step i that has to be adapted, we then add a correction offset. Therefore, the adapted footprint position p_i corresponds to:

$$p_i = p_{0,i} + \frac{i}{n}(p_n - p_{0,n}) \tag{IV.5}$$

where $p_{0,i}$ is the footprint position in the original sequence, p_n is the corrected footprint position at the time of interaction t_i and $p_{0,n}$ is the footprint position at the time of interaction t_i in the original sequence. This adaptation corresponds to taking $\frac{1}{n}$ of the error into account at each step (Figures IV.4 and IV.8.e).

Then, MKM [Kulpa 05b, Multon 09] is used to adapt the original preparatory motion to the new correct footprints and solve the resulting kinematic constraints in an efficient manner.

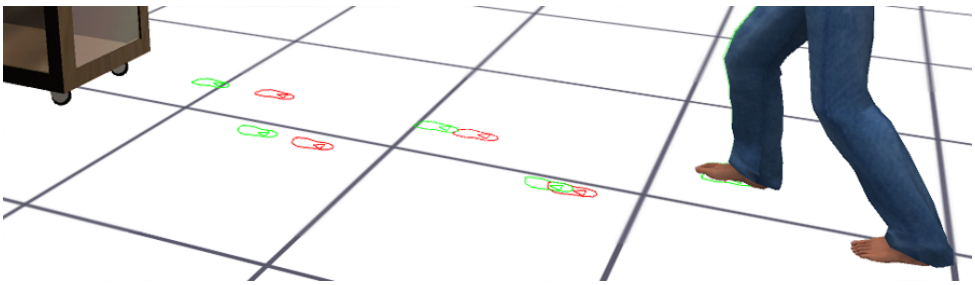

Figure IV.4: New footprints (red) adapted from original footprints (green) to reach the new preparation configuration

Footprint generation In some cases, we do not have future footprints compatible with the upcoming interaction. It happens for instance when a user activates an interaction at the last time: the interaction will happen during the current foot sequence. In that case, the preparatory algorithm has to generate new footprints to satisfy the foot position constraints.

Figure IV.5 presents the process for generating new steps. The original (green) and required (red) feet positions are used as inputs. The process is the following

1. If the current foot sequence is a single support phase, we start by putting the swing foot on the floor. Positions of both feet on the floor are then considered as the original feet positions.
2. The first foot is moved to its corrected location (red). This first foot corresponds to the one that will not support balance at the the time of interaction.
3. Finally, the *supporting foot* is also moved to its required location.

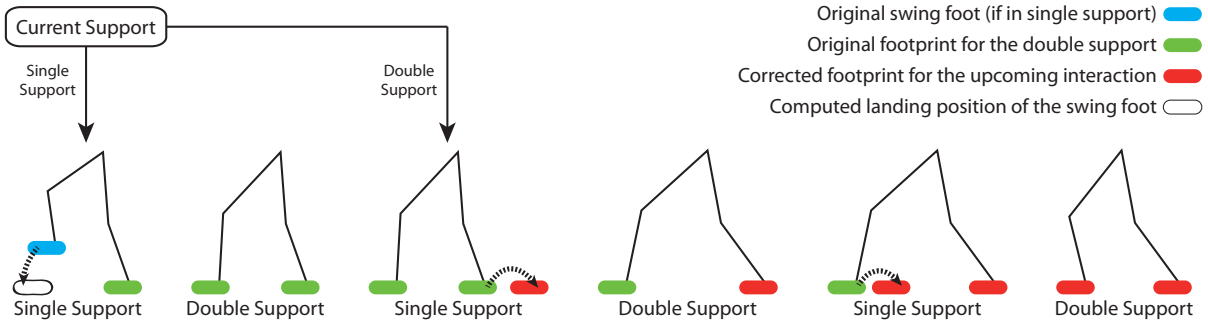

Figure IV.5: Process used to generate the new footprint sequence. Firstly, if the current foot sequence is a single support phase, the swing foot is put on the floor. Positions of both feet on the floor are then considered as the original feet positions. Then, the first foot is moved to its corrected location (red). Finally, the *supporting foot* is also moved to its corrected location.

For single support phases, the trajectory of the swing foot is based on a motion clip corresponding to a forward or backward step and adapted according to the situation. This example is time-warped, scaled and rotated to match the parameters of the step. MKM is again used to drive the root of the character and satisfy the kinematic constraints corresponding to the position of the feet [Kulpa 05b, Multon 09].

Figure IV.6.a presents the generation of steps for two motions. Figures IV.6.b and IV.8.a,b,c,d presents examples of the desired generated footprints.

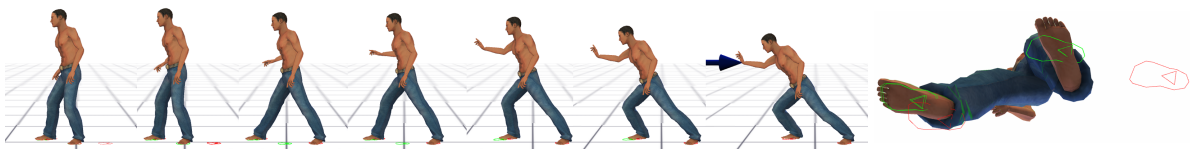

(a) (b)

Figure IV.6: a) Step generation. b) Corresponding footprints from another view: generated (red) and original (green) footprints.

Correction of the sequence In both cases, it is necessary to also adapt the character's motion to reach the required configuration computed in Step 1. Thus, once the feet are positioned for the upcoming event, the pose of the virtual character is filtered toward the required configuration imposed by Step 1. In this work, this process has been designed in an empirical manner but further biomechanical experiments should be carried-out to analyze the natural strategies used to reposition the feet.

IV.2.3 Adaptation of the interaction

Once the character is in a correct configuration for the upcoming constraints, it is then necessary to adapt the following interaction sequence during which the additional external forces are maintained. The experiment described in Chapter III has shown that the velocity profile of some body parts conveys a lot of information about the dynamics of the motion. Thus, only modifying the global pose of the character without considering time is not enough to take this information into account. To this end, we retime the resulting motion, as proposed in previous works [Majkowska 07].

Hence, once the interaction has begun, the character starts to perform its action while taking the perturbations that were not present in the original motion into account. Thus, the system changes the pose while assuming zero acceleration and retimes the current action. Our method adapts each frame in real time to take these new perturbations into account. If the speed at which was performed the original motion is suitable for the original constraint, it might not be the case with the new current interaction.

Many possibilities are available to retime a motion. Our previous experiments based on lifting various weights have shown that there is a shift of the peak of velocity when the mass increases. Hence, the motion is somehow delayed, maybe to let the muscle force reach the required intensity. However, we have also seen that this shifting of the velocity peak suddenly changes beyond a given mass. The peak occurs earlier, but with a higher acceleration value. Thus, for this specific motion the motor strategy seems composed of a continuous adaptation with some discontinuities corresponding to changes of strategies. As we do not get any formal description of these strategies in the literature, we propose to let the user tune the retiming function to control the style of the character. In the future, it would be necessary to carry-out experiments to better understand this phenomenon.

Thus, we let users tune the following parameters for retiming:

- Maximum force f_{max} handled by the character for interactions: if the sum of the external interaction forces is higher than f_{max}, the character cannot perform the interaction.
- Time delay Δf_{max} for the maximum force: it corresponds to the shift of the peak of velocity for the maximum handled force f_{max}. Then, it is linearly interpolated to compute the time delay Δf for forces f lower than f_{max}.
- Speed coefficient c_{speed}: it corresponds to the speed at which the interaction should be performed: coefficients $c_{speed} = 1$, $c_{speed} < 1$ and $c_{speed} > 1$ respectively keep the speed of the original motion, accelerate or decelerate the original motion, using the following Equation:

$$new\_duration = original\_duration * c_{speed} \tag{IV.6}$$

These parameters are used to produce the retiming function. Figure IV.7 presents different examples of retiming functions generated using these parameters.

When the interaction stops, an immediate suppression of the additional external force would create a discontinuity. Thus, additional external forces are smoothly decreased to generate continuous transition to the sequence after the interaction.

IV.3 Results

We have applied the results of our method to various motions involving interactions with different dynamic properties. Figure IV.8 shows the current pose (textured characters) when an interaction is

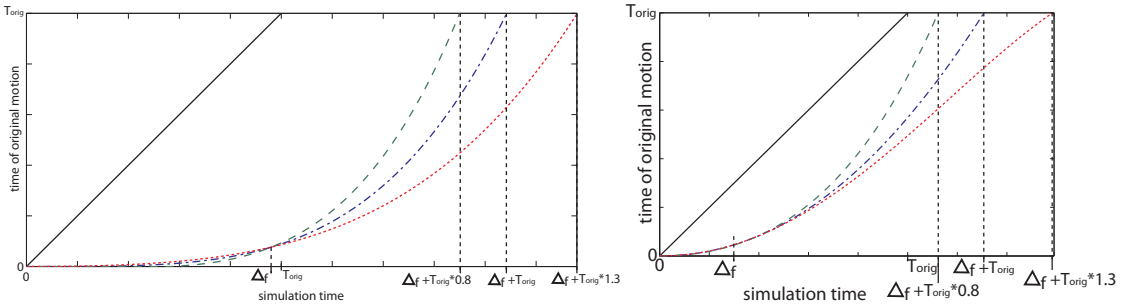

Figure IV.7: Examples of retiming functions generated using user defined parameters. Solid black: time function of the original motion. Retiming functions respectively correspond to a speed coefficient of $c_{speed} = 1$ (blue dotted-dashed), $c_{speed} = 0.8$ (green dashed) and $c_{speed} = 1.3$ (red dotted). Figure a) and b) respectively present a time delay Δf_{max} of 2.5s and 1s, for a maximal force of 800N. As the force f was set to 200N is these examples, the corresponding Δf were a) 0.62s ($0.95 * T_{original}$) and b) 0.25s ($0.38 * T_{original}$).

detected in the near future. The green character represents the pose after adaptation at interaction time. Figure IV.9 compares the results of our method to experimental data. Compared to the original sequence (pulling or pushing nothing), the resulting motion seems to be more adapted to reacting to an external force of 200N.

Table IV.1 presents computation time for the different phases (standard laptop Dualcore 2.33GHz CPU, 2GB RAM and NVidia Quadro FX 2500M GC). Column A presents the time needed to compute the correct interaction pose and the new foot sequences in reaction to the upcoming interaction. Column B and C present respectively the average time for correction of poses in the preparatory phase (to satisfy the new feet positions and prepare the character for interaction) and during the interaction phase. Column D presents the number of iterations for the linearization of the static equations of Section IV.2.1. For the implementation presented in this work, the maximum computation time for one frame is always under 1ms per character. Thus, it is possible to animate up to 15 characters with dynamic interactions at 60Hz, without visualization.

To evaluate the error made during this process, we have compared the trajectory of the CoP (using Equation IV.1) for the original and the corrected motion (see Figure IV.10). In this figure, the blue solid curve represents the original motion without changes, the green dotted one depicts the trajectory of the CoP if we consider 200N additional force without adaptation, and the red dashed one stands for the final adapted motion. By definition, the trajectory of the CoP is restricted to remain inside the base of support (depicted with black dot lines). Figure IV.10 clearly shows that the CoP of the adapted motion remains close to the CoP of the original one, inside the base of support.

In some applications, the virtual character may not have any time to prepare for the upcoming action. It can be the case if the perturbation is not the cause of an interaction (a strong wind suddenly rises in the environment, centrifugal forces during turning, etc) or if the character is interacting from the beginning of the application (holding a suitcase for instance). The preparatory phase is then ignored and only the dynamic adaptation phase is taken into account. In that case, the external forces applied to the virtual character should be activated continuously otherwise the motion may exhibit discontinuities.

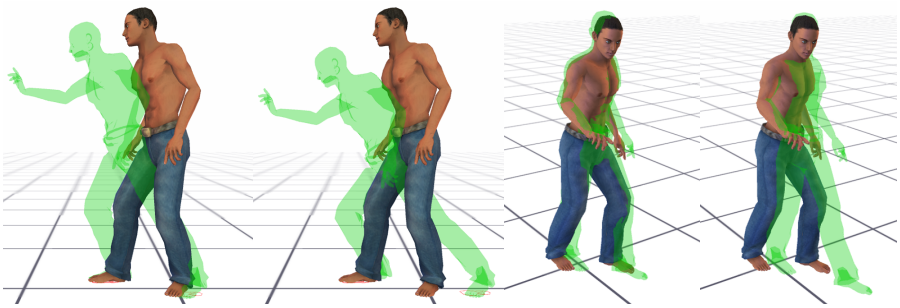

(a) (b) (c) (d)

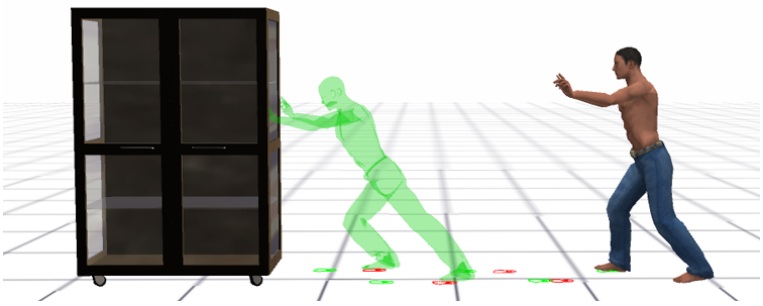

(e)

Figure IV.8: Textured character: current pose of the simulation. Green character: corrected pose at the time of interaction to handle the physical constraint. Red footprints: generated/modified footprints for the new sequence. Green footprints: footprints of the original motion. Motions: pushing with an additional force of a) 50N and b) 150N, and pulling with an additional force of c) 50N and d) 150N. e) pushing a 60kg cupboard (175N additional force using a 0.2 coefficient of friction). Footprints were generated for a, b, c and d and modified from original footprints in e.

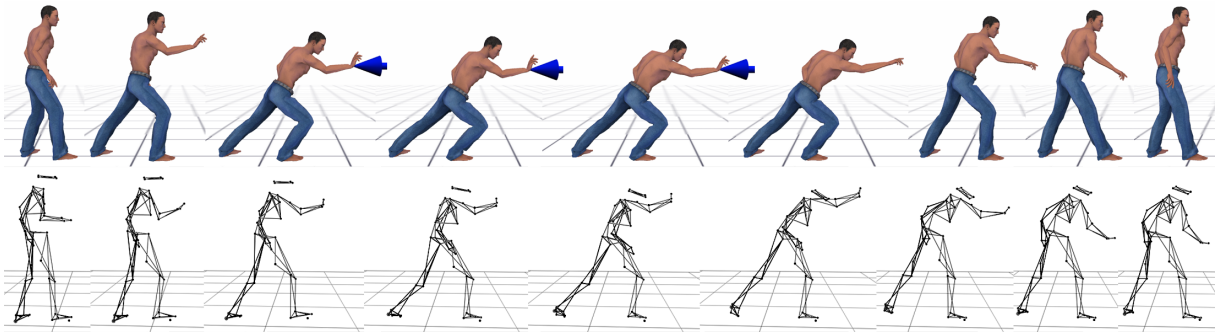

(a)

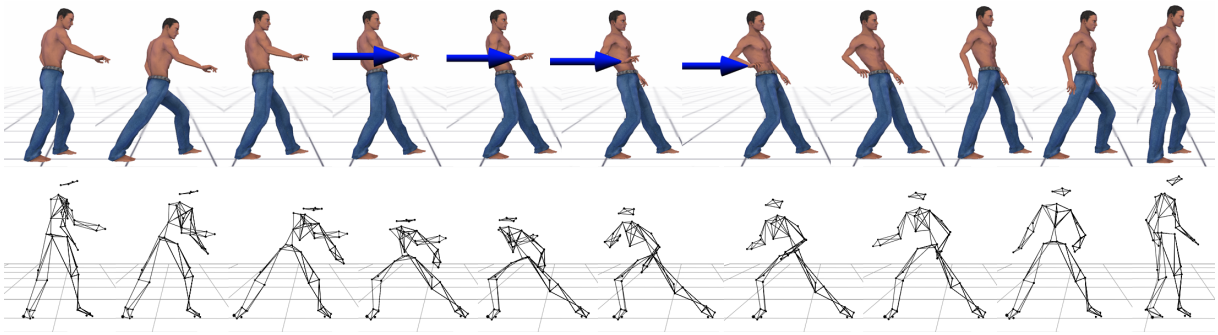

(b)

Figure IV.9: Motions subject to a 200N external perturbation corrected with our method compared to motions interacting with a similar intensity captured on a real subject for a) pushing and b) pulling.

Motion	Additional force	A	B	C	D
Push right hand	20N	0.23ms	0.005ms	0.27ms	1
	100N	0.24ms	0.005ms	0.35ms	2
	200N	0.26ms	0.005ms	0.51ms	2.15
Pull right hand	20N	0.24ms	0.005ms	0.43ms	1.92
	100N	0.24ms	0.005ms	0.40ms	2
	200N	0.24ms	0.005ms	0.42ms	1.99

Table IV.1: Comparison of the method for different scenarios (Motion × Additional force). A: time needed to compute the correct pose for the time of interaction. B: mean time needed for the foot sequence modification/generation of one frame. C: mean time needed for the dynamic correction of one frame and D: mean number of iterations needed to converge toward a correct static pose with the method of Section IV.2.1.

Figures E.4, IV.12 and IV.13 present different examples of dynamic correction where no preparatory phase is available. In Figure E.4, the character is walking while holding an object, which mass m creates a vertical force along the gravity direction. The additional external forces may also depends on the environment, such as in Figures IV.12.a and IV.12.b where the character is walking face or back on a strong wind for instance. Finally, forces might be created by the adaptation of the motion such as

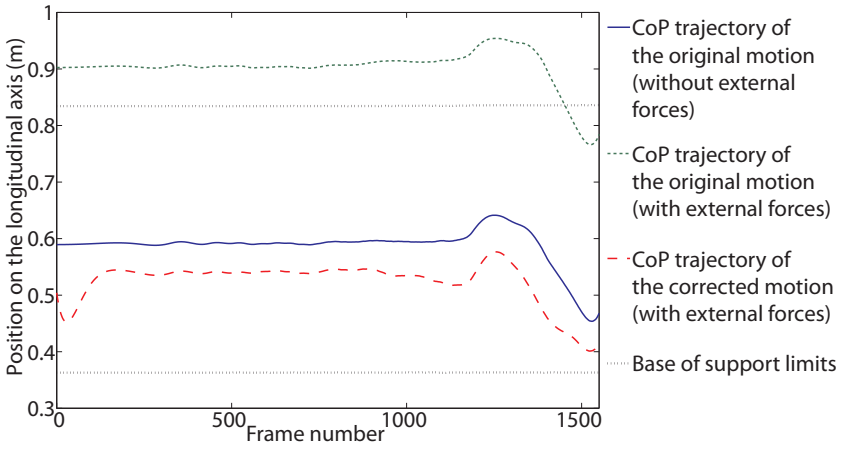

Figure IV.10: Trajectory of the CoP for pulling with an external force of 200N. Original motion without taking external force into account (solid blue), taking this force into account but without adaptation (dotted green) and final adapted motion (dashed red)

compensating centrifugal force while turning (Figure IV.13.a and IV.13.b).

In the case of compensation of centrifugal forces (Figure IV.13), the original motion is a straight walk which is converted into a curved walk. Thus, the green character (original motion) remains straight while turning. However, an acceleration normal to the curvature (directed towards the center of the curvature) appears at the center of mass of the character when turning. This normal acceleration is computed as follows:

$$a_N = v^2/r \tag{IV.7}$$

where v is the norm of the velocity of the center of mass on the XY plane and r is the radius of curvature. This acceleration, applied at G and directed towards the center of the curvature (unit vector $\vec{N}$), is considered as an external force F_{a_N} applied at G (Equation IV.8). As a consequence, the character naturally bends into the curve to compensate this additional external force.

$$F_{a_N} = m.a_N.\vec{N} \tag{IV.8}$$

IV.4 Discussion

Based on the preliminary results presented in Chapter III, we have proposed a two-steps process to adapt the motion to physical perturbations. This method has been successfully applied to produce natural adaptations such as pushing, pulling, or carrying various masses, modifications of the environment conditions (such as representing a strong wind) and natural behavior to dynamic effects (compensations of centrifugal forces).

In Figure IV.9, we present the adaptation of a light pulling motion to a heavy one. In the comparison with the real pulling scenario, the actor decided to perform a completely different strategy, which is not possible to obtain with our method. To correctly compare captured and adapted data, it would have been necessary to prevent the actor from changing its strategy. However, different strategies are available for

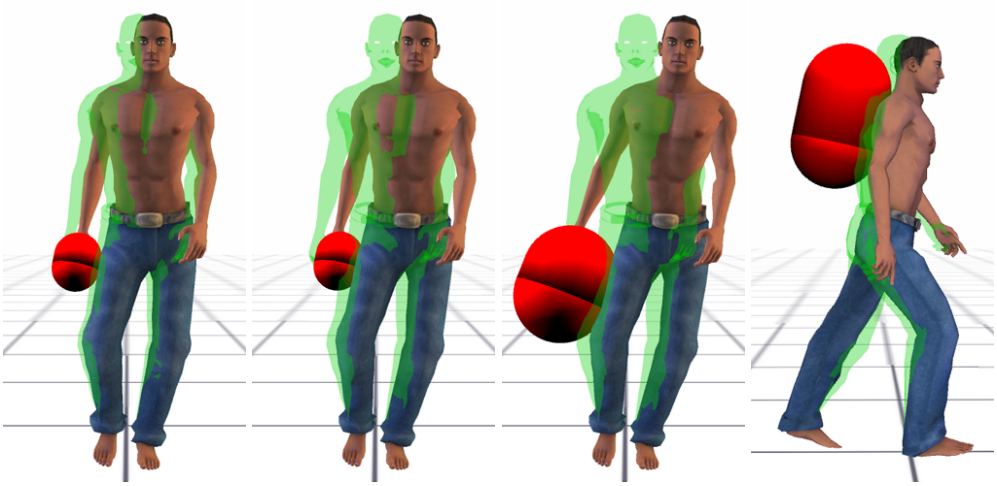

(a) (b) (c) (d)

Figure IV.11: Various examples of dynamic correction for carrying objects. Green character: original motion without correction. Textured character: each object creates a new additional forces directed along the gravity. The motion is dynamically corrected to handle this new force. Objects can be carried all over the body, such as hand (a) 10kg, b) and c) 25kg) or on the back (d) 20kg), and of various size (object inc) is bigger than in d) which implies to move the hand away from the thigh to prevent inter penetrations. This distance increases the momentum created by the object).

humans to perform the same task. Thus, the naturalness of the adapted motion may still be acceptable but should be confirmed by further experiments.

Furthermore, this process is based on the assumption that the pose and the velocity profile can be adapted separately. This assumption obviously leads to inaccuracies. However, The comparison of CoP trajectories for original and corrected motions (Figure IV.10) clearly shows that the CoP of the adapted motion remains close to the CoP of the original one, inside the base of support. Thus, we assume that these inaccuracies remain acceptable from the perception point of view, as suggested by the perceptual study of Chapter III.

In the adaptation of the preparatory phase, foot sequences are either adapted or generated. In the case of the adaptation of existing foot sequences, we based our method on the results of [Laurent 88], which state humans modify only their three last steps prior to a new situation such as climbing stairs. However, these results were obtained from situations where humans do not need to stop before the new situations. Thus, the assumption that this knowledge can be extended to upcoming interactions should be verified from biomechanical data.

In the same vein, we observed from several behaviors during motion capture sessions that the subject's supporting foot is generally close to the projection of the center of mass on the ground at the interaction time. We use this empirical knowledge to generate natural interactions, but this assumption should also be validated thanks to specific biomechanical analyzes and experiment.

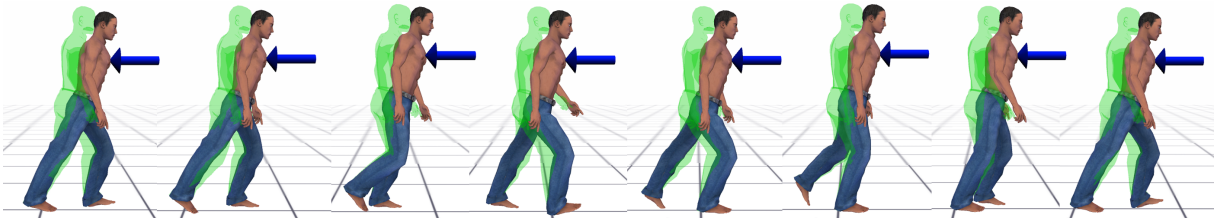

(a) Walking facing a strong wind (60N)

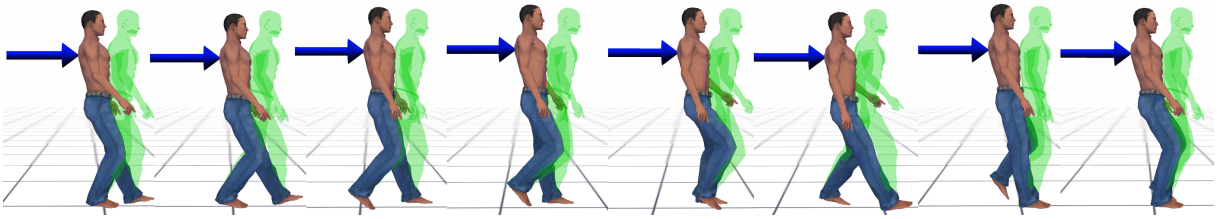

(b) Walking while being continuously pushed on the back (100N)

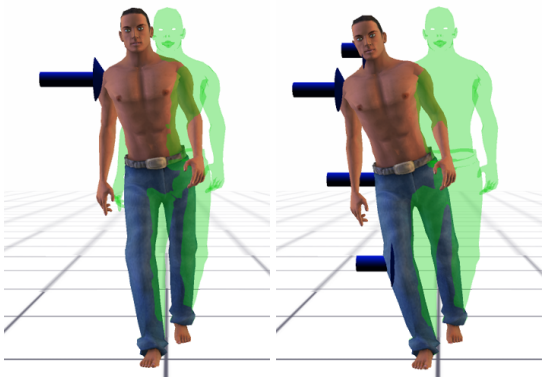

(c) Walking while being continuously pushed on the side (50N)

(d) Walking while being continuously pushed on the side from various locations

Figure IV.12: Various examples of dynamic correction without preparatory phase. Green character: original motion without correction. Textured character: dynamic correction using the method of Section IV.2.

Last, we proposed a Motion Retiming process to enhance the effect of the additional external forces on the motion. This solution is based on user defined parameters that drive the shift of the peak of velocity and the speed at which the motion should be performed. In the future, this process should be improved thanks to specific biomechanical experiments.

IV.5 Conclusion

In this Chapter, we proposed a two-steps process to adapt the motion to physical perturbations based on the preliminary results presented in Chapter III. This process is based on the assumption that the pose and the velocity profile can be adapted separately, which seems acceptable regarding CoP comparisons and users' accuracy of dynamic properties.

Hence, the first step consists in solving the problem by considering the system as static (null ac-

celerations). At this stage, the base of support and the global orientation of the character are adapted, as suggested in the biomechanical literature to maintain balance [Hof 07]. If necessary, either the few preliminary footprints are adapted (if the task follows displacements) or the system generates new steps (if no displacement occur) to ensure balance (by adapting the base of support).

The second step consists in retiming the motion, as suggested in [Majkowska 07]. This is an important issue as it is supposed to convey lot of information about the dynamic status of the system. The results show that computation time enables us to animate dozens of characters at 30Hz on a common PC. Other methods, such as physical simulation with controllers or spacetime constraints would certainly not reach this performance. Now, the key question is to determine if people can perceive the errors induced by our method. As a perspective we thus wish to carry-out perceptual experiments to check this point.

Using the perception skills of subjects to design appropriate simulation methods is a promising approach for the future. The studies and the methods reported in this Chapter are clearly preliminary but offer promising results. They should be improved by further experiments and biomechanical analyzes.

Related publications

Journal papers

F. Multon, R. Kulpa, L. Hoyet and T. Komura (2009): Interactive animation of virtual humans based on motion capture data. Computer Animation and Virtual Worlds, Volume 20 , Issue 5-6 (September 2009), pages 491-500, 2009

International conferences

L. Hoyet, F. Multon, T. Komura and A. Lecuyer (2010): Perception based real-time dynamic adaptation of human motions. Lecture Notes in Computer Science, MIG2010 special issue, Volume 6459/2010, pages 266-277, 2010

F. Multon, R. Kulpa, L. Hoyet and T. Komura (2008): From Motion Capture to Real-Time Character Animation. Lecture Notes in Computer Science LNCS 5277, MIG2008 special issue, pages 72-81, 2008.

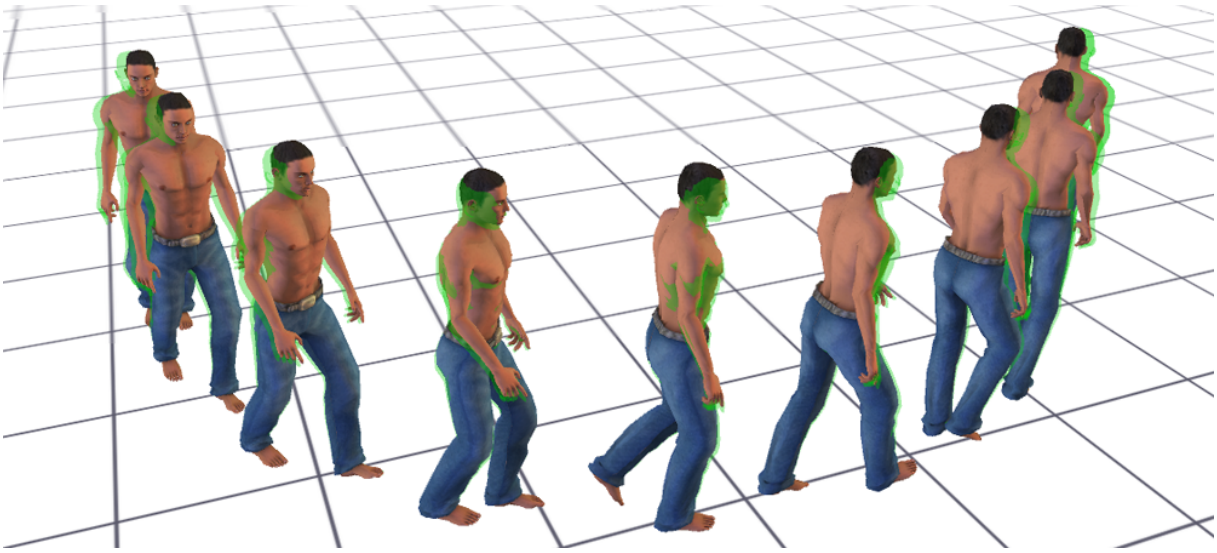

(a) Large turning (radius of curvature: 3m).

(b) Sharp turning (radius of curvature: 1.5m).

Figure IV.13: Various examples of dynamic correction for turning motions. Green character: original motion without correction. Textured character: dynamic correction using the method of Section IV.2, with different radius of curvature. Textured character bends in the curve to compensate for centrifugal forces.

Conclusion

This PhD aimed at proposing a novel approach for generating physically-valid and natural-looking motions for virtual humans that are subject to various physical constraints. To this end, this work has been divided into three main parts: analyzing real motor strategies, understanding how people perceive physical constraints in natural motions and proposing an approach to generate natural-looking adaptations of human motion to physical constraints. The method is supposed to be compatible with interactive applications, such as videogames or virtual reality. Hence, computation time and the capability to avoid using a complete knowledge of the future are key issues to make a virtual human react to unpredictable events imposed by a user.

Reacting to physical constraints has been addressed in computer animation with three main approaches: using physical models and controllers, applying spacetime optimization and reusing motion capture data with adaptation facilities. To evaluate the relevance of each of these approaches, three main properties have to be considered.

Firstly, the method should offer a simple and efficient control of the virtual human: the goal is to satisfy the constraints imposed by the scenario and the users' orders. Most of the above techniques offer an impressive control of virtual humans that have to deal with physical constraints. During the last few years, many works have been carried-out to improve their controllability based on physical models. However, there are still many parameters to tune in order to make the virtual human react correctly to external events.

Secondly, computation time is a key issue, especially for real-time or interactive applications. Thanks to the increase of the processing power of computers, it is now possible to simulate a physical model of virtual human in almost real-time. However, most of the applications generally require high computation time for many other tasks, such as rendering, artificial intelligence, management of clever interfaces, etc. Computation time is thus still a key point to address all the tasks involved in a complete application.

Thirdly, virtual humans are viewed by users who are very experienced in watching natural motions and behaviors. As a result, the naturalness of the simulated motion is one of the main key-point to produce credible animations, especially for applications which require a complete involvement of the user in the experiment (named Presence in virtual reality). From a long time now, most of the approaches have proposed to reuse motion capture data to address this problem. Indeed, it ensures to produce natural motions if no important modifications are applied. However, reusing motion capture data for inappropriate constraints leads to unnatural motions, as for controllers. However, for the moment, it seems to be the unique method to efficiently deal with natural styles, as it is very complex model.

In this PhD, we contributed in designing a new method that tries to take all the above points into account. The key idea is to offer an easy control of the virtual human motion, with few computation time, while preserving the naturalness of a unique example of motion clip.

To achieve this goal, we have first studied how to model the influence of physical constraints on relevant parameters, such as balance. In this first study, the key point is to determine a criterion that could efficiently predict the loss of balance for any static or dynamic situation. Many papers in computer animation and robotics used the Zero Moment Point to detect loss of balance in low dynamic motions. In this PhD, we have studied the behavior of this criterion from quasi-static to highly dynamic motions. As this point is theoretically equivalent to the center of pressure, it should not go outside the base of support by definition. However, we have shown that this is not the case for highly dynamic motions, especially when high vertical accelerations occur (such as preparing a jump). We have also shown that the models chosen to represent the virtual character lead to more or less important innaccuracies between computed ZMPs and measured CoP. For instance, the pendulum model clearly fails to capture dynamic properties of motions, especially when the limbs are significantly moving.

From the fundamental point of view, as ZMP should be equal to CoP in most cases (if no torque is applied on the border of the feet), computing a ZMP outside the base of support seems to be mainly due to inaccuracies linked to the model. As a result, designing a criterion based on detecting when the CoP or ZMP goes outside the base of support is difficult to justify from the biomechanical point of view. The only idea could be that when the ZMP goes outside the base of support it could also lead to torques applied to the feet, which could correspond to placing the CoP very close to the border of the base of support.

However, other criteria have been designed in the literature to measure the balance status of characters. To our point of view, the XcoM seems to be a very promising criterion even if it fails, like the other ones, to accurately detect loss of balance for highly dynamic motions. Moreover, as it is based on velocities instead of accelerations (compared to ZMP), it would be more robust to noise in simulations or measurements, even if it should still be extended to deal with highly dynamic motions. An idea could be to replace the inverted pendulum model by a more complex representation of the virtual character, as in the case of the ZMP computation.

In order to design efficient criteria measuring the balance status of characters, one of the key fundamental question is to clearly define what balance is in dynamic situations. From the experimental point of view, determining the time at which the motion switches from balanced to unbalanced is very difficult. Let us consider the motion that consists in reaching an object if front of us. When the user has to step, it is certainly associated with a loss of balance. However, it is still difficult to determine the exact time at which the situation is felt as unbalanced by the subject. For really slow motions, or with a constant velocity, the dynamic laws clearly state that recovering balance is possible if the projection of the center of mass on the ground belongs to the base of support. For less static situations, it is less clear. For instance, walking is supposed to be a succession of forward falling according to many authors. In that case, unbalance could be intuitively viewed as the necessity to place the swing foot forward and the impossibility to replace this foot at the original position (backward). If we can experiment this with subjects, detecting the exact time when this loss of balance actually occurs is however very difficult, especially when non-negligible accelerations occur. In this PhD, we failed in designing a protocol to experimentally detect this time. In the future, it would be very important to design a clear criterion to detect this loss of balance in dynamic situations, especially as our experiments clearly show that none of the tested criteria succeed in detecting balanced and unbalanced situations for highly dynamic motions. They detected false loss of balance most of the time, while the subject is continuing his motion without any visible need to step or act to preserve balance. This is a key problem that might be studied with a multidisciplinary approach as it rises challenging experimental set-ups.

As stated above, dynamic balance is a key point in understanding motion adaptation to external physical perturbations. Indeed, human beings mainly stand on a small surface (where interactions occur) while a greater surface (mainly spread along the vertical axis) might be subject to many perturbations. Thus, it creates angular momentums that have direct consequences on balance. Although no clear criterion arises from this study, balance must be taken into account for motion adjustments to external constraints.

In addition to balance maintenance, other parameters may be affected when dealing with various physical constraints. In a second study, we have carried-out experiments to identify the relevant kinematic data that were modified when applying even small changes in physical constraints. In this experiment, we focused on lifting more or less heavy dumbbells which mass ranged from 2kg to 10kg with a one-kilogram step. The statistical analysis shows that human being mostly adapt the velocity profile of joints that are close to the physical constraints (such as the elbow and wrist joints for lifting motions). Of course this result is preliminary as it is only based on lifting motions, with one subject, and for small masses. However the preliminary results are really promising and tend to show that adaptations of velocity profiles could be good candidates to naturally adapt motions to dynamic constraints.

In future works, it would be necessary to confirm and complete this result. Firstly, it would be important to evaluate if this statement is valid for many other types of motions, such as pulling, pushing, punching, carrying, manipulating tools, etc. Secondly, it should be verified on a wider range of people in order to eliminate the possible bias of an individual and unique behavior. Thirdly, it should be extended to a wider range of external constraints, asking people to perform motions until reaching their own maximum voluntary muscle contraction. Thanks to these improvements, it should be possible to identify global strategies for motion adjustments to external physical constraints. During the experiments, we have shown that the velocity profile continuously changes according to the increase of the lifted mass until a given threshold. When this threshold is reached, we observed a complete change of strategy, which seems to show that the adaptation strategy is made of continuous and discontinuous parts.

As these strategies have a direct impact on joint kinematics, people can theoretically perceive these adaptations. Our perceptual experiments showed that it is effectively the case but with a lower accuracy than expected when analyzing kinematic variables thanks to statistical tests. Our preliminary results show that a difference of 3kg (corresponding to almost 50% of the studied mass) in lifting motions is not always detected while a 1kg difference leads to statistical differences in the kinematic data. One has to notice here that statistics only provides information about the difference between two kinematic curves but cannot provide information to know which one is associated with the heaviest mass. People may also perceive the difference in kinematic data but could fail in interpreting this difference to determine which one is associated with the heaviest mass. Other protocols should be designed in collaboration with neuroscientists in order to efficiently answer such type of questions.

As for the biomechanical experiments, these results should be verified on a wider range of masses and motions. In the same way, we should also compare motions performed by different experimenters who manipulate the dumbbells. Indeed, it could be interesting to study the capability of human beings to determine the amount of physical constraints applied to various people with various physical activity status. In that case, strong people might be differently affected by physical loads than inactive people. A collaboration with experts in physical activity (such as M2S lab in University Rennes 2) will be useful to standardize and design this type of protocol.

Despite these limitations, our preliminary results tend to show that the accuracy of human beings for recognizing dynamic constraints in biological motions is low. We have also demonstrated that this skill is not affected when watching virtual humans compared to videos. These results are key points to provide assumptions in order to simplify the animation process which is responsible for adapting motions

to physical constraints.

According to this knowledge, we have proposed a new approach for adapting motion capture data to physical constraints. Compared to most of the modern approaches that consist in dealing with databases of motion capture data, such as motion graphs, the key idea here is to efficiently adapt a unique motion according to new physical constraints. Recent works have proposed to design controllers to mimic human motion, especially locomotion, but it is still difficult to obtain natural-looking motions, even with the high computation load of these approaches. Indeed, style is really difficult to model because it conveys abstract information such as emotions, social status, etc. However, many previous works have demonstrated that style plays an important role to recognize human motions as people could recognize another person by simply watching to point lights animated with motion capture data. At this moment, we do not know how to take this type of information into account when designing models. We thus have decided to take a unique example of motion capture data and to adapt it to various physical constraints. The assumption is to preserve the intrinsic style while adapting the motion to the situation. Another assumption is that the motor strategy is not adapted to the situation. For example, carrying a very heavy box may totally change the way people choose to position their hands.

In this PhD, we did not address this type of problem but proposed a new method to adapt a given strategy to the situation (taking real-time kinematic and dynamic constraints into account). To solve this problem, classical approaches generally rely on solving the constraints in the state space while minimizing a set of criteria. The main problem is to design these criteria in order to obtain natural-looking motions (such as minimizing energy, square torques, Jerk, etc). The selection of the good criteria with the relevant weights is still a challenge. To skip this problem, we decided to study the relevant biomechanical parameters that are affected by physical constraints and how they are perceived by people. The key idea is to develop direct adaptation methods that enable to adjust the motion to the imposed constraints using natural biological and perceptual knowledge.

To efficiently produce natural motions, our method relies on the results obtained in the two previous studies. Although the first study confirmed that dynamic balance is difficult to model, it is a key issue for adapting motions to external perturbations. Similarly, the velocity profile of distal joints is a relevant parameter but is not perceived with a good accuracy by people. Although these results are preliminary, they can drive our method to simulate natural-looking motions in real-time. Our main assumption to efficiently animate virtual characters subject to physical constraints is to subdivide the solving process into two separated steps: adjusting the pose of the character at interaction time with the static equations and then retiming the resulting motion to adapt the velocity profile.

The results are promising as we can deal with 15 characters at 60Hz on a common laptop while adapting the motion to external physical constraints. The inaccuracy is difficult to quantify but we assume that the adaptations performed by our method are natural enough to make users perceive the physical constraints applied to the virtual human. It is a key point in many interactive applications where the user cannot directly perceive the physical constraints of the virtual environment, such as the weight of an object. Therefore, the virtual human should be able to provide this information to the user through adaptations of its performance.

Obviously, this method has some limitations as it is based on adapting a global mechanical system. There is no adaptation of the local body segments according to the physical constraints. In the example where a virtual human is carrying a heavy object on his side, we have only adapted the global orientation of the character: the arm which is carrying the heavy object is not adapted. As a result, the amplitude and the frequency of the arm swing is not appropriate for heavy objects, which may affect the global naturalness of the simulation. Hence this preliminary work should be completed by other contributions

to address this type of problem. As in the MKM system developed in Bunraku, we could imagine a hierarchical solving process. The work presented in this PhD could affect the global motion of the character and the same idea could then be applied to each limb in a hierarchical manner.

Another problem introduced above is the coupling of continuous and discontinuous changes in human motion control. Even in the lifting motion, we have shown a continuous shift of the pick of acceleration until a given mass is reached. Beyond this mass, the subject changed his motor strategy in a discontinuous manner. In future works, it would be necessary to carry-out wider experiments on a wider set of motions and physical constraints, in order to propose hybrid models that can mimic this mixture of continuous and discontinuous adaptations.

However, one of the main difficulty in computer animation is validation. How do we validate that a motion is natural or not, especially with the wide variety of motor adjustments. Computing a distance between real and simulated motions may fail because of this variety of motor strategies. For example, comparing lifting motions performed by an inactive actor and a physically trained one may should lead to great differences while the simulated motion is still correct with the virtual inactive human. In the future, it will be necessary to develop new validation protocols, in collaboration with experts in human motion. It would also be necessary to carry-out perceptual experiments to evaluate the naturalness of the resulting animations. In fact, we could use the same type of protocol than the one used in the second study to compare captured and adapted motions.

From the fundamental point of view, we have to improve our knowledge on the perception of natural motions. In this PhD, we have proposed a pilot study, which should be completed with other studies to validate and extend our results. It could also be interesting to evaluate Presence in virtual environment where a user has to interact with a virtual human to perform a complex task, such as maintenance training. Previous works in M2S lab have shown that despite some negative subjective feelings of people immersed in such a virtual environment, the performance of these subjects could be similar to the one they have in real world for the same situation. Therefore if the application aims at training people and evaluating their performance to perform a given task, this type of validation is clearly more appropriate.

To conclude, we would like to remind the three main contributions of this PhD

1. Firstly, we presented a study on measuring the dynamic balance status using biological captured motions. Our experiments with highly dynamic motions clearly showed that none of the tested criteria succeeded in accurately detecting balanced and unbalanced situations. They detected false loss of balance most of the time, while subjects were continuing their motion without any visible need to act to preserve balance.

2. Secondly, we carried-out an experiment to study the accuracy of users to differentiate the mass of a dumbbell lifted either by a real (video) or virtual human (computer animation). The results show that users do not manage to accurately differentiate small mass differences. However, it seems that they reach a similar level of accuracy when comparing computer animation sequences and videos of real motions.

3. Finally, we proposed a new perception-based method for natural dynamic adaptation of human motions subject to physical constraints, using biomechanical and perceptual knowledge from the two first studies. This method has been successfully applied to produce natural adaptations such as pushing, pulling, or carrying various masses and natural behavior to dynamic effects (compensations of centrifugal forces, walking against a strong wind, etc).

Appendix A

Zero Moment Point - Equations

By definition, the Zero Moment Point (ZMP) is the point on the ground where the tipping moment acting on the character, due to gravity and inertia forces, equals zero. The tipping moment being defined as the component of the moment tangential to the supporting surface. Depending on the model used to represent the virtual human, different terms are involved in the computation of the ZMP, terms which influence its computation time and its accuracy. Section A.1 presents the ZMP equations for three common virtual human models.

Several authors [Goswami 99, Sardain 04, Popovic 05] demonstrated that this point is theoretically equivalent to the center of pressure, which can be measured using a forceplate. This demonstration is reminded in Section A.2.

A.1 Equations

The ZMP trajectory is computed from the equations of the dynamics presented in Equation I.15. For simplicity, these equations are reminded here:

$$\left\{ \begin{array}{rcl} \mathbf{P} + \mathbf{GRF} + \sum_j \mathbf{F}_j & = & m.\mathbf{a} \\ \mathbf{OG} \times \mathbf{P} + \mathbf{OCoP} \times \mathbf{GRF} + \sum_j \mathbf{OA_j} \times \mathbf{F}_j & = & \dot{\mathbf{H}}_{/O} \end{array} \right. \tag{A.1}$$

Using ZMP notation instead of the term CoP, these equations are rewritten:

$$\left\{ \begin{array}{rcl} \mathbf{GRF} & = & m.\ddot{\mathbf{OG}} - \mathbf{P} - \sum_j \mathbf{F}_j \\ \mathbf{OZMP} \times \mathbf{GRF} & = & \dot{\mathbf{H}}_{/O} - \mathbf{OG} \times \mathbf{P} - \sum_j \mathbf{OA_j} \times \mathbf{F}_j \end{array} \right. \tag{A.2}$$

As this equation is only valid on the axis tangent to the supporting surface (X and Y in our case), and using the fact that the Z component of the ZMP has to be constant (flat floor hypothesis), Equation A.2 can be rewritten:

$$ZMP_X = \frac{mgOG_X + ZMP_Z(m\ddot{OG}_X - \sum_j (F_j)_X) - \dot{H}_{Y/O} + (\sum_j \mathbf{OA_j} \times \mathbf{F}_j)_Y}{m\ddot{OG}_Z + mg - \sum_j (F_j)_Z} \tag{A.3}$$

$$ZMP_Y = \frac{mgOG_Y + ZMP_Z(m\ddot{OG}_Y - \sum_j (F_j)_Y) + \dot{H}_{X/O} - (\sum_j \mathbf{OA_j} \times \mathbf{F}_j)_X}{m\ddot{OG}_Z + mg - \sum_j (F_j)_Z} \tag{A.4}$$

where the subscripts $_X$, $_Y$ and $_Z$ represent respectively the X, Y and Z components of the vector.

A.1.1 Inverted pendulum

In the inverted pendulum model, the virtual human is represented as a particle of mass m located at the center of mass G of the character. We can define the following parameters:

$$\begin{aligned}
\mathbf{OG} &= [\quad x \quad y \quad z \quad] \\
\ddot{\mathbf{OG}} &= [\quad \ddot{x} \quad \ddot{y} \quad \ddot{z} \quad] \\
\mathbf{H_O} &= \mathbf{OG} \times m\dot{\mathbf{OG}} \text{ (see Appendix C.2.1)} \\
\dot{\mathbf{H}}_{\mathbf{O}} &= m[\quad y\ddot{z} - z\ddot{y} \quad z\ddot{x} - x\ddot{z} \quad x\ddot{y} - y\ddot{x} \quad]
\end{aligned}$$

Thus, Equations A.3 and A.4 become:

$$ZMP_X = \frac{mx(g+\ddot{z}) + (ZMP_Z - z)m\ddot{x} - ZMP_Z \sum_j (F_j)_X + (\sum_j \mathbf{OA_j} \times \mathbf{F}_j)_Y}{m(\ddot{z}+g) - \sum_j (F_j)_Z} \tag{A.5}$$

$$ZMP_Y = \frac{my(g+\ddot{z}) + (ZMP_Z - z)m\ddot{y} - ZMP_Z \sum_j (F_j)_Y - (\sum_j \mathbf{OA_j} \times \mathbf{F}_j)_X}{m(\ddot{z}+g) - \sum_j (F_j)_Z} \tag{A.6}$$

When no additional external forces are applied on the virtual character, equations become:

$$ZMP_X = x + \frac{(ZMP_Z - z)\ddot{x}}{\ddot{z}+g} \tag{A.7}$$

$$ZMP_Y = y + \frac{(ZMP_Z - z)\ddot{y}}{\ddot{z}+g} \tag{A.8}$$

A.1.2 System of particles

In the system of particles model, the virtual human is represented as a set of particles. Each segment i of the virtual human body is represented by a particle of mass m_i located at the center of mass G_i of the segment:

$$\begin{aligned}
\mathbf{OG} &= \tfrac{1}{m} \textstyle\sum_{i=1}^{N} m_i \mathbf{OG_i} \\
\mathbf{OG_i} &= [\quad x_i \quad y_i \quad z_i \quad] \\
\mathbf{H_O} &= \textstyle\sum_{i=1}^{N} \mathbf{OG_i} \times m_i \dot{\mathbf{OG}}_\mathbf{i} \text{ (see Appendix C.2.2)} \\
\dot{\mathbf{H}}_{\mathbf{O}} &= \textstyle\sum_{i=1}^{N} m_i[\quad y_i\ddot{z}_i - z_i\ddot{y}_i \quad z_i\ddot{x}_i - x_i\ddot{z}_i \quad x_i\ddot{y}_i - y_i\ddot{x}_i \quad]
\end{aligned}$$

Thus, Equations A.3 and A.4 become:

$$ZMP_X = \frac{\sum_{i=1}^{N} m_i x_i(\ddot{z}_i+g) + m_i\ddot{x}_i(ZMP_Z - z_i) - ZMP_Z \sum_j (F_j)_X + (\sum_j \mathbf{OA_j} \times \mathbf{F}_j)_Y}{\sum_{i=1}^{N} m_i(\ddot{z}_i+g) - \sum_j (F_j)_Z} \tag{A.9}$$

$$ZMP_Y = \frac{\sum_{i=1}^{N} m_i y_i(\ddot{z}_i+g) + m_i\ddot{y}_i(ZMP_Z - z_i) - ZMP_Z \sum_j (F_j)_Y + (\sum_j \mathbf{OA_j} \times \mathbf{F}_j)_X}{\sum_{i=1}^{N} m_i(\ddot{z}_i+g) - \sum_j (F_j)_Z} \tag{A.10}$$

When no additional external forces are applied on the virtual character, equations become:

$$ZMP_X = \frac{\sum_{i=1}^{N} m_i x_i(\ddot{z}_i+g) + m_i\ddot{x}_i(ZMP_Z - z_i)}{\sum_{i=1}^{N} m_i(\ddot{z}_i+g)} \tag{A.11}$$

$$ZMP_Y = \frac{\sum_{i=1}^{N} m_i y_i(\ddot{z}_i+g) + m_i\ddot{y}_i(ZMP_Z - z_i)}{\sum_{i=1}^{N} m_i(\ddot{z}_i+g)} \tag{A.12}$$

A.1.3 Rigid body model

In the rigid body model, the virtual human is represented as a set of rigid segments. Each segment i of the virtual human body is represented by an object with a mass m_i, a center of mass G_i and an inertia matrix $\mathbf{I}_i$:

$$\begin{aligned} \mathbf{OG} &= \tfrac{1}{m}\textstyle\sum_{i=1}^{N} m_i \mathbf{OG_i} \\ \mathbf{OG_i} &= [\ x_i \quad y_i \quad z_i\ ] \\ \mathbf{H_{/O}} &= \textstyle\sum_{i=1}^{N} \mathbf{I}_i\omega_i + \mathbf{OG_i} \times m_i \dot{\mathbf{OG}}_\mathbf{i} \text{ (see Appendix C.2.3)} \end{aligned}$$

Thus, Equations A.3 and A.3 become:

$$ZMP_X = \frac{\sum_{i=1}^{N} m_i x_i(\ddot{z}_i + g) + m_i\ddot{x}_i(ZMP_Z - z_i) - ZMP_Z\sum_j (F_j)_X + (\sum_j \mathbf{OA_j} \times \mathbf{F}_j)_Y - (I_i\dot{\omega}_i - \dot{I}_i\omega_i)_Y}{\sum_{i=1}^{N} m_i(\ddot{z}_i + g) - \sum_j (F_j)_Z} \tag{A.13}$$

$$ZMP_Y = \frac{\sum_{i=1}^{N} m_i y_i(\ddot{z}_i + g) + m_i\ddot{y}_i(ZMP_Z - z_i) - ZMP_Z\sum_j (F_j)_Y + (\sum_j \mathbf{OA_j} \times \mathbf{F}_j)_X + (I_i\dot{\omega}_i - \dot{I}_i\omega_i)_X}{\sum_{i=1}^{N} m_i(\ddot{z}_i + g) - \sum_j (F_j)_Z} \tag{A.14}$$

When no additional external forces are applied on the virtual character, equations become:

$$ZMP_X = \frac{\sum_{i=1}^{N} m_i x_i(\ddot{z}_i + g) + m_i\ddot{x}_i(ZMP_Z - z_i) - (I_i\dot{\omega}_i - \dot{I}_i\omega_i)_Y}{\sum_{i=1}^{N} m_i(\ddot{z}_i + g)} \tag{A.15}$$

$$ZMP_Y = \frac{\sum_{i=1}^{N} m_i y_i(\ddot{z}_i + g) + m_i\ddot{y}_i(ZMP_Z - z_i) + (I_i\dot{\omega}_i - \dot{I}_i\omega_i)_X}{\sum_{i=1}^{N} m_i(\ddot{z}_i + g)} \tag{A.16}$$

A.2 CoP and ZMP equivalence

Using the Newton-Euler equations and the previous formulations, we obtain for the force equation:

$$\mathbf{R}^c + m\mathbf{g} = m\mathbf{a}_G \tag{A.17}$$

where $\mathbf{R}^c$ is the sum of the contact forces. If $\mathbf{R}^g$ represents the sum of inertia and gravity forces, then:

$$\mathbf{R}^c + \mathbf{R}^{g_i} = \mathbf{0} \tag{A.18}$$

Momentum equations are thus expressed as:

$$\mathbf{QCoP} \times \mathbf{R}^c + \mathbf{QG} \times m\mathbf{g} = \dot{\mathbf{H}}_G + \mathbf{QG} \times m\mathbf{a}_G \tag{A.19}$$

$$\mathbf{M}_Q^c + \mathbf{M}_Q^{g_i} = \mathbf{0} \tag{A.20}$$

with:

$$\mathbf{M}_Q^c = \mathbf{QCoP} \times \mathbf{R}^c \qquad \text{and} \qquad \mathbf{M}_Q^{g_i} = \mathbf{QG} \times m\mathbf{g} - \dot{\mathbf{H}}_G - \mathbf{QG} \times m\mathbf{a}_G \tag{A.21}$$

where $\mathbf{M}_Q^c$ is the sum of contact momentums computed at point Q and $\mathbf{M}_Q^g$ is the sum of inertia and gravity momentum computed at point Q.

If we choose $Q = CoP$ in equation A.20, we obtain:

$$\mathbf{M}^{c}_{CoP} + \mathbf{M}^{g_i}_{CoP} = \mathbf{0} \tag{A.22}$$

As presented in equation II.10, the momentum of the ground reaction force is null on the axis tangential to the contact surface. Then equation A.22 becomes:

$$(\mathbf{M}^{c}_{CoP}.\mathbf{n})\mathbf{n} + \mathbf{M}^{g_i}_{CoP} = \mathbf{0} \tag{A.23}$$

If we look at the axis tangential to $\mathbf{n}$ we obtain:

$$\mathbf{M}^{c}_{CoP\perp\mathbf{n}} + \mathbf{M}^{g_i}_{CoP\perp\mathbf{n}} = \mathbf{0} \tag{A.24}$$

Then:

$$\mathbf{M}^{g_i}_{CoP\perp\mathbf{n}} = \mathbf{0} \tag{A.25}$$

However, there exist only one point where the tipping momentum of inertia forces is null. As this point is the ZMP, equation A.25 shows that the CoP and the ZMP are the same point [Goswami 99, Sardain 04, Popovic 05].

Appendix B

Foot Rotation Indicator - Equations

The Foot Rotation Indicator (FRI) was presented by Goswami [Goswami 99] to measure the rotational state of the foot of humanoids: “foot rotation is an indication of postural instability and should be carefully treated in dynamically stable motions and avoided altogether in statically stable ones” [Goswami 99]. He used this point to characterize postural instability of the gait during single support phases of the locomotion.

The dynamic equilibrium Equation of the foot can be expressed as:

$$\mathbf{OG_{foot}} \times \mathbf{P_{foot}} + \mathbf{OCoP} \times \mathbf{GRF} + \mathbf{OA_{ankle}} \times \mathbf{F_{ankle}} + \tau_{\mathbf{ankle}} = \dot{\mathbf{H}}_{\mathbf{foot}/0} \tag{B.1}$$

where G_{foot} is the center of mass of the foot, $\mathbf{P_{foot}}$ is the weight force of the foot applied at G_{foot}, A_{ankle} is the position of the joint linking the foot with the shinbone, $\mathbf{F_{ankle}}$ and $\tau_{\mathbf{ankle}}$ are the force and the torque applied by the rest of the body on the foot, and $\dot{\mathbf{H}}_{\mathbf{foot}/0}$ is the derivative of the angular momentum of the foot expressed at the point O. These points are represented in Figure B.1

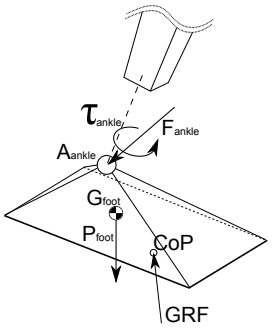

Figure B.1: Sketch of a 3D foot with the different forces and torques applied on the foot, and the forces locations.

Thus, the equations for the static equilibrium of the foot are obtained by setting the dynamic terms in Equation B.1 to zero:

$$\mathbf{OG_{foot}} \times \mathbf{P_{foot}} + \mathbf{OCoP} \times \mathbf{GRF} + \mathbf{OA_{ankle}} \times \mathbf{F_{ankle}} + \tau_{\mathbf{ankle}} = \mathbf{0} \tag{B.2}$$

Expressing Equation B.2 at CoP on the axes tangential to the support surface leads to:

$$\left(\mathbf{CoPG_{foot}} \times \mathbf{P_{foot}} + \mathbf{CoPA_{ankle}} \times \mathbf{F_{ankle}} + \tau_{\mathbf{ankle}}\right)_{\perp \mathbf{n}} = \mathbf{0} \tag{B.3}$$

where the subscript $_{\perp\mathbf{n}}$ implies the tangential components (orthogonal to the vecteur **n** normal to the contact surface). In the presence of an unbalanced torque on the foot Equation B.3 is not satisfied for any point within the support polygon. One may, however, still find a point FRI outside the support boundary which satisfies Equation B.2, i.e.:

$$\Big(\mathbf{FRIG_{foot}} \times \mathbf{P_{foot}} + \mathbf{FRIA_{ankle}} \times \mathbf{F_{ankle}} + \tau_{\mathbf{ankle}}\Big)_{\perp\mathbf{n}} = \mathbf{0} \tag{B.4}$$

By computing at FRI the dynamics of the virtual human, minus the foot (subscript $_1$), we obtain:

$$\begin{array}{rcl} \mathbf{FRIA_{ankle}} \times \mathbf{F_{ankle}} + \tau_{\mathbf{ankle}} & = & \sum_{i=2}^{n} \Big(\mathbf{FRIG_i} \times \mathbf{P_i} - \dot{\mathbf{H}}_{i/FRI}\Big) \\ & = & \sum_{i=2}^{n} \Big(\mathbf{FRIG_i} \times \mathbf{P_i} - \dot{\mathbf{H}}_{i/G_i} - m_i * \mathbf{FRIG_i} \times \ddot{\mathbf{OG}}_{\mathbf{i}i}\Big) \end{array} \tag{B.5}$$

Thus, Equation B.4 can be rewritten as:

$$\Big(\mathbf{FRIG_{foot}} \times \mathbf{P_{foot}} + \sum_{i=2}^{n} \Big(\mathbf{FRIG_i} \times (\mathbf{P_i} - m_i * \ddot{\mathbf{OG}}_{\mathbf{i}}) - \dot{\mathbf{H}}_{i/G_i}\Big)\Big)_{\perp\mathbf{n}} = \mathbf{0} \tag{B.6}$$

Then:

$$\Big(\mathbf{OFRI} \times \Big(\mathbf{P_{foot}} + \sum_{i=2}^{n} (\mathbf{P_i} - m_i * \ddot{\mathbf{OG}}_{\mathbf{i}})\Big)\Big)_{\perp\mathbf{n}} = \Big(\mathbf{OG_{foot}} \times \mathbf{P_{foot}} + \sum_{i=2}^{n} \Big(\mathbf{OG_i} \times (\mathbf{P_i} - m_i * \ddot{\mathbf{OG}}_{\mathbf{i}}) - \dot{\mathbf{H}}_{i/G_i}\Big)\Big)_{\perp\mathbf{n}} \tag{B.7}$$

Finally:

$$OFRI_x = \frac{NUM_x}{DEN} \qquad OFRI_y = \frac{NUM_y}{DEN} \tag{B.8}$$

with:

$$\begin{array}{rcl} NUM_x & = & m_{foot} * x_{foot} * g + \sum_{i=2}^{n} mi\Big(x_i(\ddot{z}_i + g) + \ddot{x}_i(FRI_z - z_i)\Big) - (\dot{\mathbf{H}}_{i/G_i})_Y \\ NUM_y & = & m_{foot} * y_{foot} * g + \sum_{i=2}^{n} mi\Big(y_i(\ddot{z}_i + g) + \ddot{y}_i(FRI_z - z_i)\Big) + (\dot{\mathbf{H}}_{i/G_i})_X \\ DEN & = & m_{foot} * g + \sum_{i=2}^{n} m_i * (\ddot{z}_i + g) \end{array} \tag{B.9}$$

Appendix C

Angular Momentum

Angular momentum is a quantity that is useful in describing the rotational state and the inertial properties of a physical system. In a system where no external forces or torques are applied, there is a conservation of the angular momentum. This explains many phenomenas, such as the increase of spinning of an figure ice skater when the skater's arm are fold up, or such as the creation of a twist when a trampolinist move his arms during a somersault.

C.1 Definitions

Depending on the system, the angular momentum $\mathbf{H}$ can be composed of a rotational inertia term $\mathbf{H}_{rot}$ and a translational inertia term $\mathbf{H}_{trans}$. The total angular momentum is then defined as:

$$\mathbf{H} = \mathbf{H}_{rot} + \mathbf{H}_{trans} \tag{C.1}$$

In the case of a mass particle in translation, the angular momentum about a given origin O is limited to the translational inertia $\mathbf{H}_{trans}$. It is defined by:

$$\mathbf{H}_{trans/O} = \mathbf{c} \times m\dot{\mathbf{c}} \tag{C.2}$$

where $\mathbf{c}$ is the position vector of the particle relatively to the origin O, $\dot{\mathbf{c}}$ is the velocity and m is the mass of the particle.

For an object with a fixed mass that is only rotating about its center of mass, the angular momentum about a given origin O is limited to the rotational inertia $\mathbf{H}_{rot}$. It is expressed as the product of the inertia matrix $\mathbf{I}$ of the object in the global coordinates and its angular velocity vector ω:

$$\mathbf{H}_{rot} = \mathbf{I}\omega \tag{C.3}$$

In a system composed of several elements (mass particles or rigid bodies), the angular momentum of the whole system corresponds to the sum of the angular momentum H_i of each individual element i. Thus, the total angular momentum of a N element system is:

$$\mathbf{H} = \sum_{i=1}^{N} \mathbf{H}_i = \sum_{i=1}^{N} \mathbf{H}_{i,rot} + \mathbf{H}_{i,trans} \tag{C.4}$$

C.2 Angular momentum for common virtual human models

Different models can be used to represent a virtual human, from a simple inverted pendulum to a full rigid body model. Certainly, the choice of the model will increase the computation time of the angular momentum. The equations of angular momentum for three common virtual human models are presented in the following of the section. These three common virtual human models are represented in Figure C.1

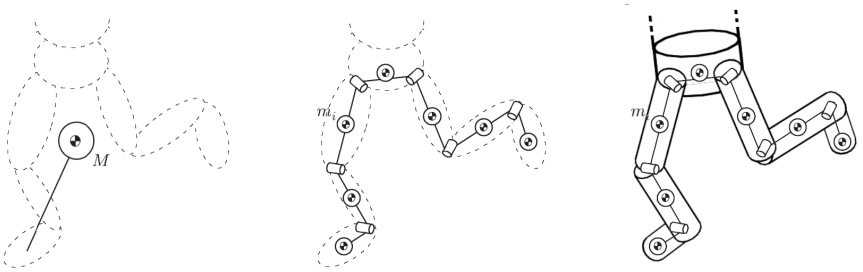

(a) Pendulum model (b) System of particles model (c) Articulated rigid body model

Figure C.1: Three main models commonly used in the literature. The virtual human is represented as a) a particle of mass m located at the center of mass of the character (pendulum model), b) a set of particles (system of particles model) or c) a set of rigid segments (articulated rigid body model). Only the lower body is represented by simplicity.

C.2.1 Inverted pendulum

In the inverted pendulum model, the virtual human is represented as a particle of mass M located at the center of mass G of the character. This particle is only in translation, hence $\mathbf{H}_{rot} = \mathbf{0}$. The angular momentum about an origin O is thus defined by:

$$\mathbf{H}_{inverted\_pendulum/O} = \mathbf{OG} \times M\dot{\mathbf{OG}} \tag{C.5}$$

C.2.2 System of particles

In the system of particles model, the virtual human is represented as a set of particle. Each segment i of the virtual human body is represented by a particle of mass m_i located at the center of mass G_i of the segment. All these particles are considered without rotation, hence $\forall i, \mathbf{H}_{i,rot} = \mathbf{0}$. The angular momentum about an origin O is thus defined by:

$$\mathbf{H}_{system\_of\_particles/O} = \sum_{i=1}^{N} \mathbf{H}_{i/O} = \sum_{i=1}^{N} \mathbf{OG_i} \times m_i\dot{\mathbf{OG_i}} \tag{C.6}$$

It is often convenient to consider the angular momentum of a collection of particles about their center of mass G. In that case, Equation C.6 is rewritten :

$$\mathbf{H}_{system\_of\_particles/G} = \sum_{i=1}^{N} \mathbf{H}_{i/G} = \sum_{i=1}^{N} \mathbf{GG_i} \times m_i\dot{\mathbf{GG_i}} \tag{C.7}$$

C.2.3 Rigid body model

In a rigid body model, the virtual human is represented as a set of rigid segments. Each segment i of the virtual human body is represented by an object with a mass m_i, a center of mass G_i and an inertia matrix I_i. The angular momentum about an origin O is thus defined by:

$$\mathbf{H}_{rigid\_body/O} = \sum_{i=1}^{N} \mathbf{H}_{i/O} = \sum_{i=1}^{N} I_i \omega_{\mathbf{i}} + \mathbf{OG_i} \times m_i \dot{\mathbf{OG}}_{\mathbf{i}} \tag{C.8}$$

with $\mathbf{I_i}$ and ω_i defined in the global coordinate system.

It is often convenient to compute the angular momentum of a virtual human represented using a rigid body model about its center of mass G. In that case, Equation C.8 is rewritten:

$$\mathbf{H}_{rigid\_body/G} = \sum_{i=1}^{N} \mathbf{H}_{i/G} = \sum_{i=1}^{N} I_i \omega_{\mathbf{i}} + \mathbf{GG_i} \times m_i \dot{\mathbf{GG}}_{\mathbf{i}} \tag{C.9}$$

Appendix D

Questionnaire of the perceptual study

In the perceptual study of Chapter III, participants were asked to fill-in an intermediate questionnaire after each session of the experiment, as well as a final one after the last session. These questionnaires are presented hereafter.

D.1 Intermediate questionnaire

1. What strategy did you use to estimate the weights from the presented motions?

2. Which cues seemed pertinent to differentiate the different weights? Which body part?

D.2 Final questionnaire

1. Which difference did you feel between real and virtual motions?

2. Did you find similarities between real and virtual motions?

3. Did you change the strategy used to differentiate weights when comparing real or virtual motions?

4. Do you think that the virtual character was similar enough to the real character? If not, what differences did you feel?

5. Comments about the experiments?

6. How did you feel the difficulty/easiness of the task?

7. How did you feel the tiredness linked with the experiments?

8. Did you use one of the following cue for the experiment showing real motions only? Tick the right boxes.
   □ Position □ Velocity □ Acceleration
   □ Hand □ Elbow □ Shoulder
   Comments and details: ...

9. Same question about the experiment with virtual motions only.
   □ Position □ Velocity □ Acceleration
   □ Hand □ Elbow □ Shoulder
   Comments and details: ...

10. Same question about the experiment with both real and virtual motions.
    □ Position □ Velocity □ Acceleration
    □ Hand □ Elbow □ Shoulder
    Comments and details: ...

Annexe E

Résumé en français du mémoire

E.1 Introduction

Depuis plusieurs années, la simulation du mouvement des humanoïdes virtuels est devenue un enjeu important dans de nombreux domaines. Le problème consiste à produire des humains virtuels qui se comportent et se déplacent de façon naturelle, c.à.d. qui ont le même comportement qu'un véritable humain dans la même situation. Dans le cas d'applications interactives, il est de plus important que ces humains virtuels réagissent rapidement aux ordres de l'utilisateur.

Dans de telles applications, les humains virtuels interagissent avec leur environnement : ils se déplacent sur des sols plus ou moins complexes, portent et déplacent des objets plus ou moins lourds, ou interagissent avec d'autres humains virtuels. Pour réaliser toutes ces tâches, les humains virtuels doivent donc prendre en compte différentes contraintes :

- des contraintes **cinématiques**, se basant sur les positions, telle que la position d'un objet à attraper dans l'environnement virtuel,
- des contraintes **cinétiques**, qui gèrent l'équilibre quasi-statique (sans accélérations) de l'humain virtuel en contrôlant son centre de masse,
- des contraintes **mécaniques**, qui prennent en compte les lois de la physique, cruciales lorsque l'humain virtuel est soumis à des forces extérieures,
- d'autres contraintes telles que le style, la morphologie ou une incapacité physique qui influencent le naturel du mouvement.

La simulation d'humains virtuels a apporté de nombreuses méthodes pour contrôler naturellement des personnages virtuels dans des environnements complexes, tout en prenant en compte les différentes contraintes précédentes. Deux principales familles de méthodes existent dans la littérature pour animer de façon naturelle ces humains virtuels. La première consiste à réutiliser de façon intelligente des mouvements capturés sur des acteurs, pour les appliquer à de nouvelles situations : le naturel des mouvements résultants dépend alors du naturel des mouvements capturés. Comme il n'est pas possible de capturer

toutes les variations d'une situation donnée, telle que toutes les vitesses possibles de marche, le problème consiste alors à proposer des méthodes pour réorganiser ou modifier les données capturées.

La seconde approche consiste à générer des mouvements sans l'aide de mouvements capturés. Ces approches offrent un contrôle du mouvement haut-niveau basé sur quelques paramètres pertinents. Cependant, le naturel des mouvements résultants n'atteint pas encore la qualité des mouvements capturés, alors que ces approches sont généralement extrêmement couteuses en temps de calcul. La génération de mouvement pose donc le problème de s'assurer qu'un algorithme est capable de générer un mouvement naturel, d'où la question suivante : « Parmi tous les mouvements réalisables par un humain virtuel, comment sélectionner ceux qu'un humain réel aurait réalisé dans la même situation ? »

Quel que soit la méthode d'animation, les humains virtuels se doivent de se comporter et de se déplacer de façon naturelle. Cependant, il est difficile de définir la limite d'un mouvement *naturel* : des animations de type cartoons peuvent sembler naturelles bien qu'elles ne respectent pas les lois de la physique, alors que les mêmes mouvements ne seront pas perçus comme naturels lorsqu' appliqués à des humains virtuels réalistes. La perception du naturel du mouvement est donc extrêmement liée à un sentiment subjectif de l'utilisateur. Par conséquence, la perception du mouvement joue un rôle important dans la crédibilité et la qualité des applications virtuelles.

Dans ce mémoire, nous nous basons sur cette observation pour proposer de nouvelles méthodes d'animation exploitant la perception du mouvement humain. D'une part, nous proposons d'examiner quelles sont les propriétés mécaniques pertinentes pour assurer le naturel du mouvement des personnages de synthèse. D'autre part, nous souhaitons étendre les connaissances de la perception du naturel des mouvements soumis à des contraintes physiques. Le but est de coupler ces études pour produire des mouvements perçus comme naturels par les utilisateurs, tout en simplifiant de façon pertinente les contraintes mécaniques appliquées au mouvement.

Ces travaux s'organisent sous trois contributions principales. La première contribution consiste à extraire les propriétés mécaniques pertinentes qui interviennent lors de réactions à des perturbations extérieures. Parmi les différentes situations possibles, nous nous sommes focalisés sur l'étude des paramètres mécaniques de l'équilibre humain. Notre première contribution consiste à comparer différents critères existants dans la littérature pour mesurer l'équilibre et le déséquilibre, et à proposer une gamme d'utilisation optimale pour chaque critère. Le but est de déterminer s'il existe un critère capable de mesurer précisément la perte d'équilibre. Comme les êtres humains ont une station préférentiellement bipodale, donc une faible surface d'interaction avec leur environnement, leur équilibre est facilement mis en danger et implique un contrôle permanent. Par conséquent, le fait d'être soumis à des forces extérieures implique d'adapter et de contrôler son équilibre. De nombreux travaux ont proposé des méthodes pour contrôler l'équilibre en condition statique (pas d'accélérations) ou quasi-statique (accélérations négligeables). Cependant, le problème est plus complexe en situation d'équilibre dynamique.

L'un des challenges en animation consiste à produire des mouvements qui sont perçus comme naturels par les utilisateurs plutôt que de produire des mouvements uniquement physiquement corrects. Dans cette optique, notre seconde contribution est l'étude des propriétés physiques perçues par les utilisateurs lorsqu'ils regardent et comparent des mouvements soumis à différentes contraintes mécaniques. Nous avons mis en place une expérience pour évaluer la précision des utilisateurs à différencier des mouvements soulevant différentes charges. Les résultats de cette expérience perceptive peuvent alors être réutilisés pour proposer de nouvelles méthodes d'animation se basant sur la précision de la perception humaine pour produire des mouvements perçus comme naturels.

La dernière contribution de ce mémoire consiste alors à réutiliser les connaissances acquises lors des études précédentes pour développer une nouvelle méthode d'animation simulant de façon naturelle la réaction des personnages de synthèse à des perturbations externes. Comme remarqué précédemment, il existe une infinité de réactions correctes à une perturbation donnée. L'idée principale consiste à utiliser un exemple de réaction possible et à adapter cet exemple aux nouvelles contraintes qui s'appliquent sur l'humain virtuel. Cette méthode se base donc sur les connaissances acquises lors de l'étude de l'équilibre dynamique pour modifier la posture de l'humain virtuel au moment de l'interaction. Cependant, contrairement aux approches classiques qui se basent sur des optimisations extrêmement couteuses, notre méthode sélectionne automatiquement une réaction naturelle en se basant sur les stratégies motrices mises en évidence lors des premières expériences. De plus, nous intégrons les résultats de l'expérience perceptive présentée auparavant pour simplifier le problème. Ainsi, au lieu de prendre en compte des équations non-linéaires complexes, nous proposons de diviser le problème en deux sous-problèmes (nous faisons l'hypothèse ici que l'erreur liée à cette simplification n'est pas perceptible par les utilisateurs) :

1. adapter chaque posture sous hypothèse d'accélérations nulles,

2. modifier l'échelle temporelle du mouvement résultant pour prendre en compte les informations de vitesse.

Le résumé de ce mémoire est organisé de la façon suivante. La section E.2 présente l'étude de différents critères couramment utilisés en biomécanique et en robotique pour mesurer l'état d'équilibre d'un humanoïde (réel, virtuel ou robot). L'étude de la précision de ces critères est un point clé pour prendre en compte les ajustements mécaniques lors de perturbations extérieures. Un autre point clé est la capacité des utilisateurs à percevoir ce type d'ajustements. Ainsi, la section E.3 présente une étude biomécanique combinée à une étude perceptive évaluant si les êtres humains sont capables de distinguer des différences de perturbations mécaniques sur des mouvements capturés sur des acteurs. Enfin, la section E.4 présente une nouvelle méthode d'animation basée sur ces deux premières contributions : nous proposons une nouvelle méthode temps-réelle pour adapter un mouvement soumis à diverses perturbations.

E.2 Mesure de l'équilibre dynamique

S'il est connu depuis de nombreuses années que les propriétés mécaniques jouent un rôle important dans le naturel du mouvement humain, leur intégration dans les processus d'animation n'est pas encore directe. Différentes simplifications sont généralement nécessaires pour contrôler physiquement ces humains virtuels, tel que contrôler la position du centre de pression ou minimiser la variation du moment cinétique durant la locomotion. Cependant, parmi toutes les solutions possibles, seulement un sous-ensemble sera perçu comme naturel. Simuler des mouvements naturels requière donc de comprendre le fonctionnement des mécanismes physiques de l'être humain, dans le but de comprendre comment les humains virtuels doivent se comporter en fonction de la situation (perturbations, déplacements, interactions, etc).

L'un des éléments important pour obtenir des mouvements naturels consiste à gérer des comportements réalistes de conservation équilibre. La mesure de cet équilibre mécanique intéresse de nombreux domaines, tels que la biomécanique, la robotique ou l'animation de personnages, mais reste un challenge. Une question toujours ouverte consiste notamment à savoir comment définir l'état d'équilibre ainsi que de définir un critère performant pour mesurer l'équilibre ou la perte d'équilibre.

L'un des problèmes principal de l'être humain est qu'il gère son équilibre de part une faible surface de contact avec son environnement comparée à l'étendue de la surface corporelle où des perturbations peuvent avoir lieu. Le maintien de cet équilibre est donc lié à cette surface de contact couramment appelée base de support. En animation, la base de support est généralement représentée par un polygone, appelé polygone de sustentation.

De nombreux critères de mesure de l'équilibre ont déjà été présentés dans la littérature. Ils se basent généralement sur l'écart d'un point représentatif par rapport à la base de support pour mesurer l'équilibre/déséquilibre du mouvement. Pour les mouvements avec accélérations négligeables (condition *quasi-statique*), la projection du centre de masse sur le sol (GCOM) est couramment utilisée pour détecter la perte d'équilibre lorsqu'elle réside en dehors de la base de support [Dyson 77, Winter 95]. Ce critère a notamment été utilisé en animation pour contrôler l'équilibre quasi-statique d'un personnage [Boulic 96, Baerlocher 00, Kulpa 05a].

Cependant, l'utilisation du GCOM est très limitée à cause de l'hypothèse *quasi-statique*. Pai et son groupe on notamment démontré que cette condition est insuffisante pour des mouvements où les accélérations ne peuvent être négligées [Pai 97, Iqbal 00]. Conserver son équilibre peut alors être impossible même si la projection du centre de masse réside dans la base de support, par exemple si la vitesse du centre de masse est dirigée vers l'extérieur. L'inverse est bien entendu aussi possible. En se basant sur ces observations, Hof [Hof 05] a proposé de modéliser l'équilibre de mouvements avec faibles accélérations (*faible dynamique*) en utilisant le Extrapolated Center of Mass (XcoM). Ce critère étend la notion de projection du centre de masse en prenant en compte la vitesse du centre masse pour mesurer l'équilibre dynamique.

Dans le cas de mouvements avec de fortes accélérations (*forte dynamique*), d'autres critères existent dans la littérature. Le centre de pression (CdP) et son homologue robotique le Zero Moment Point (ZMP) sont, par définition, restreints à n'exister que dans la base de support. Le CdP, lié aux forces de contact, est mesuré en utilisant une plate-forme de forces. Le ZMP, lié aux forces inertielles et d'accélérations, est calculé à partir des données capturées. A cause des limitations inhérentes à ces critères, d'autres auteurs ont proposé de mesurer l'équilibre dynamique en se basant sur l'équilibre en rotation. Goswami et col. [Goswami 99] ont proposé de mesurer la rotation du pied, ou Foot Rotation Index (FRI), pour détecter un déséquilibre lors des phases unipodales. Pour étendre la détection aux phases bipodales, Ils ont aussi proposé de se baser sur la variation de rotation du corps (Zero Rate of Angular Momentum, ZRAM [Goswami 04]) pour mesurer le déséquilibre en rotation.

Par conséquent, les différents critères existant dans la littérature pour mesurer l'état d'équilibre d'un humanoïde sont valides dans des conditions différentes. Le chapitre de ce mémoire sur la mesure de l'équilibre dynamique des humanoïdes présente les principaux avantages et désavantages de chaque critère et évalue leur performance en fonction du type de mouvement réalisé.

Dans ce chapitre, nous évaluons la capacité de chaque critère à mesurer l'équilibre et le déséquilibre. Treize participants ont réalisé plusieurs séries de mouvements (Figure E.1) : mouvements lents (quasi-statiques), avec faibles accélérations (faible dynamique) ou avec fortes accélérations (forte dynamique). Un système de capture de mouvements Vicon MX40 (12 caméras) enregistrait la position de 45 marqueurs placés sur le corps des participants. Une plateforme de force AMTI OR6 était de plus synchronisée avec le système de capture de mouvement pour enregistrer la position du centre de pression. Les trajectoires articulaires recalculées à partir des données capturées ont alors été utilisées pour calculer les différents critères d'équilibre dynamique, dans le but d'évaluer leur efficacité dans différentes situations.

Quasi-statique	
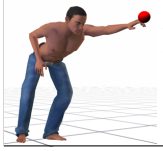	**Attraper :** essayer d'atteindre une cible en conservant les deux pieds en contact avec le sol.
Faible dynamique	
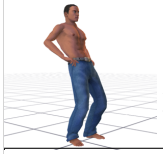	**Oscillations :** oscillations volontaires de plus en plus importantes avec bras fixes.
	**Marche :** marche à vitesse de comfort et arrêt brusque au signal.
	**Virages :** marche à vitesse de comfort et virages soudains à 90° et 180°.
Forte dynamique	
	**Oscillations fortes :** oscillations volontaires de plus en plus importantes avec utilisation des bras.
	**Appui un pied :** mouvements rapides de balancier d'une jambe.
	**Toupie :** un ou deux tours sur soi-même sur un pied.
	**Course et saut :** course et saut au signal.

TABLE E.1 – Liste des mouvements réalisés par les sujets. Les mouvements sont representés sur un personnage de synthèse dans un but uniquement informatif.

Les résultats de cette étude montrent qu'aucun des critères évalués ne détecte correctement les équilibres et déséquilibres. Des déséquilibres sont majoritairement détectés alors que le sujet continue son mouvement sans besoin visible d'agir pour récupérer son équilibre (récupération, mouvement des bras, hésitation, etc). Les résultats montrent aussi que le ZMP, en théorie équivalent au CdP, diffère grandement de ce dernier, en particulier pour les mouvements à *forte dynamique*. Ainsi, calculer un ZMP en dehors de la base de support (comme souvent utilisé en robotique) semble davantage être lié à des erreurs de modèle.

Cependant, l'une des questions fondamentale découlant de cette étude est de définir clairement la notion d'équilibre en situation dynamique. La question se pose notamment pour la locomotion, considérée comme une succession de chutes vers l'avant en biomécanique. Il serait particulièrement intéressant de définir la limite à partir de laquelle un mouvement de marche n'est plus considéré comme en équilibre. D'un point de vue expérimental, il est très difficile de définir l'instant à partir duquel le mouvement passe de l'état d'équilibre à celui de déséquilibre. Dans l'étude de ce chapitre, aucun des critères testés n'a réussi à détecter automatiquement cet instant. Par conséquent, de futures études conduites avec un protocole spécifique et une approche multidisciplinaire est clairement nécessaire.

E.3 Perception des propriétés mécaniques du mouvement humain

Si l'équilibre dynamique est important pour simuler des humains virtuels crédibles et autonomes, ces humains virtuels doivent aussi interagir de façon réaliste avec leur environnement (porter des objets,

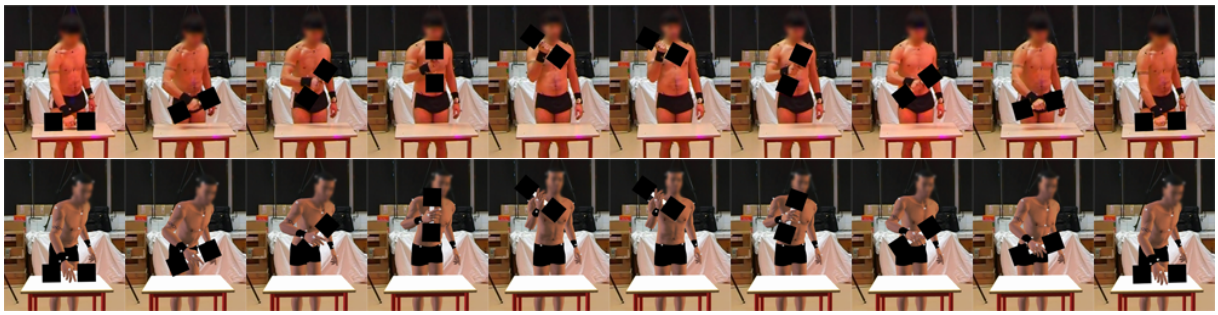

FIGURE E.1 – Extraits de vidéos d'un acteur soulevant un haltère de six kilogrammes : vidéo d'un mouvement réel (haut) et vidéo d'un mouvement capturé appliqué à un personnage de synthèse (bas).

se déplacer dans une scène complexe, réaliser différentes actions à différentes vitesses ou forces, etc). Réaliser ces actions nécessite de prendre en compte différentes contraintes, telle que la prise en compte des propriétés physiques de l'environnement. Différents modèles sont alors nécessaires, dont la précision est liée à la complexité. Si des modèles complexes peuvent générer des simulations très précises, il est cependant possible que les utilisateurs finaux ne soient pas en mesure de percevoir un tel degré de détail.

Cependant, si de nombreux travaux s'intéressent à la perception du mouvement humain, peu de travaux étudient la perception des paramètres physiques [O'Sullivan 03, Reitsma 03, Yeh 09]. Dans ce second chapitre, nous proposons d'évaluer la capacité des utilisateurs à percevoir des différences dans les paramètres physiques du mouvement humain. Nous nous intéressons plus particulièrement à la perception de la différence de masse pour des mouvements de soulever de charge.

Pour le besoin de cette expérience, un acteur réalisa des mouvements de soulever d'haltères dont le poids s'étendait de deux à dix kilogrammes par tranche d'un kilogramme. Un système de capture de mouvement équipé de 12 caméras Vicon MX40 captura la position de 45 marqueurs réfléchissant positionnés sur le corps de l'acteur, tandis qu'une caméra vidéo filmait ses mouvements.

Dans la première partie de l'étude, les trajectoires articulaires sont réutilisées pour évaluer si un critère biomécanique est capable de percevoir une différence de charge de seulement un kilogramme. Six critères sont étudiés : la position et la vitesse de l'épaule, du coude et de la main. Les résultats montrent que la vitesse de la main et de l'épaule parviennent à détecter une différence d'un kilogramme dans plus de 80% des cas. Ainsi, le profil de vitesse semble être un paramètre pertinent pour percevoir les différences de paramètres physiques.

Dans la seconde partie de l'étude, nous évaluons la capacité des utilisateurs à percevoir une différence de charge pour des mouvements réels (vidéos de l'acteur) ou virtuels (mouvements capturés réappliqués sur un personnage de synthèse). La figure E.1 présente un exemple des séquences présentées aux utilisateurs. Dans chaque cas (réels ou virtuels), les utilisateurs comparent des vidéos par paires : après avoir visualisé séquentiellement les deux vidéos, ils désignent la vidéo dont l'acteur réel ou virtuel porte la charge la plus lourde.

Les résultats de cette étude perceptive sont présentés sur la figure E.2. En règle générale, les masses légères (deux et trois kilogrammes) sont bien perçues lorsque comparées à la masse de référence de six kilogrammes. Les masses de dix et quatre kilogrammes sont aussi correctement perçues. Cependant, les autres masses (cinq, sept, huit et neuf kilogrammes) sont assez mal perçues lorsque comparées à

la référence de six kilogrammes. Ces résultats semblent montrer la difficulté des sujets à comparer les masses entre cinq et huit kilogrammes.

Il semble donc que les utilisateurs ne soient pas capables de percevoir une différence de charge d'un kilogramme. Pour le cas du soulever d'une charge, il semblerait qu'ils soient davantage capable de percevoir une différence de l'ordre de trois kilogrammes (ou 50% de la charge de référence). Cependant, les résultats montrent que les participants ont une capacité de perception similaire lors de la comparaison de mouvements réels ou virtuels.

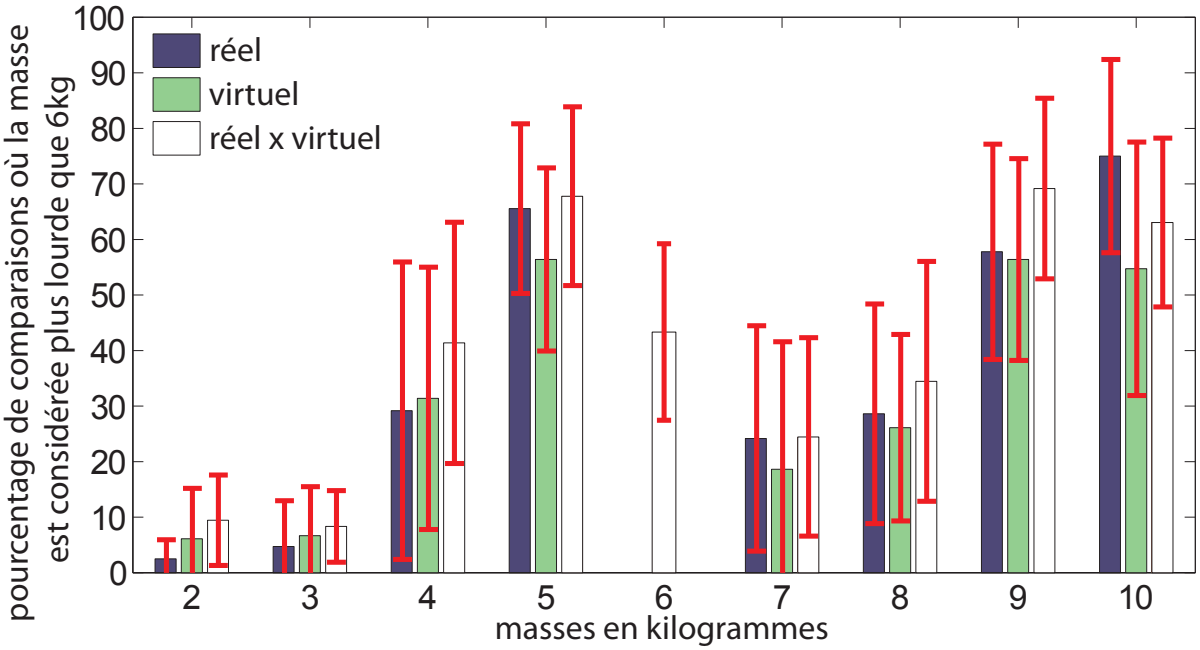

FIGURE E.2 – Résultats de l'étude perceptive : pourcentage de comparaisons où la masse en abscisse $m_j \in [2..10]$, $j \neq 6kg$ est considérée plus lourde que la masse de référence de 6kg. Les trois conditions sont : comparaison de paires de mouvements réels (vidéos) en bleu, comparaison de paires de mouvements appliqués sur un personnage de synthèse (animation) en vert, et comparaison de paires de mouvements composées d'un mouvement réel et d'un mouvement virtuel en blanc.

E.4 Adaptation du mouvement en réaction à des perturbations physiques

Comme les humanoïdes de synthèse sont de plus en plus présents dans les applications virtuelles, il est nécessaire de produire des interactions réalistes avec l'environnement virtuel pour la crédibilité de l'application. Le mouvement humain étant grandement dirigé par les lois de la physique, il est nécessaire de développer des algorithmes produisant des comportements physiques naturels. De plus, ces applications nécessitent généralement des interactions en temps-réel entre l'utilisateur et les humanoïdes virtuels dans le but de contrôler le personnage (attraper un objet, se déplacer, ajouter des perturbations, modifier les paramètres physiques de l'environnement, etc). Pour satisfaire la contrainte temps-réel, il est nécessaire de prendre en compte le problème du temps de calcul lors du développement des algorithmes physiques,

et de trouver un compromis entre réalisme physique et temps de calcul.

De notre point de vue, la perception du mouvement par l'utilisateur nous semble plus importante que l'exactitude physique dans la plupart des applications. Un paradoxe en animation est que des mouvements peuvent paraître totalement crédibles alors que les lois de la physique ne sont pas respectées, comme dans le cas des personnages de type cartoon. Dans ce dernier chapitre, nous présentons donc une nouvelle méthode d'animation temps-réelle basée perception pour la prise en compte des paramètres physiques lors de l'animation de personnage de synthèse. Cette méthode se base sur la faible sensibilité des utilisateurs à percevoir les propriétés physiques pour simplifier le processus d'animation physique. Nous présentons comment utiliser les résultats acquis dans les études des chapitres précédents pour animer en temps-réel des humains virtuels soumis à diverses perturbations physiques. Notre méthode traite séparément l'adaptation posturale et temporelle du mouvement, entraînant une légère imprécision au profit d'une amélioration considérable du temps de calcul. Le mouvement obtenu est davantage adapté aux contraintes dynamiques que ne l'était celui d'origine, à moindre coût de calcul.

Cette méthode a été appliqué à différents types de mouvements : pousser ou tirer (Figure E.3), porter de charge (Figure E.4), accélérations centrifuges, perturbations externes, etc.

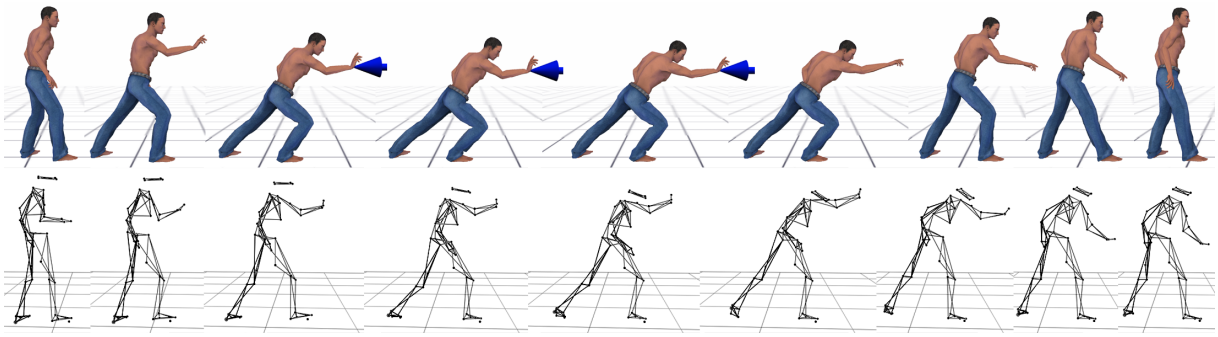

(a)

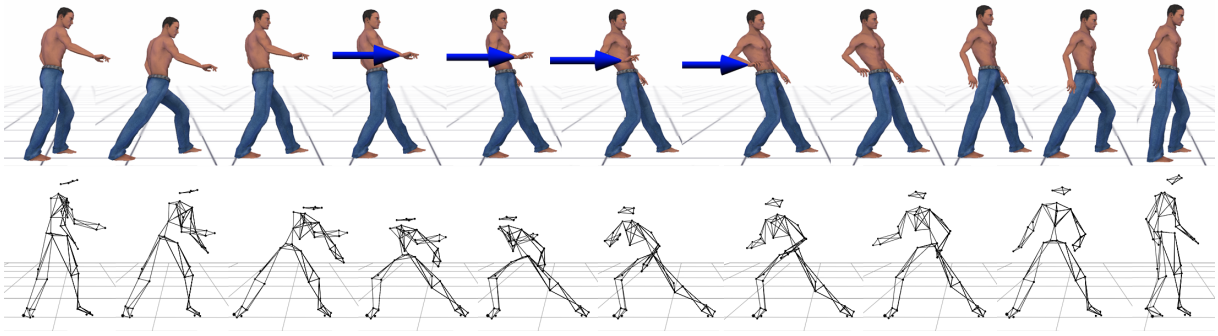

(b)

FIGURE E.3 – Personnage de synthèse soumis à une force extérieure de 200N non présente dans le mouvement d'origine. Le mouvement est corrigé par notre méthode en séparant l'adaptation posturale de l'adaptation temporelle, pour des mouvements a) de pousser et b) de tirer. Les mouvements corrigés (en couleur) sont comparés à des mouvements capturés sur un acteur avec des interactions du même ordre de grandeur.

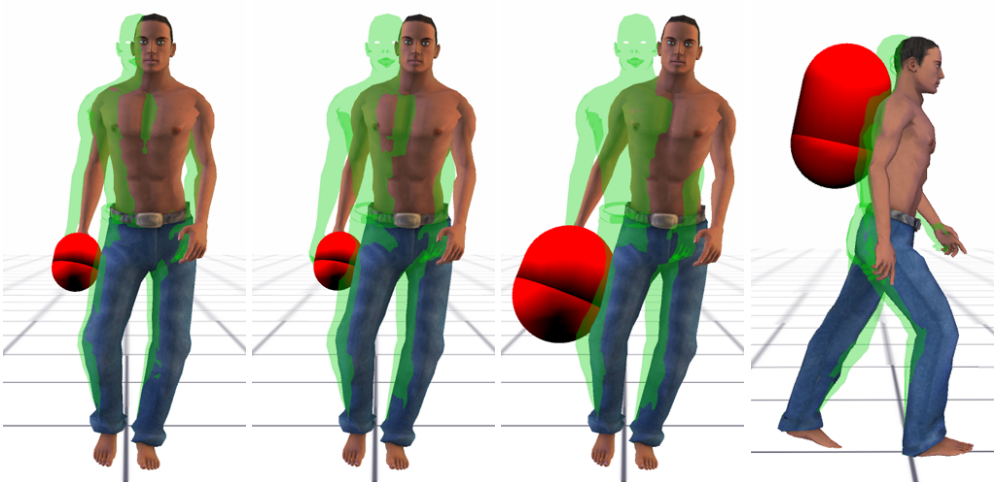

(a) (b) (c) (d)

FIGURE E.4 – Corrections pour des mouvements portant des charges. Personnage vert : mouvement d'origine non corrigé. Personnage texturé : chaque objet créé une force extérieure supplémentaire dirigée dans la direction de la gravité. Le mouvement est corrigé pour prendre en compte cette force : a) 10kg, b) et c) 25kg, d) 20kg.

E.5 Conclusion

Ce doctorat s'est intéressé à l'étude des paramètres mécaniques du mouvement humain dans le but de générer des mouvements réalistes à faible coût pour des personnages de synthèse. Il en a résulté la proposition d'une nouvelle méthode d'animation pour générer des mouvements perçus comme physiquement corrects lorsque les personnages de synthèse sont soumis à de nouvelles contraintes physiques. Pour parvenir à ces résultats, ces travaux ont été divisés en trois principales parties : analyser les stratégies motrices de mouvements capturés sur des acteurs, comprendre comment les utilisateurs perçoivent les contraintes physiques lorsqu'ils observent les mouvements d'acteurs (réels ou virtuels), et proposer une nouvelle approche pour prendre en compte de façon naturelle les nouvelles contraintes physiques appliquées sur le personnage de synthèse. La méthode proposée est de plus orientée applications interactives, tels que les jeux vidéo ou la réalité virtuelle, et se base sur les connaissances des deux premières études pour atteindre de faibles temps de calcul.

En animation, l'effet des contraintes physiques sur le mouvement des personnages de synthèse a été prise en compte principalement de trois façons : avec le couplage d'un modèle physique et d'un contrôleur, avec une optimisation sous contraintes spatio-temporelles, ou en réutilisant des mouvements capturés sur des acteurs et en les modifiant pour prendre en compte ces nouvelles contraintes. Pour évaluer la pertinence de chaque méthode, trois propriétés principales doivent être considérées :

1. La méthode doit proposer un contrôle simple et efficace de l'humain virtuel : le but est de prendre en compte les contraintes imposées par le scénario ou par l'utilisateur. Les méthodes présentées offrent généralement un très bon contrôle de l'humanoïde, mais de nombreux paramètres sont encore à régler avant d'obtenir des mouvements réalistes.

2. Le temps de calcul inhérent à la méthode est un problème clé, plus spécialement dans le cas des

applications interactives. Si la simulation de modèles physiques complexes a été rendue possible par l'augmentation de la puissance des ordinateurs, la plupart des applications requièrent aussi de la puissance de calcul pour de nombreuses autres tâches que l'animation de mouvements (rendu, intelligence artificielle, interfaces, collaboration entre utilisateurs, etc). Ainsi, réduire le temps de calcul est nécessaire pour pouvoir prendre en compte toutes les tâches composant une application.

3. Les humains virtuels sont observés et évalués par des utilisateurs réels qui ont une longue expérience des mouvements et comportements naturels humains. Par conséquent, assurer le naturel des mouvements des personnages de synthèse est crucial pour produire des animations de haut niveau. Ceci est encore plus vrai pour les applications qui recherchent une immersion de l'utilisateur dans le monde virtuel. De nombreuses approches cherchent à réutiliser les mouvements capturés sur des acteurs pour s'assurer du naturel des mouvements. Cependant, réutiliser ces mouvements dans des situations non appropriées entraine des artefacts et des mouvements non naturels, d'où la nécessité de proposer des méthodes pour modifier ces mouvements capturés. Néanmoins, cette approche semble être actuellement la seule capable de prendre en compte correctement le style propre aux mouvements humains.

Ce mémoire de doctorat a contribué à proposer une nouvelle méthode d'animation prenant en compte tous les points mentionnés précédemment. L'idée est d'offrir à l'utilisateur un contrôle simple de l'humanoïde de synthèse, avec peu de temps de calculs et en préservant le réalisme d'un mouvement de référence. Pour atteindre ce but, nous nous sommes appuyés sur deux études pour évaluer les propriétés mécaniques pertinentes de l'équilibre dynamique des personnages de synthèse et pour évaluer la sensibilité de perception des utilisateurs aux paramètres physiques du mouvement.

Pour résumer, les trois principales contributions de ce doctorat sont :

1. Premièrement, nous avons présenté une étude portant sur la mesure de l'équilibre dynamique, basée sur des mouvements biologiques capturés sur un ensemble de sujets. Nos expériences avec les mouvements à forte dynamique montrent clairement qu'aucun des critères actuellement utilisés pour détecter la perte d'équilibre ne parvient à correctement détecter les phases d'équilibre ou de déséquilibre. Ces critères détectent majoritairement des pertes d'équilibre alors que les participants continuent leurs mouvements sans réaction apparente.

2. Deuxièmement, nous avons mené une étude sur la capacité des utilisateurs à percevoir une différence de masse soulevée par un acteur réel (vidéos) ou par un personnage de synthèse (animations). Les résultats montrent clairement que les utilisateurs ne parviennent pas à distinguer précisément une faible différence de charge. Cependant, nous observons des résultats similaires lors de la comparaison de vidéos réelles ou virtuelles.

3. Finalement, nous avons proposé une nouvelle méthode d'animation basée sur la perception humaine pour adapter des mouvements sujets à des perturbations extérieures. Cette méthode utilise les connaissances biomécaniques et perceptives obtenues dans les deux premières études. Elle a été appliquée pour produire des adaptations naturelles pour des interactions de type pousser, tirer ou porter, ou en réaction à des effets physiques (force centrifuge, marche contre le vent, etc).

INSA de Rennes
Service des formations

AVIS DU JURY SUR LA REPRODUCTION DE LA THESE SOUTENUE

Titre de la thèse : Adaptation dynamique de mouvements humains.

Nom Prénom de l'auteur : HOYET Ludovic

Membres du jury :
- Monsieur BOULIC
- Monsieur LAUMOND
- Monsieur MULTON
- Monsieur ARNALDI
- Monsieur EGGES
- Monsieur KOMURA

Président du jury : Bruno ARNALDI

Date de la soutenance : 18/11/2010

Reproduction de la thèse soutenue :

- ☒ Thèse pouvant être reproduite en l'état
- ☐ Thèse ne pouvant être reproduite
- ☐ Thèse pouvant être reproduite après corrections suggérées

Le Directeur,

A. JIGOREL

Rennes, le 18/11/2010

Signature du Président du jury

Bibliographie

[Abe 07] Yeuhi Abe, Marco da Silva & Jovan Popović. *Multiobjective control with frictional contacts*. In SCA '07 : Proceedings of the 2007 ACM SIGGRAPH/Eurographics symposium on Computer animation, pages 249–258, 2007.

[Alexander 84] R.M. Alexander. *Walking and Running*. American Scientist, vol. 72, no. 348-354, 1984.

[Arikan 02] Okan Arikan & David A. Forsyth. *Interactive motion generation from examples*. ACM Trans. Graph., vol. 21, no. 3, pages 483–490, 2002.

[Arikan 05] Okan Arikan, David A. Forsyth & James F. O'Brien. *Pushing people around*. In SCA '05 : Proceedings of the 2005 ACM SIGGRAPH/Eurographics symposium on Computer animation, pages 59–66, New York, NY, USA, 2005. ACM.

[Ashraf 00] Golam Ashraf & Kok Cheong Wong. *Generating consistant motion transition via framespace interpolation*. Eurographics, Computer Graphics Forum, vol. 19, no. 3, August 2000.

[Ashraf 01] Golam Ashraf & Kok Cheong Wong. *Constrained Framespace Interpolation*. Computer Animation 2001, pages 61–72, November 2001.

[Ashraf 03] Golam Ashraf & Kok Cheong Wong. *Semantic Representation and Correspondence for State-Based Motion Transition*. IEEE Transactions on Visualization and Computer Graphics, vol. 9, no. 4, pages 481–499, 2003.

[Assa 05] Jackie Assa, Yaron Caspi & Daniel Cohen-Or. *Action synopsis : pose selection and illustration*. ACM Trans. Graph., vol. 24, no. 3, pages 667–676, 2005.

[Aydin 99a] Yahya Aydin & Masayuki Nakajima. *Balance control and mass centre adjustment of articulated figures in interactive environments*. The Visual Computer, vol. 15, pages 113–123, 1999. 10.1007/s003710050166.

[Aydin 99b] Yahya Aydin & Masayuki Nakajima. *Realistic Articulated Character Positioning and Balance Control in Interactive Environments*. In Proceedings of the Computer Animation, CA '99, pages 160–, Washington, DC, USA, 1999. IEEE Computer Society.

[Baerlocher 98] Paolo Baerlocher & Ronan Boulic. *Task-priority formulations for the kinematic control of highly redundant articulated structures*. In Intelligent Robots and Systems, 1998. Proceedings., 1998 IEEE/RSJ International Conference on, volume 1, pages 323–329, 1998.

[Baerlocher 00] Paolo Baerlocher & Ronan Boulic. *Kinematic control of the mass properties of redundant articulated bodies*. Robotics and Automation, 2000. Proceedings. ICRA '00. IEEE International Conference on, vol. 3, pages 2557 –2562 vol.3, 2000.

[Baerlocher 04] Paolo Baerlocher & Ronan Boulic. *An inverse kinematics architecture enforcing an arbitrary number of strict priority levels*. Vis. Comput., vol. 20, no. 6, pages 402–417, 2004.

[Bingham 87] G. P. Bingham. *Kinematic form and scaling : further investigations on the visual perception of lifted weight*. Journal of experimental psychology. Human perception and performance, vol. 13, no. 2, pages 155–177, 1987.

[Boulic 92] Ronan Boulic & Daniel Thalmann. *Combined Direct and Inverse Kinematic Control for Articulated Figure MotionEditing*. Computer Graphics Forum, vol. 2, no. 4, October 1992.

[Boulic 96] Ronan Boulic, Ramon Mas & Daniel Thalmann. *A robust approach for the control of the center of mass with inverse kinetics*. Computers & Graphics, vol. 20, no. 5, pages 693 – 701, 1996. Mobile Computing.

[Boulic 97] Ronan Boulic, Pascal Bécheiraz, Luc Emering & Daniel Thalmann. *Integration of motion control techniques for virtual human and avatar real-time animation*. In VRST '97 : Proceedings of the ACM symposium on Virtual reality software and technology, pages 111–118, New York, NY, USA, 1997. ACM.

[Boulic 98] R. Boulic, P. Fua, L. Herda, M. Silaghi, J. S. Monzani, L. Nedel & D. Thalmann. *An Anatomic Human Body For Motion Capture*. In EMMSEC , Bordeaux, France, 1998.

[Bruderlin 95] Armin Bruderlin & Lance Williams. *Motion signal processing*. In SIGGRAPH '95 : Proceedings of the 22nd annual conference on Computer graphics and interactive techniques, pages 97–104, New York, NY, USA, 1995. ACM.

[Chadwick 89] J. E. Chadwick, D. R. Haumann & R. E. Parent. *Layered construction for deformable animated characters*. In SIGGRAPH '89 : Proceedings of the 16th annual conference on Computer graphics and interactive techniques, pages 243–252, New York, NY, USA, 1989. ACM.

[Chaminade 07] Thierry Chaminade, Jessica Hodgins & Mitsuo Kawato. *Anthropomorphism influences perception of computer-animated characters' actions*. Social Cognitive and Affective Neuroscience, 2007.

[Cohen 92] Michael F. Cohen. *Interactive spacetime control for animation*. SIGGRAPH Comput. Graph., vol. 26, no. 2, pages 293–302, 1992.

[Coros 10] Stelian Coros, Philippe Beaudoin & Michiel van de Panne. *Generalized biped walking control*. ACM Trans. Graph., vol. 29, no. 4, pages 1–9, 2010.

[da Silva 08a] Marco da Silva, Yeuhi Abe & Jovan Popović. *Interactive Simulation of Stylized Human Locomotion*. ACM Trans. Graph., vol. 27, no. 3, 2008.

[da Silva 08b] Marco da Silva, Yeuhi Abe & Jovan Popović. *Simulation of Human Motion Data using Short-Horizon Model-Predictive Control*. Computer Graphics Forum, vol. 27, pages 371–380, 2008.

[de Lasa 10] Martin de Lasa, Igor Mordatch & Aaron Hertzmann. *Feature-based locomotion controllers*. ACM Trans. Graph., vol. 29, no. 4, pages 1–10, 2010.

[De Leva 96] P. De Leva. *Adjustments to Zatsiorsky-Seluyanov's segment inertia parameters*. Journal of Bomechanics, vol. 29, pages 1223–1230, 1996.

[Dyson 77] GH Dyson. The mechanics of athletics. Holmes & Meier Publishers, New York, 1977.

[Ehrig 06] Rainald M Ehrig, Georg N Taylor William R ans Duda & Markus O Heller. *A survey of formal methods for determining the centre of rotation of ball joints*. Journal of Biomechanics, vol. 39, pages 2798–2809, 2006.

[Faloutsos 01a] Petros Faloutsos, Michiel van de Panne & Demetri Terzopoulos. *Composable controllers for physics-based character animation*. In SIGGRAPH '01 : Proceedings of the 28th annual conference on Computer graphics and interactive techniques, pages 251–260, New York, NY, USA, 2001. ACM.

[Faloutsos 01b] Petros Faloutsos, Michiel van de Panne & Demetri Terzopoulos. *The virtual stuntman : dynamic characters with a repertoire of autonomous motor skills*. Computers and Graphics, vol. 25, no. 6, pages 933–953, 2001.

[Fang 03] Anthony C. Fang & Nancy S. Pollard. *Efficient synthesis of physically valid human motion*. ACM Trans. Graph., vol. 22, no. 3, pages 417–426, 2003.

[Gescheider 85] George A. Gescheider. Psychophysics : Method, theory, and application. Lawrence Erlbaum Associates, 1985.

[Gleicher 97] Michael Gleicher. *Motion editing with spacetime constraints*. In I3D '97 : Proceedings of the 1997 symposium on Interactive 3D graphics, pages 139–ff., New York, NY, USA, 1997. ACM.

[Gleicher 98] Michael Gleicher & Peter Litwinowicz. *Constraint-Based Motion Adaptation*. Journal of Visualization and Computer Animation, vol. 9, no. 2, pages 65–94, 1998.

[Gleicher 01] Michael Gleicher. *Motion path editing*. In I3D '01 : Proceedings of the 2001 symposium on Interactive 3D graphics, pages 195–202, New York, NY, USA, 2001. ACM.

[Goswami 99] Ambarish Goswami. *Foot rotation indicator (FRI) point : A new gait planning tool to evaluate postural stability of biped robots*. In IEEE International Conference on Robotics and Automation, pages 47–52, 1999.

[Goswami 04] Ambarish Goswami & Vinutha Kallem. *Rate of change of angular momentum and balance maintenance of biped robots*. In Robotics and Automation, 2004. Proceedings. ICRA '04. 2004 IEEE International Conference on, volume 4, pages 3785–3790 Vol.4, 26-May 1, 2004.

[Guo 96] Shang Guo & James Robergé. *A high-level control mechanism for human locomotion based on parametric frame space interpolation*. In Proceedings of the Eurographics workshop on Computer animation and simulation '96, pages 95–107, New York, NY, USA, 1996. Springer-Verlag New York, Inc.

[H-Anim 01] H-Anim. *Human Animation Working Group*. `http://www.h-anim.org`, 2001.

[Hanafusa 81] H. Hanafusa, T. Yoshikawa & Y. Nakamura. *Analysis and Control of Articulated Robot with Redundancy*. IFAC, 8th Triennal World Congress, vol. 4, pages 1927–1932, 1981.

[Herda 00] Lorna Herda, Ralf Pl"ankers, Pascal Fua, Ronan Boulic & Daniel Thalmann. *Skeleton-Based Motion Capture for Rebust Reconstruction of Human Motion*. Proc. of Computer Animation'2000, May 2000.

[Herda 01] Lorna Herda, Pascal Fua, Ralf Pl"ankers, Ronan Boulic & Daniel Thalmann. *Using Skeleton-Based Tracking to Increase the Reliability of Optical MotionCapture*. Human Movement Science Journal, 2001.

[Herr 04] Hugh Herr & Marco Popovic. *Angular momentum in human walking*. The Journal of Experimental Biology, vol. 211, pages 467–481, 2004.

[Hicheur 05a] H. Hicheur, S. Glasauer, S. Vieilledent & A. Berthoz. *Head direction control during active locomotion in humans.* Wiener, SI, Taube, JS (Eds.), Head direction cells and the neural mechanisms of spatial orientation. MIT Press., 2005.

[Hicheur 05b] H. Hicheur, S. Vieilledent & A. Berthoz. *Head motion in humans alternating between straight and curved walking path : Combination of stabilizing and anticipatory orienting mechanisms.* Neurosci. Lett., vol. 383(1-2), pages 87–92., 2005.

[Hirukawa 06] Hirohisa Hirukawa, Shizuko Hattori, Kensuke Harada, Shuuji Kajita, Kenji Kaneko, Fumio Kanehiro, Kiyoshi Fujiwara & Mitsuharu Morisawa. *A universal stability criterion of the foot contact of legged robots - adios ZMP*. Robotics and Automation, 2006. ICRA 2006. Proceedings 2006 IEEE International Conference on, vol. , pages 1976–1983, May 2006.

[Hodgins 95] Jessica K. Hodgins, Wayne L. Wooten, David C. Brogan & James F. O'Brien. *Animating human athletics*. In SIGGRAPH '95 : Proceedings of the 22nd annual conference on Computer graphics and interactive techniques, pages 71–78, New York, NY, USA, 1995. ACM.

[Hodgins 98] Jessica K. Hodgins, James F. O'Brien & Jack Tumblin. *Perception of Human Motion With Different Geometric Models*. IEEE Trans. on Visualization and Computer Graphics, vol. 4, no. 4, pages 307–316, 1998.

[Hof 05] A. L. Hof & M. G. J. Gazendam. *The condition for dynamic stability*. Journal of Biomechanics, vol. 38, pages 1–8, 2005.

[Hof 07] A. L. Hof. *The equations of motion for a standing human reveal three mechanisms for balance.* Journal of Biomechanics, vol. 40, pages 451–457, 2007.

[Iqbal 00] Kamran Iqbal & Yi-Chung Pai. *Predicted region of stability for balance recovery : : motion at the knee joint can improve termination of forward movement*. Journal of Biomechanics, vol. 33, no. 12, pages 1619 – 1627, 2000.

[Johansson 73] G. Johansson. *Visual Perception of biological motion and a model for its analysis*. Perception and Psychophysics, vol. 14, no. 2, pages 201–211, 1973.

[Kajita 09] Shuuji Kajita, Hirohisa Hirukawa, Kensuke Harada & Kazuhito Yokoi. Introduction à la commande des robots humanoïdes : De la modélisation à la génération du mouvement. Springer, 2009.

[Ko 96] Hyeongseok Ko & N.I. Badler. *Animating human locomotion with inverse dynamics*. Computer Graphics and Applications, IEEE, vol. 16, no. 2, pages 50 –59, March 1996.

[Komura 05] Taku Komura, Edmond S. L. Ho & Rynson W. H. Lau. *Animating reactive motion using momentum-based inverse kinematics : Motion Capture and Retrieval*. Comput. Animat. Virtual Worlds, vol. 16, no. 3-4, pages 213–223, 2005.

[Kondo 91] Koichi Kondo. *Inverse Kinematics of a Human Arm*. Journal of Robotics and Systems, vol. 2, pages 115–175, 1991.

[Korein 82] J. U. Korein & N. I. Badler. *Techniques for Generating the Goal-Directed Animation of Articulated Structures*. IEEE Computer Graphics and Applications, vol. 2, no. 9, pages 71–81, November 1982.

[Kovar 02] Lucas Kovar, Michael Gleicher & Frédéric Pighin. *Motion graphs*. ACM Trans. Graph., vol. 21, no. 3, pages 473–482, 2002.

[Kulpa 05a] Richard Kulpa & Franck Multon. *Fast inverse kinematics and kinetics solver for human-like figures*. Humanoid Robots, 2005 5th IEEE-RAS International Conference on, pages 38–43, Dec. 2005.

[Kulpa 05b] Richard Kulpa, Franck Multon & Bruno Arnaldi. *Morphology-independent representation of motions for interactive human-like animation*. Computer Graphics Forum, Eurographics 2005 special issue, vol. 24, no. 3, pages 343–352, 2005.

[Laszlo 96] Joseph Laszlo, Michiel van de Panne & Eugene Fiume. *Limit cycle control and its application to the animation of balancing and walking*. In SIGGRAPH '96 : Proceedings of the 23rd annual conference on Computer graphics and interactive techniques, pages 155–162, New York, NY, USA, 1996. ACM.

[Laurent 88] M Laurent & J A Thomson. *The role of visual information in control of a constrained locomotor task.* Journal of motor behavior, vol. 20, no. 1, pages 17–37, March 1988.

[Lee 99] Jehee Lee & Sung Yong Shin. *A hierarchical approach to interactive motion editing for human-like figures*. pages 39–48, 1999.

[Lee 02] Jehee Lee, Jinxiang Chai, Paul S. A. Reitsma, Jessica K. Hodgins & Nancy S. Pollard. *Interactive control of avatars animated with human motion data*. ACM Trans. Graph., vol. 21, no. 3, pages 491–500, 2002.

[Lee 06] Jehee Lee & Kang Hoon Lee. *Precomputing avatar behavior from human motion data*. Graph. Models, vol. 68, no. 2, pages 158–174, 2006.

[Liu 94] Zicheng Liu & Michael F. Cohen. *Decomposition of Linked Figure Motion : Diving*. 5th Eurographics Workshop on Animation and Simulation, vol. , page , 1994.

[Liu 02] Karen Liu & Zoran Popović. *Synthesis of complex dynamic character motion from simple animations*. In SIGGRAPH '02 : Proceedings of the 29th annual conference on Computer graphics and interactive techniques, pages 408–416, New York, NY, USA, 2002. ACM.

[Liu 05] C. Karen Liu, Aaron Hertzmann & Zoran Popović. *Learning physics-based motion style with nonlinear inverse optimization*. ACM Trans. Graph., vol. 24, no. 3, pages 1071–1081, 2005.

[Liu 10] Libin Liu, KangKang Yin, Michiel van de Panne, Tianjia Shao & Weiwei Xu. *Sampling-based contact-rich motion control*. ACM Trans. Graph., vol. 29, no. 4, pages 1–10, 2010.

[Macchietto 09] Adriano Macchietto, Victor Zordan & Christian R. Shelton. *Momentum Control for Balance*. ACM Transactions on Graphics / SIGGRAPH, vol. 28, no. 3, 2009.

[Majkowska 07] Anna Majkowska & Petros Faloutsos. *Flipping with physics : motion editing for acrobatics*. In Proceedings of SCA '07, pages 35–44. Eurographics Association, 2007.

[Marey 94] M. Marey. *Mécanique animale*. New-York : Appleton & Co., vol. 119, 1894.

[Matsunaga 07] M. Matsunaga & V. B. Zordan. *A dynamics-based comparison metric for motion graphs*. In CGI, 2007.

[Ménardais 01] Stéphane Ménardais, Franck Multon & Bruno Arnaldi. *Amélioration des trajectoires acquises par des systèmes optiques pour l'animation de personnages synthétiques*. Revue Internationale de CFAO, pages 99–103, January 2001.

[Ménardais 03] Stéphane Ménardais. *Fusion et adaptation temps réel de mouvements acquis pour l'animation d'humanoidessynthétiques*. PhD thesis, Université Rennes 1, January 2003.

[Ménardais 04a] Stéphane Ménardais, Franck Multon, Richard Kulpa & Bruno Arnaldi. *Motion blending for real-time animation while accounting for the environment*. In Computer Graphics International, June 2004.

[Ménardais 04b] Stéphane Ménardais, Franck Multon, Richard Kulpa & Bruno Arnaldi. *Synchronization for dynamic blending of motions*. In Proceedings of ACM SIGGRAPH/Eurographics Symposium on Computer Animation, pages 325–336, Grenoble, France, August 2004.

[Mitake 09] Hironori Mitake, Kazuyuki Asano, Takafumi Aoki, Marc Salvati, Makoto Sato & Shoichi Hasegawa. *Physics-driven Multi Dimensional Keyframe Animation for Artist-directable Interactive Character*. Comput. Graph. Forum, vol. 28, no. 2, pages 279–287, 2009.

[Molet 96] Tom Molet, Ronan Boulic & Daniel Thalmann. *A real time anatomical converter for human motion capture*. In Proceedings of the Eurographics workshop on Computer animation and simulation '96, pages 79–94, New York, NY, USA, 1996. Springer-Verlag New York, Inc.

[Molet 97] T. Molet, Z. Huang, R. Boulic & D. Thalmann. *An Animation Interface Designed for Motion Capture*. In Computer Animation'97, pages 77–85, 1997.

[Mordatch 10] Igor Mordatch, Martin de Lasa & Aaron Hertzmann. *Robust physics-based locomotion using low-dimensional planning*. ACM Trans. Graph., vol. 29, no. 4, pages 1–8, 2010.

[Mori 70] Masahiro Mori. *Bukimi no tani, The uncanny valley*. (K. F. MacDorman & T. Minato, Trans.). Energy, vol. 7(4), pages 33–35, 1970.

[Multon 09] Franck Multon, Richard Kulpa, Ludovic Hoyet & Taku Komura. *Interactive animation of virtual humans based on motion capture data*. Comput. Animat. Virtual Worlds, vol. 20, no. 5&dash ;6, pages 491–500, 2009.

[O'Sullivan 03] Carol O'Sullivan, John Dingliana, Thanh Giang & Mary K. Kaiser. *Evaluating the visual fidelity of physically based animations*. ACM Trans. Graph., vol. 22, no. 3, pages 527–536, 2003.

[Otten 99] E Otten. *Balancing on a narrow ridge : biomechanics and control*. Philosophical Transactions of the Royal Society of London, vol. Series B 354, pages 869–875, 1999.

[Pai 97] Yi-Chung Pai & James Patton. *Center of mass velocity-position predictions for balance control*. Journal of Biomechanics, vol. 30, no. 4, pages 347 – 354, 1997.

[Park 02] Sang Il Park, Hyun Joon Shin & Sung Yong Shin. *On-line locomotion generation based on motion blending*. In SCA '02 : Proceedings of the 2002 ACM SIGGRAPH/Eurographics symposium on Computer animation, pages 105–111, New York, NY, USA, 2002. ACM.

[Park 04] Sang Il Park, Tae-hoon Kim, Hyun Joon Shin & Sung Yon Shin. *on-line motion blending for real-time locomotion generation*. Computer Animation and Virtual Worlds, vol. 15, no. 3-4, pages 125–138, July 2004.

[Penrose 55] Roger Penrose. *A Generalized Inverse for Matrices*. Proc. Cambridge Philos. Soc., vol. 51, pages 406–413, 1955.

[Pettré 06] Julien Pettré & Jean-Paul Laumond. *A motion capture based control-space approach for walking mannequins*. Computer Animation and Virtual Worlds, vol. 17, no. 2, pages 109–126, 2006.

[Pollard 01] Nancy Pollard & Paul Reitsma. *Animation of humanlike characters : Dynamic motion filtering with a physically plausible contact model*. in : Yale Workshop on Adaptive and Learning Systems, 2001.

[Popovic 04] Marko Popovic, Andreas Hofmann & Hugh Herr. *Zero spin angular momentum control : definition and applicability*. In Proceedings of the IEEE-RAS/RSJ International Conference on Humanoid Robots, pages 478–493, 2004.

[Popovic 05] Marko Popovic, Ambarish Goswami & Hugh Herr. *Ground reference points in legged locomotion : Definitions, biological trajectories and control implications*. The International Journal of Robotics Research, vol. 24, no. 12, pp. 1013-1032, 2005, vol. 24, no. 12, pages 1013–1032, 2005.

[Raibert 91] Marc H. Raibert & Jessica K. Hodgins. *Animation of dynamic legged locomotion*. SIGGRAPH Comput. Graph., vol. 25, no. 4, pages 349–358, 1991.

[Reitsma 03] Paul Reitsma & Nancy Pollard. *Perceptual metrics for character animation : sensitivity to errors in ballistic motion*. ACM Trans. Graph., vol. 22, no. 3, pages 537–542, 2003.

[Reitsma 08] Paul Reitsma, James Andrews & Nancy Pollard. *Effect of Character Animacy and Preparatory Motion on Perceptual Magnitude of Errors in Ballistic Motion*. In Proc. of Eurographics '08, 2008.

[Reitsma 09] Paul Reitsma & Carol O'Sullivan. *Effect of scenario on perceptual sensitivity to errors in animation*. ACM Trans. Appl. Percept., vol. 6, no. 3, pages 1–16, 2009.

[Ren 05] Liu Ren, Alton Patrick, Alexei A. Efros, Jessica K. Hodgins & James M. Rehg. *A data-driven approach to quantifying natural human motion*. ACM Trans. Graph., vol. 24, no. 3, pages 1090–1097, 2005.

[Rose 94] J. Rose & J.G Gamble. Human walking, 2nd edition. Williams and Wilkins, Baltimore, MD, 1994.

[Runeson 81] S. Runeson & G. Frykholm. *Visual perception of lifted weight*. Journal of Experimental Psychology : Human Perception and Performance, vol. 7, pages 733–740, 1981.

[Safonova 04] Alla Safonova, Jessica K. Hodgins & Nancy S. Pollard. *Synthesizing physically realistic human motion in low-dimensional, behavior-specific spaces*. ACM Trans. Graph., vol. 23, no. 3, pages 514–521, 2004.

[Safonova 05] Alla Safonova & Jessica K. Hodgins. *Analyzing the physical correctness of interpolated human motion*. In SCA '05 : Proceedings of the 2005 ACM SIGGRAPH/Eurographics symposium on Computer animation, pages 171–180, New York, NY, USA, 2005. ACM.

[Sardain 04] Philippe Sardain & Guy Bessonnet. *Forces acting on a biped robot. Center of pressure-zero moment point*. Systems, Man and Cybernetics, Part A, IEEE Transactions on, vol. 34, no. 5, pages 630–637, 2004.

[Shin 01] Hyun Joon Shin, Jehee Lee, Sung Yong Shin & Michael Gleicher. *Computer puppetry : An importance-based approach*. ACM Trans. Graph., vol. 20, no. 2, pages 67–94, 2001.

[Shin 03] Hyun Joon Shin, Lucas Kovar & Michael Gleicher. *Physical Touch-Up of Human Motions*. In PG '03 : Proceedings of the 11th Pacific Conference on Computer Graphics and Applications, page 194, Washington, DC, USA, 2003. IEEE Computer Society.

[Shiratori 09] Takaaki Shiratori, Brooke Coley, Rakié Cham & Jessica K. Hodgins. *Simulating balance recovery responses to trips based on biomechanical principles*. In SCA '09 : Proceedings of the 2009 ACM SIGGRAPH/Eurographics Symposium on Computer Animation, pages 37–46, New York, NY, USA, 2009. ACM.

[Siciliano 91] B. Siciliano & J.-J.E. Slotine. *A general framework for managing multiple tasks in highly redundant robotic systems*. In Advanced Robotics, 1991. 'Robots in Unstructured Environments', 91 ICAR., Fifth International Conference on, volume 2, pages 1211–1216, 19-22 1991.

[Tak 00] Seyoon Tak, Oh young Song & Hyeong-Seok Ko. *Motion Balance Filtering*. Computer Graphics Forum, vol. 19, no. 3, pages 437–446, 2000.

[Tak 02] Seyoon Tak, Oh young Song & Hyeong-Seok Ko. *Spacetime Sweeping : An Interactive Dynamic Constraints Solver*. Computer Animation, vol. 0, page 261, 2002.

[Tak 05] Seyoon Tak & Hyeong-Seok Ko. *A physically-based motion retargeting filter*. ACM Trans. Graph., vol. 24, no. 1, pages 98–117, 2005.

[Takenaka 94] T. Takenaka, T. Hasegawa, & Honda. *Gait Generation System for a Legged Mobile Robot,*. US Patent 5357433, 1994.

[Tolani 00] Deepak Tolani, Ambarish Goswami & Norman I. Badler. *Real-time inverse kinematics techniques for anthropomorphic limbs*. Graph. Models Image Process., vol. 62, no. 5, pages 353–388, 2000.

[Tsai 10] Yao-Yang Tsai, Wen-Chieh Lin, Kuangyou B. Cheng, Jehee Lee & Tong-Yee Lee. *Real-Time Physics-Based 3D Biped Character Animation Using an Inverted Pendulum Model*. IEEE Transactions on Visualization and Computer Graphics, vol. 16, no. 2, pages 325–337, 2010.

[Unuma 91] Munetoshi Unuma & Ryozo Takeuchi. *Generation of human motion with emotion*. In Proceedings of Computer Animation'91, pages 77–88, 1991.

[Unuma 93] Munetoshi Unuma & Ryozo Takeuchi. *Generation of human walking motion with emotion for computer animation*. In Trans. Inst. Electron. Inf. Commun. Eng., pages 77–88, 1993.

[Unuma 95] Munetoshi Unuma, Ken Anjyo & Ryozo Takeuchi. *Fourier principles for emotion-based human figure animation*. In Proceedings of the 22nd annual conference on Computer graphics and interactivetechniques, pages 91–96. ACM Press, 1995.

[van Basten 09] B. J. H. van Basten & A. Egges. *Evaluating distance metrics for animation blending*. In Proceedings of the 4th International Conference on Foundations of Digital Games, FDG '09, pages 199–206, New York, NY, USA, 2009. ACM.

[van de Panne 94] Michiel van de Panne, Ryan Kim & Eugene Flume. *Virtual Wind-up Toys for Animation*. In Proceedings of Graphics Interface '94, pages 208–215, 1994.

[Vignais 10] Nicolas Vignais, Richard Kulpa, Cathy Craig, Sébastien Brault, Franck Multon & Benoit Bideau. *Influence of the graphical levels of detail of a virtual thrower on the perception of the movement.* Presence : Teleoper. Virtual Environ., vol 19(3), 2010, vol. 19, no. 3, 2010.

[Vukobratovic 69] M. Vukobratovic & D. Juricic. *Contribution to the synthesis of biped gait*. IEEE Trans. Biomed. Eng., vol. 16, no. 1, pages 1–6, 1969.

[Vukobratovic 90] M. Vukobratovic, B. Borovac, D. Surla & D. Stokic. Scientific fundamentals of robotics 7. biped locomotion : Dynamics, stability, control and application. Berlin, Germany : Springer-Verlag, 1990.

[Vukobratović 04] Miomir Vukobratović & Branislav Borovac. *Zero-Moment Point- Thirty Five Years of its Life*. Int. Jour. of Humanoid Robotics, vol. 1, pages 157–173, 2004.

[Wang 99] X Wang. *A behavior-based inverse kinematics algorithm to predict arm prehension postures for computer-aided ergonomic evaluation*. Journal of Biomechanics, vol. 32, no. 5, pages 453 – 460, 1999.

[Wang 03] Jing Wang & Bobby Bodenheimer. *An evaluation of a cost metric for selecting transitions between motion segments*. In SCA '03 : Proceedings of the 2003 ACM SIGGRAPH/Eurographics symposium on Computer animation, pages 232–238, Aire-la-Ville, Switzerland, Switzerland, 2003. Eurographics Association.

[Wang 10] Jack M. Wang, David J. Fleet & Aaron Hertzmann. *Optimizing walking controllers for uncertain inputs and environments*. ACM Trans. Graph., vol. 29, no. 4, pages 1–8, 2010.

[Wikipedia] Wikipedia. *Uncanny valley*. `http://en.wikipedia.org/wiki/Uncanny_valley`.

[Wiley 97] D.J. Wiley & J.K. Hahn. *Interpolation Synthesis of Articulated Figure Motion*. IEEE Computer Graphics and Application, vol. 17, no. 6, November 1997.

[Winter 95] DA Winter. *Human balance and posture control during standing and walking*. Gait & Posture, vol. 3, no. 4, pages 193 – 214, 1995.

[Witkin 88] Andrew Witkin & Michael Kass. *Spacetime constraints*. In SIGGRAPH '88 : Proceedings of the 15th annual conference on Computer graphics and interactive techniques, pages 159–168, New York, NY, USA, 1988. ACM.

[Witkin 95] A. Witkin & Z. Popović. *Motion warping*. In Proceedings of the 22nd annual conference on Computer graphics and interactivetechniques, pages 105–108. ACM Press, 1995.

[Wooten 96] Wayne L. Wooten & Jessica K. Hodgins. *Animation of Human Diving*. Computer Graphics Forum, vol. 15, no. 1, pages 3–14, 1996.

[Wooten 00] Wayne L. Wooten & Jessica K. Hodgins. *Simulation of leaping, tumbling, landing, and balancing humans*. IEEE International Conference On Robotics ans Automation, 2000.

[Wu 10] Jia-chi Wu & Zoran Popović. *Terrain-adaptive bipedal locomotion control*. ACM Trans. Graph., vol. 29, no. 4, pages 1–10, 2010.

[Yamane 00] Katsu Yamane & Yoshihiko Nakamura. *Dynamics Filter - Concept and Implementation of On-Line Motion Generator for Human Figures*. In Proceedings of the 2000 IEEE International Conference on Robotics and Automation, pages 688–695, San Francisco, CA, USA, 2000.

[Yamane 03] Katsu Yamane & Yoshihiko Nakamura. *Dynamics Filter - concept and implementation of online motion Generator for human figures*. Robotics and Automation, IEEE Transactions on, vol. 19, no. 3, pages 421–432, 2003.

[Ye 10] Yuting Ye & C. Karen Liu. *Optimal feedback control for character animation using an abstract model*. ACM Trans. Graph., vol. 29, no. 4, pages 1–9, 2010.

[Yeh 09] Thomas Y. Yeh, Glenn Reinman, Sanjay J. Patel & Petros Faloutsos. *Fool me twice : Exploring and exploiting error tolerance in physics-based animation*. ACM Trans. Graph., vol. 29, no. 1, 2009.

[Yin 07] KangKang Yin, Kevin Loken & Michiel van de Panne. *SIMBICON : simple biped locomotion control*. ACM Trans. Graph., vol. 26, no. 3, page 105, 2007.

[Zatsiorsky 90] V.M. Zatsiorsky, V.N. Seluyanov & L.G. Chugunova. *Methods of determining mass-inertial characteristics of human body segments*. In : Chernyi, G.G., Regirer, S.A. (Eds.), Contemporary Problems of Biomechanics, CRC Press, Massachusetts., 1990.

[Zatsiorsky 98] D.L. Zatsiorsky V.M. abd King. *An algorithm for determining gravity line location from posturographic recordings.* Journal of Biomechanics, vol. 31, pages 161–164, 1998.

[Zordan 02] Victor Brian Zordan & Jessica K. Hodgins. *Motion capture-driven simulations that hit and react*. In SCA '02 : Proceedings of the 2002 ACM SIGGRAPH/Eurographics symposium on Computer animation, pages 89–96, New York, NY, USA, 2002. ACM.

[Zordan 05] Victor Brian Zordan, Anna Majkowska, Bill Chiu & Matthew Fast. *Dynamic response for motion capture animation*. ACM Trans. Graph., vol. 24, no. 3, pages 697–701, 2005.

Table des figures

Chapter I – Background

Chapter II – Modeling dynamic balance in biological motions

Chapter III – Perception of dynamic properties in virtual human motions

Appendix B – Foot Rotation Indicator

Appendix C – Angular Momentum

Liste des tableaux

Chapter II – Modeling dynamic balance in biological motions

Résumé

Depuis plusieurs années, la simulation de mouvements d'humains virtuels est devenue un enjeu important pour de nombreux domaines. Comprendre le fonctionnement du mouvement humain et le simuler intéresse des disciplines variées, telles que l'animation par ordinateur, la robotique, la biomécanique, etc. Dans le cas de l'animation d'humains virtuels, le but est d'utiliser ces connaissances pour créer des humanoïdes aussi réalistes que possible. De nombreux travaux ont été déjà été réalisés, permettant désormais de gérer de nombreuses tâches avec des mouvements fidèles à ce qu'un humain aurait réalisé. L'une des contraintes importante du réalisme du mouvement humain est le respect des lois de la dynamique. Tout humain est soumis à ces lois inviolables, faisant partie des lois de la physique. Dans cette thèse, nous nous intéressons à l'étude et la modélisation simplifiée de la dynamique du mouvement humain afin d'atteindre des performances compatibles avec des applications interactives. Le travail proposé se décompose donc en trois parties : analyser le comportement de l'être humain face à certaines contraintes dynamiques, évaluer la capacité d'un utilisateur à percevoir les subtilités gestuelles induites par ces contraintes et proposer une nouvelle méthode d'animation d'humains virtuels tirant le meilleur profit de ces connaissances.

Dans le cadre de cette thèse, nous nous sommes donc tout d'abord penchés sur l'étude de la mesure d'équilibre dynamique du mouvement humain. Différents critères de mesure de l'équilibre et du déséquilibre du mouvement humain existent depuis des années en biomécanique et robotique. Dans le but d'évaluer l'efficacité de ces critères, nous avons réalisé une étude portant sur différent types de mouvements pour catégoriser le domaine d'utilisation optimal de chaque critère.

Cependant, si la dynamique joue un rôle crucial dans le réalisme du mouvement, peu de travaux traitent de la perception des propriétés dynamiques. Dans le but de définir un seuil de perception, nous avons étudié la capacité des utilisateurs à détecter la masse d'un objet porté par un humain réel (vidéo) ou virtuel (animation). Il sort de l'étude réalisée qu'une faible différence de charge portée par un humain n'est pas perçue. Cependant, nous ne notons pas différence de précision si la séquence provient d'une vidéo ou d'une animation en images de synthèse. Ainsi, malgré le fait que des informations soient perdues lors du processus de capture de mouvements et de synthèse, les éléments liés à la dynamique du mouvement sont préservées et perçus par l'utilisateur.

Au vu de l'imprécision avec laquelle un utilisateur perçoit les adaptations gestuelles dues à des contraintes dynamiques, nous avons proposé un modèle simplifié d'adaptation du mouvement en réponse à de nouvelles contraintes dynamiques. Lorsqu'un humain virtuel est soumis à des perturbations non présentes dans le mouvement d'origine, la méthode traite séparément l'adaptation posturale et temporelle du mouvement, entraînant une légère imprécision au profit d'une amélioration considérable du temps de calcul. Le mouvement obtenu est davantage adapté aux contraintes dynamiques que ne l'était celui d'origine, à moindre coût de calcul.

Abstract

For years, understanding and simulating human motion has become an important issue for various fields, such as computer animation, robotics, biomechanics, etc. In computer animation, the goal is to use this knowledge to create virtual humans as realistic as possible. With the amount of work already done, it is now possible for virtual humans to handle various tasks as realistically as a real human would do. One important key point in the realism of virtual motions is to verify dynamic laws. Every human being is subject to these laws. This PhD thesis deals with understanding the dynamics of virtual human motion and modeling simplified dynamics to reach interactive applications. This work is divided in three parts. First, we analyze human behavior to different dynamic constraints. Then, we evaluate users' perception of subtle differences in human motion due to dynamic constraints. Finally, we propose a new method for dynamic adaptation of human motion using the knowledge obtained from our previous studies.

In the first part of this work, we present a study on measuring the dynamic balance of human motion. Using different criteria previously proposed in biomechanics and robotics literature, we evaluate their efficiency on different types of motions with varying degrees of dynamics. Then, we propose a preferential utilization range for each criterion.

If dynamics plays an important role in the realism of virtual human motions, few works deal with the perception of dynamic properties. In order to define a perception threshold, we studied the accuracy of users to differentiate the mass of a dumbbell lifted either by a real (video) or a virtual human (animation). We observed that users do not manage to differentiate small mass differences. However, we did not perceive significant differences between comparing real videos or virtual animations. Thus, even if some information is lost in the process transforming a real motion into a virtual one, principal dynamic information are preserved and perceived by users.

Regarding the accuracy reached by users on the perception of dynamic constraints, we proposed a new perception-based method for dynamic adaptation of human motions subject to new external constraints, using the knowledge obtained from the perception study. When a virtual character is subject to external perturbations that were not present in the original motion, our method separates postural and temporal adaptation of the motion. It introduces small inaccuracies but generates natural looking reactions to external perturbations while drastically decreasing computation time. Thus, the final motion is more dynamically correct than the original motion with the new perturbations, with low computation load.

N°d'ordre : **D10-023**

Institut National des Sciences Appliquées de Rennes
20, Avenue des Buttes de Coësmes . CS 14315 . F-35043 Rennes Cedex
Tel : 02 23 23 82 00 – Fax : 02 23 23 83 96